Investigation of the interaction between salt movement, faulting and deposition, using high-resolution 3-D seismic data; Eugene Island South Addition, Gulf of Mexico

---

A Thesis

Presented to

the Faculty of the Department of Earth and Atmospheric Sciences

University of Houston

In Partial Fulfillment

of the Requirements for the Degree

Master of Science

By

Ozbil Yapar

August 2013

Investigation of the interaction between salt movement, faulting and deposition, using high-resolution 3-D seismic data; Eugene Island South Addition, Gulf of Mexico

_____

Ozbil Yapar

APPROVED:

_____

Dr. Michael A. Murphy

_____

Dr. Paul Mann

_____

Dr. Pete Emmet

_____

_____

Dean, College of Natural Sciences and Mathematics

ACKNOWLEDGEMENTS

My special thanks go to my advisor Dr. Michael Murphy for his invaluable guidance and assistance in the preparation of this research. I would also like to thank my thesis committee members, Dr. Paul Mann and Dr. Pete Emmet. I acknowledge and thank Selin Akhun, Omer Akbas, Rebecca Neill, and all my Turkish friends for significant contribution for this research.

My sincerest appreciation and deepest gratitude goes to Turkish Petroleum Corporation for their encouragement support and funding of my master thesis.

Last, but not least, my deepest gratitude goes to my fiancé Gulsah and my family for believing in me.

Investigation of the interaction between salt movement, faulting and deposition, using high-resolution 3-D seismic data; Eugene Island South Addition, Gulf of Mexico

---

An Abstract of a Thesis

Presented to

the Faculty of the Department of Earth and Atmospheric Sciences

University of Houston

In Partial Fulfillment

of the Requirements for the Degree

Master of Science

By

Ozbil Yapar

August 2013

ABSTRACT

Investigation of the interaction between salt movement, faulting and deposition, using high-resolution 3-D seismic data; Eugene Island South Addition, Gulf of Mexico

Deformation on the Louisiana shelf results from the complex interaction between salt movement, faulting, and deposition. The goal of this study is to investigate the relationship between these processes through detailed structural interpretation of data from Eugene Island South Addition, Gulf of Mexico. I used a high-resolution 3D seismic dataset that is an approximately $1850\mathrm{km}^2$ seismic survey acquired by Petroleum Geo-Services in 1995-1996. The seismic data were processed through Kirchhoff prestack time migration.

I interpreted the fault systems, sedimentary bodies, and salt geometries based on 3D seismic data, well data, and previous studies in adjacent areas. I calculated the displacement-length values based on the faults and horizons interpretations. Fault displacement-length data were used to evaluate the pattern of deformation and how it evolved. I used 29 publically available wells to convert the 3D time data to depth.

I interpreted 31 faults and 10 horizons. The fault systems in the study area consist of 25 concave basinward normal faults. Most of the faults sole into salt, a salt weld, or a salt roller. I show that most normal faults were active during the Pleistocene (0.46-0.65 Ma) based on the age of growth strata in their hanging walls. This implies that salt movement and fault displacement are contemporaneous with sedimentation.

Strain analysis of the fault system shows that extension is primarily accommodated by the major faults which include fault 1, fault 2 and fault 2-e located in the central part of the study area. My results show the location of kinematically linked faults. Fault 1 consists of at least three major linked faults. Fault linkage along fault 1 is observed along strike and in the dip

direction. Fault 2 and fault 2-e are linked by fault 2-d. D*L plots show that fault 2 is linked to several smaller faults. Fault 2-e consists of at least two major segments that grew by lengthening until they overlapped and subsequently linked.

My research shows that faults in the study area are kinematically linked and act as a system which accommodates Pliocene and Pleistocene extensional strata that were deposited in mostly north-south-oriented basins. Since most of the faults in the study area sole into salt, it implies that the kinematics of salt deformation are the same or at least similar to the kinematics of faulting.

CONTENTS

1. Introduction

1.1 Project Summary

Deformation on the Louisiana shelf results from the complex interaction between salt movement, faulting, and deposition. The goal of this study is to investigate the relationship between these processes through detailed structural interpretation of Eugene Island South Addition, Gulf of Mexico. In order to accomplish this goal, faults and their growth strata were interpreted, along with associated salt and depositional facies. These features were used to construct fault network maps, displacement-length plots, and displacement histories.

I used a high-resolution 3D seismic survey that it is approximately 1850 km^2 and was acquired by Petroleum Geo-Services in 1995-1996. Twenty-nine publicly available wells were used to convert the 3D data time to depth. These wells included velocity, depth, and lithology information.

I interpreted 31 faults and 10 horizons. The fault systems in the study area consist of 25 concave-basinward normal faults which are part of roller fault families and rollover fault families. Most of the faults offset Pleistocene-age horizons. A majority of them dip south-south east. All faults root into salt, a salt weld, or a salt roller.

I examined the sedimentary infill within the study area. Two fluvial channels are interpreted between the Plac A-Plac B (0.49 Ma- 0.65Ma) and Plac B- Sm Gap (0.65 Ma- 0.9Ma) horizons. The developing deltas are interpreted to have loaded the underlying salt and caused, in part, mobilization of the salt, causing it to flow up-section, both laterally and vertically.

Displacement vs. Length (D*L) along the fault that are used to observe how displacement is changing along the fault and what type of relationship exists between the faults in the system (e.g. Morley and Wonganan, 2000; Peacock 2002; Morley et al., 2007). In this research D*L plots are constructed to assess fault relationships (linkage and interaction), fault growth intervals and displacement distribution along faults. In order to investigate the strain distribution in the study area, D*L plots were constructed for four faults. Plots were generated for six interpreted horizons. Moreover, interaction between the fault 2, fault 2-d and fault 2-e were compared by using D*L plots along the oldest interpreted horizon (Plac B).

The research presented in this thesis helps provide a better understanding of the evolution of normal faults during sedimentation, and salt movement on the Louisiana shelf.

1.2 Geologic Overview of the Area

Paleogeographic reconstructions indicate that the Gulf of Mexico Basin developed as a consequence of the southward drift of the Yucatan Peninsula Tectonic Block away from the North American plate during the Late Triassic (Salvador, 1987; Salvador, 1991; Bird et al., 2005) (Table 1). Rifting continued at a slow rate during the Early and Middle Jurassic and then at a higher rate after Middle Jurassic salt deposition.

Rifting Begins	Salt Deposition	Sources
Late Triassic to end of the Middle Jurassic	Late Middle Jurassic	Salvador, 1987
Late Triassic to Early Jurassic	Late Middle Jurassic to Early Late Jurassic	Salvador, 1991
Middle to Late Triassic	Late Callovian- Early Oxfordian to Kimmeridgian	Bird et al., 2005

Table 1: Beginning of Rifting and Salt Deposition (Salvador, 1987; Salvador, 1991; Bird et al., 2005)

Middle Jurassic salt became mobile soon after its deposition. In general, it moved down slope, as well as up-section along faults and as diapirs. This resulted in the formation of salt canopies (Figures 2 and 3). The salt bodies within the study area are part of a regionally-extensive canopy.

Interpretation of the regional structures of the northern Gulf of Mexico (GOM) is challenging due to the presence of three-dimensionally complex structures and variability of deep structures in many areas that are not well imaged by current seismic methods (Diegel et al., 1995). Tectono -stratigraphic maps of the GOM show eight significant regions within which distinctive structural styles may be described (Figure 1) (Modified from Diegel et al., 1995).

The area between the onshore and the shelf margin is dominated by listric growth faults that sole into a sub-horizontal detachment and extend into a large salt dome-minibasin province. The study area is located in a Pliocene-Pleistocene detachment province which may be separated into 'organized' and 'disorganized' roho systems (Sumner et al., 1990; Diegel et al., 1995).

The organized systems are located in the western and eastern parts of the Pliocene-Pleistocene detachment province and the disorganized systems are located in the central part of the Pliocene-Pleistocene detachment province. The organized roho system is a combination of extensive salt welds and listric basinward normal faults that developed more uniform structures than the disorganized roho system. The study area is located exactly on a disorganized roho system which is a combination of residual salt wings, evacuation surfaces, and windows between salt bodies that developed more complex structures (Diegel et al., 1995).

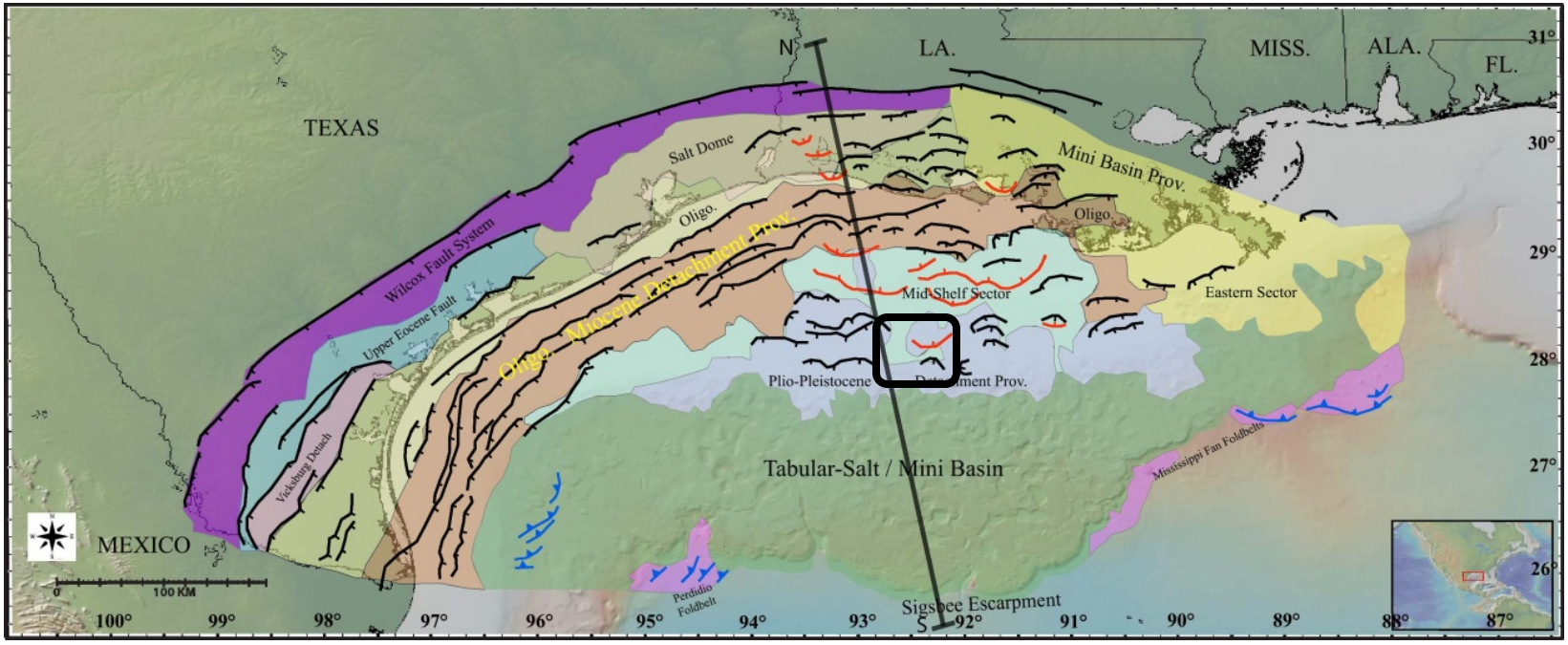

Figure 1: Structural summary map of the Northern Gulf of Mexico Basin and Tectono- Stratigraphic provinces (Modified from Diegel et al., 1995).

Figure 2 shows a generalized cross section across the northern Gulf of Mexico. From north to south it shows, thin transitional crust to oceanic crust. The generalized stratigraphic and structural elements are shown on this crustal structure. The study area is located within the northern part of the shoreline provinces (modified from Galloway et al., 2005) (Figure 2).

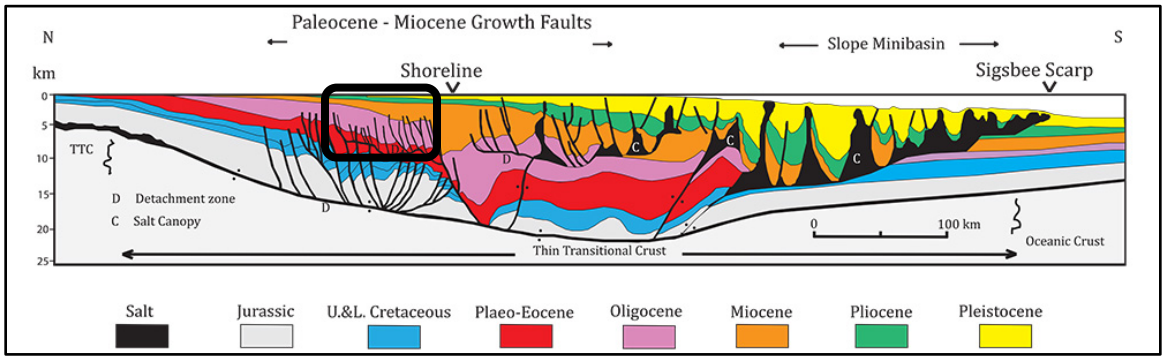

Figure 2: North-South cross-section of crustal types, generalized stratigraphy, and structural elements of the Northern Gulf of Mexico (see figure 1 for location) (Modified from Galloway et al., 2005). Black square shows the general location of study area.

The location of the continent-ocean transition zone (COTZ) in the Gulf of Mexico has been interpreted by a number of authors using a variety of different methods. Figure 3 shows the different interpretations in map view. The study area is located approximately 150 km to the north of the COTZ as defined by Bird et al. (2005). Transitional oceanic crust lies adjacent to, and to the northeast of, Keathley Canyon (KC) (Bird et al., 2005).

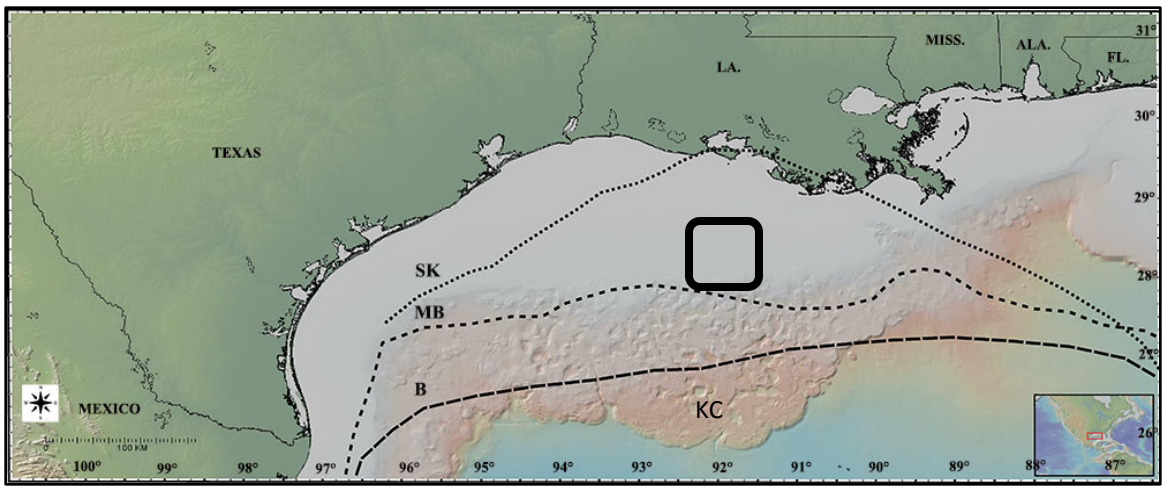

Figure 3: B, MB and SK are interpreted position of the continent-ocean transition zone (COTZ). B (Bird et al., 2005), MB (Marton and Buffler., 1994), SK (Schouten and Klitgor., 1994), (Modified from Bird et al., 2005). KC= Keathley Canyon. Black square shows the general location of study area.

1.2.1 Salt-related Structures

A schematic block diagram shows geologic elements present in the study area (Figure 4). In the study area, these structures are observed and interpreted in both cross sections and map views.

The roller fault family consists of extensional faults and they generally develop on autochthonous salt or allochthonous salt sheet (Rowan et al., 1999). The dip direction of these faults is basinward and the faults are defined as listric growth faults that sole into the salt layer (Rowan et al., 1999). If salt has been evacuated, the roller faults have triangular salt rollers in their footwalls. If salt exists, faults merge with the top salt horizon. In cross section, roller faults generally comprise landward tilted rollover monoclines or anticlines with an expanded growth section. Displacement expands downward and strata thicken landward on their hanging walls. In map view, roller faults develop concave-shape fault arrays (Diegel et. al., 1995; Rowan et al., 1999).

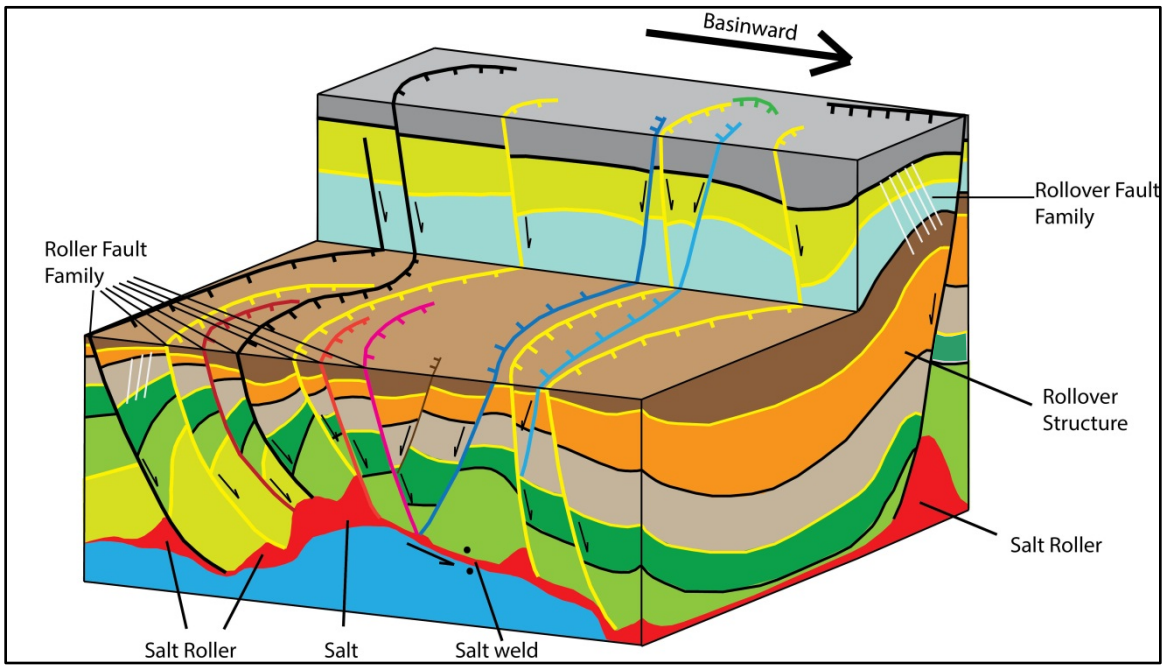

Figure 4: Schematic block diagram of typical fault families in the study area.

The rollover fault family consists of extensional faults and they generally develop on the hanging walls of roller faults or salt welds. The dip direction of rollover faults is antithetic to the adjacent roller fault. Also, rollover strata and roller faults have same dip direction. In cross section, they are planar and they do not reach downward into salt (Rowan et al., 1999).

Salt and salt welds have been described by a number of authors. Salt welds form when formerly separated strata are joined together because of salt evacuation. In seismic cross sections, salt welds are defined as discontinuous, high amplitude reflectors (Alexander and Fleming, 1995; Rowan et al., 1999). According to Diegel et al. (1995), an updip salt weld characterizes the downdip part of the Pliocene-Pleistocene detachment province.

1.2.2 Depositional Facies

Within the study area the sedimentary sequences can be divided into three general depositional facies (Figure 5); these include prodelta facies, proximal facies, and fluvial facies. The prodelta facies comprise the part of a delta lying beyond the delta front, and sloping slowly down to the basin floor of the delta; it is entirely below the water level and includes bathyal and prodelta shales, turbidites, and distal deltaic shales. The proximal deltaic facies are comprised of coarse clastic sediment deposited near the source and includes shelf margin delta-derived sand, silt, and clay. The fluvial facies (A sedimentary deposit of material transported by or suspended in a river) consist of sediment deposited shallow marine deltas and rivers (Alexander and Flemings, 1995).

More than 4 km of sediment was deposited within the minibasins during late Pliocene and Pleistocene. Total sedimentary thickness increases from east to west and from south to north, and it approaches a maximum of 17 km (Pliocene age) under the Texas-Louisiana Shelf (Ebeniro, 1988).

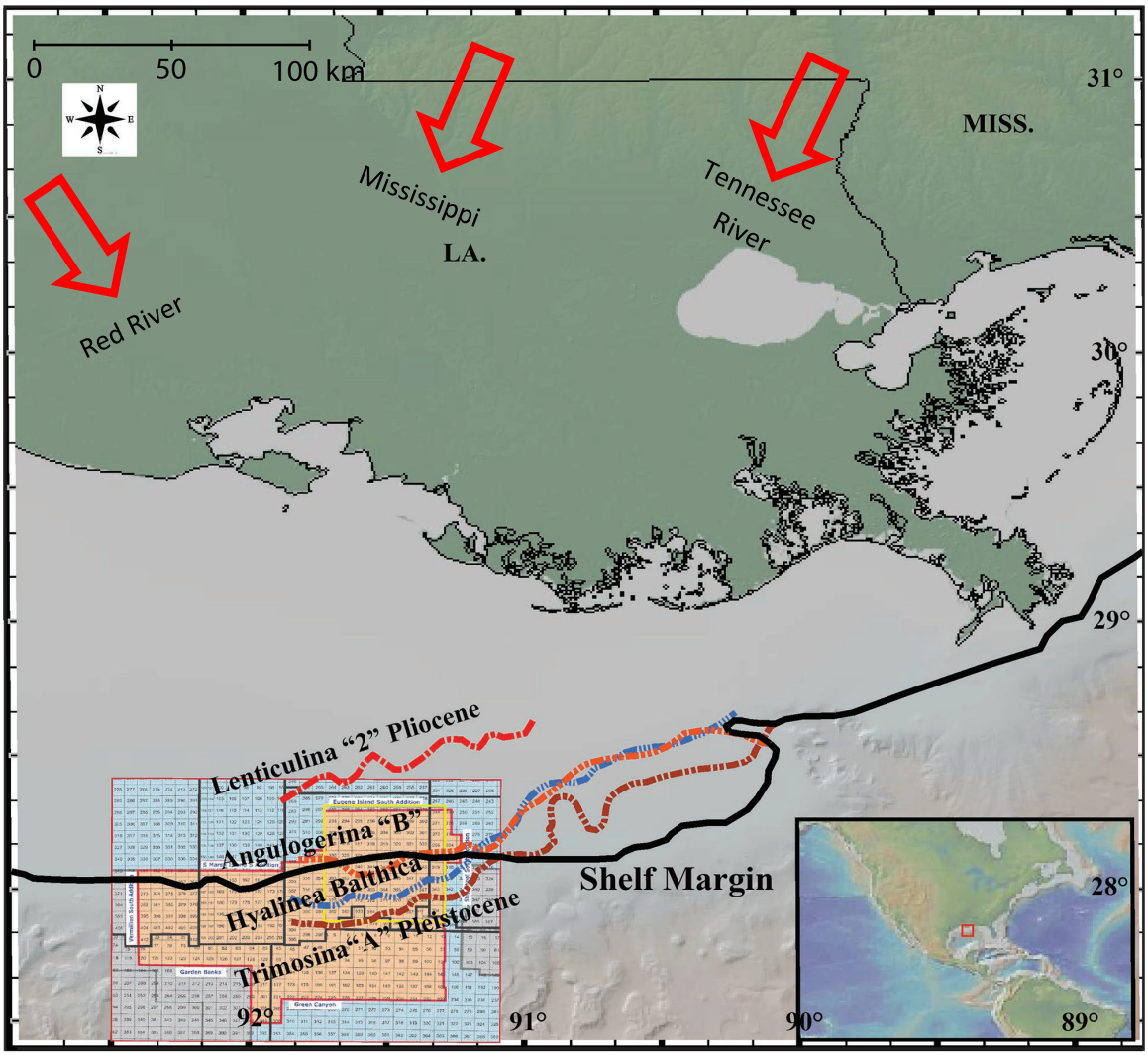

Figure 5: Paleontologically constrained shelf margin development from the late Pliocene (Lenticulina 1 stage) through late Pleistocene (Trimosina A stage) (Modified from Alexander and Fleming, 1995). Red arrows indicate the geographic location of Cenozoic fluvial input axes around the study area (Galloway et al., 2011).

Fluvial input of Gulf of Mexico shows that the study area is deposited mainly by three river systems which are the Red River, the Mississippi River and the Tennessee River (Figure 6) (Galloway)(See figure 5 for location). To better understand the evolution of the study area, structure maps of three transgressive surfaces (Plac A, Plac B, and Sm Gep) and four high amplitude events were constructed from seismically correlated horizons.

Between the Plac B and Sm Gep transgressive surfaces, two main sand intervals were deposited. These are interpreted to be deltaic sands and incised-valley fill (Alexander and Flemings, 1995). Between the Plac B and Plac A transgressive surfaces, two main sands intervals were also deposited. These are interpreted to be incised-valley fill deposits (Alexander and Flemings, 1995). These specific observations were made in the Eugene Island South Addition blocks 332, 331, 330, 309, 317, and 337 in the western part of the study area.

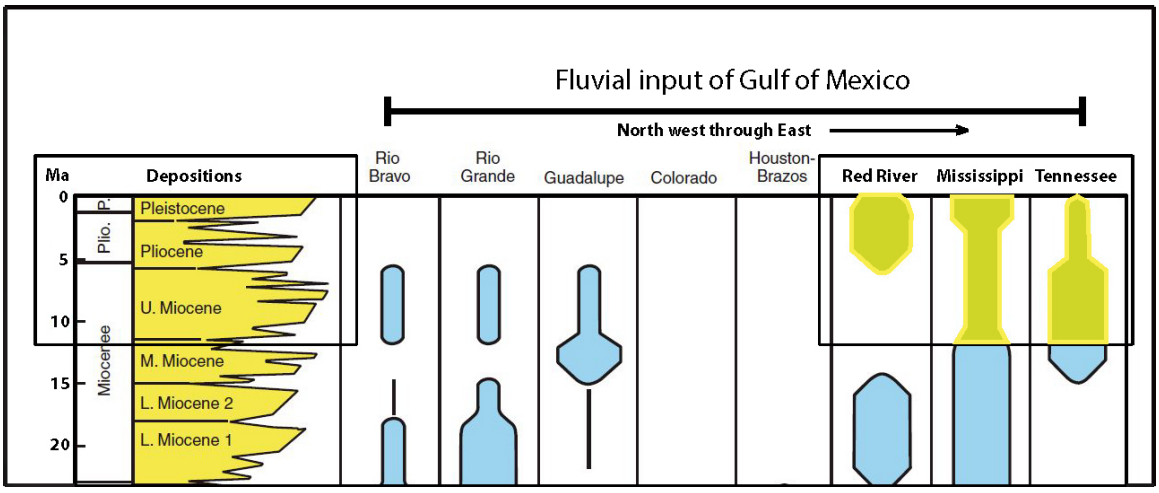

Figure 6: Depositional history of Pliocene-Pleistocene in Gulf of Mexico (Modified from Galloway et al., 2011). Blue and yellow areas represent the depocenters sediment supply. Width of bars indicates relative amount of supply.

1.3 Previous work in Eugene Island South Addition

A previous study, in Eugene Island South Addition, Gulf of Mexico, was done on block 330 by Alexander and Fleming (1995). My study area covers the block 330, but the block 330 is cropped from the focus area that it is located eastern part of the block 330.

Although Alexander and Fleming interpreted faults, depositional facies, and transgressive surfaces, and assessed the stacking pattern and geologic evolution of the block 330, their research did not evaluate the kinematic linkage of faults, nor their relationship with salt bodies and structural analysis of faults by using displacement-length plots.

Faults, depositional facies, and five transgressive surfaces are interpreted based on seismic and well data, plus previous interpretation by Alexander and Fleming (1995), Diegel et al. (1995), Rowan et al. (1998), Barry C. McBride et al. (1998), and Rowan et al. (1999).

1.4 Thesis Scope and Organization

Deformation on the Louisiana shelf results from the complex interaction between salt movement, faulting, and deposition. The scope of this thesis is to investigate the relationship between these processes through detailed structural interpretation of Eugene Island South Addition. This was conducted by integrating seismic interpretation and structural analysis of faults. Seismic interpretation is described in the ‘‘Structural Interpretation’’ section of this thesis. Structural analysis of faults is performed using displacement-length plots.

The main focus of this thesis is structural interpretation and structural analysis, based on seismic data interpretation, as well as interpretation of displacement-length plots and observations. Schematic workflow shows the sequence of this research (Figure 7).

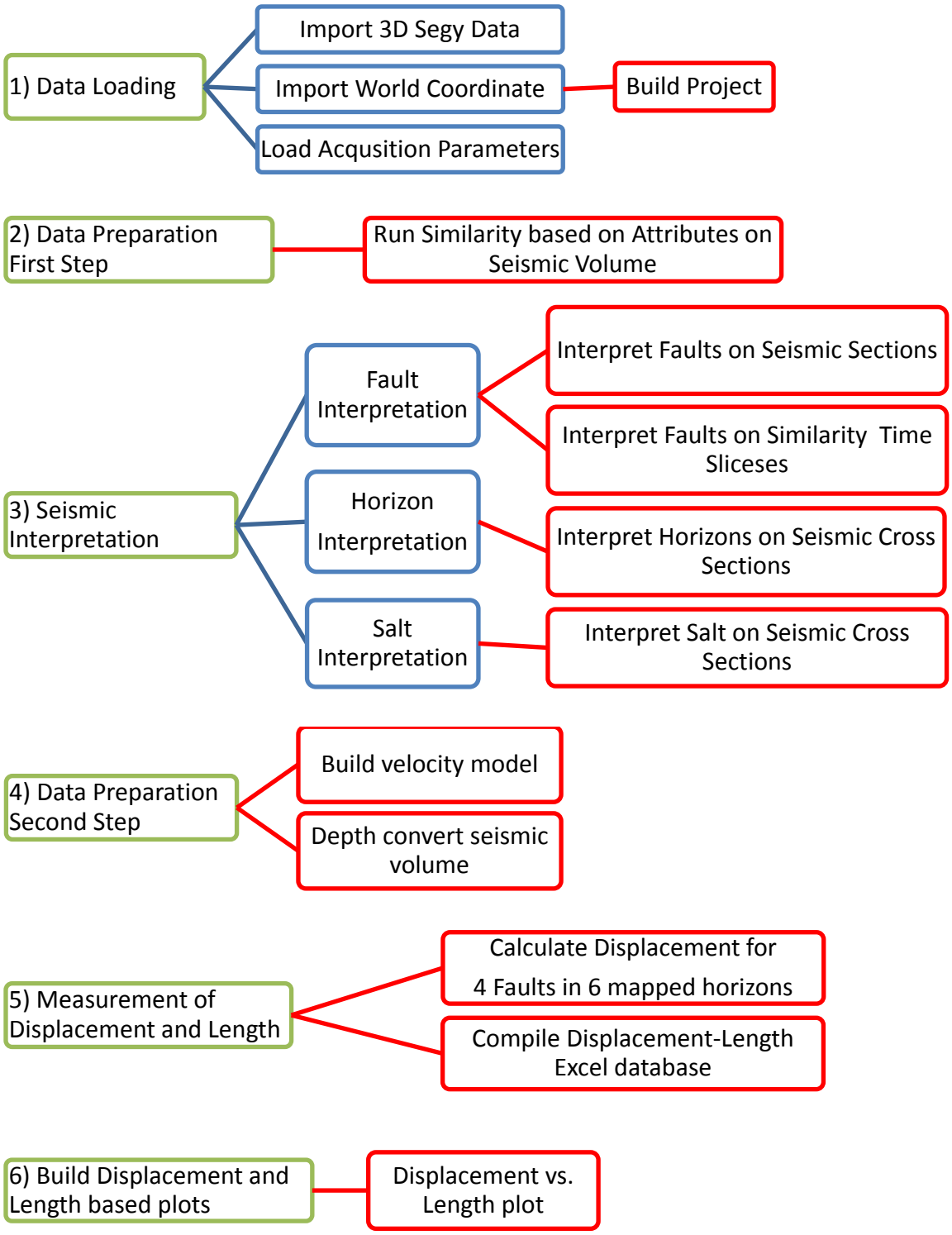

Figure 7: Schematic workflow of thesis research.

2. Data and Methodology

2.1 Seismic Data

The high resolution 3D seismic data set that was used for this study was acquired by Petroleum Geo-Services in 1995-1996 and covers an area of approximately 1850 km^2. It was processed using a Kirchhoff prestack time migration. The seismic dataset has a record length of 10.0 seconds of two-way travel time. In this study, the upper 6.0 seconds were used. The output bin dimension is 25 m x 37.5 m. The seismic data were acquired with a dominant frequency near the surface of 50 Hz, and as a result have a vertical resolution in the shallow part of the volume of approximately 3 m. At a depth of 6500 meters, the dominant frequency of 12 Hz gives a vertical resolution of approximately 115 m. The lateral resolution of the data is approximately equivalent to the spacing of the inlines, 25 m, and crosslines, 37.5 m.

2.2 Velocity Model Time to Depth Conversion

In the study area, there are more than 100 wells. The locations of the 29 wells used in this study are shown in (Figure 8). These wells were selected to generate a velocity model for time-depth conversion by using MATLAB. Available data for these wells were used to constrain interpretations of lithology, age, and time-depth conversion velocities.

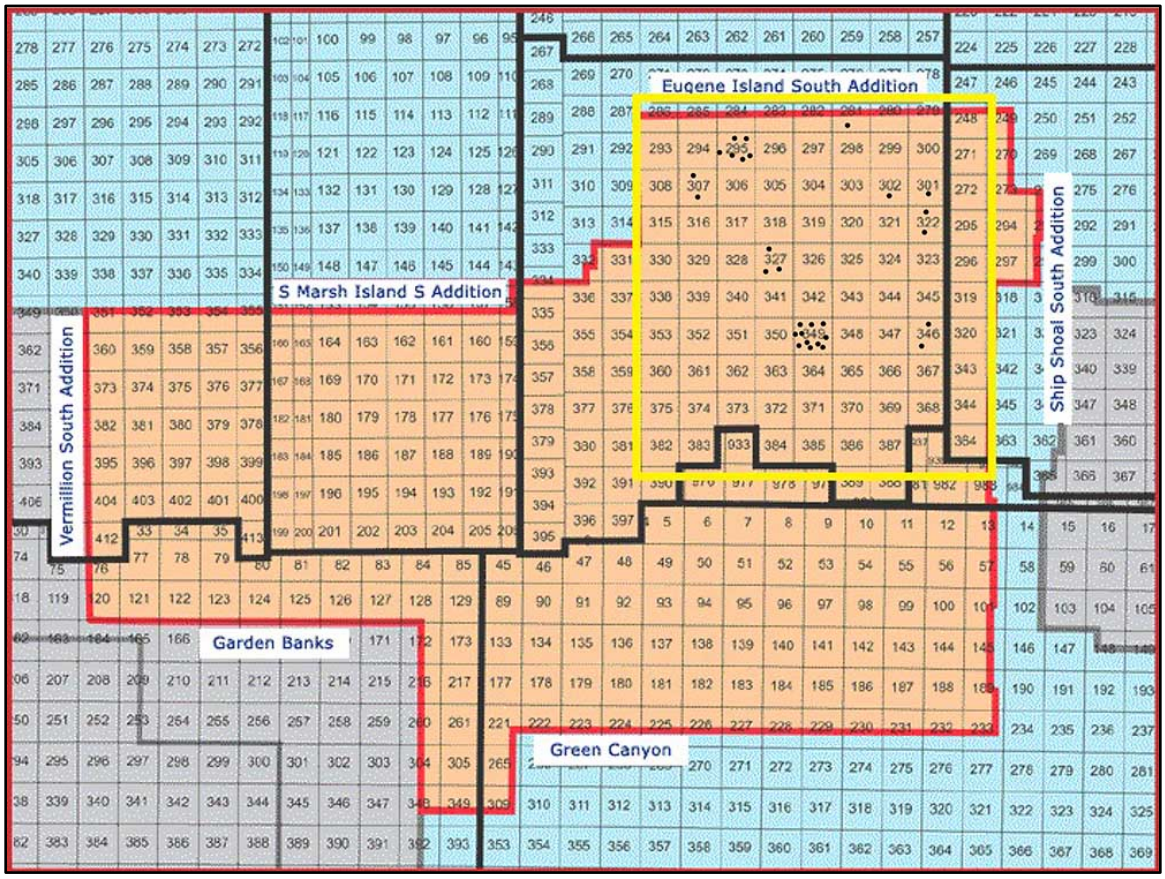

Figure 8: Project map showing the approximate location of 29 wells with available time-depth curves and blocks in the study area.

A velocity versus depth plot was calculated by using a publicly available one-way travel time versus depth data set. Depth values were converted from feet to meters and time values were converted from one-way travel time to two-way travel time. Finally, velocity values were calculated by using V=x/t equation (V= Velocity (m/s), x= depth (m) t= time (second) for each wells. Figure 7 shows the study area velocity function from 29 wells. Linear velocity function was calculated by using least square methods in MATLALB (Figure 9).

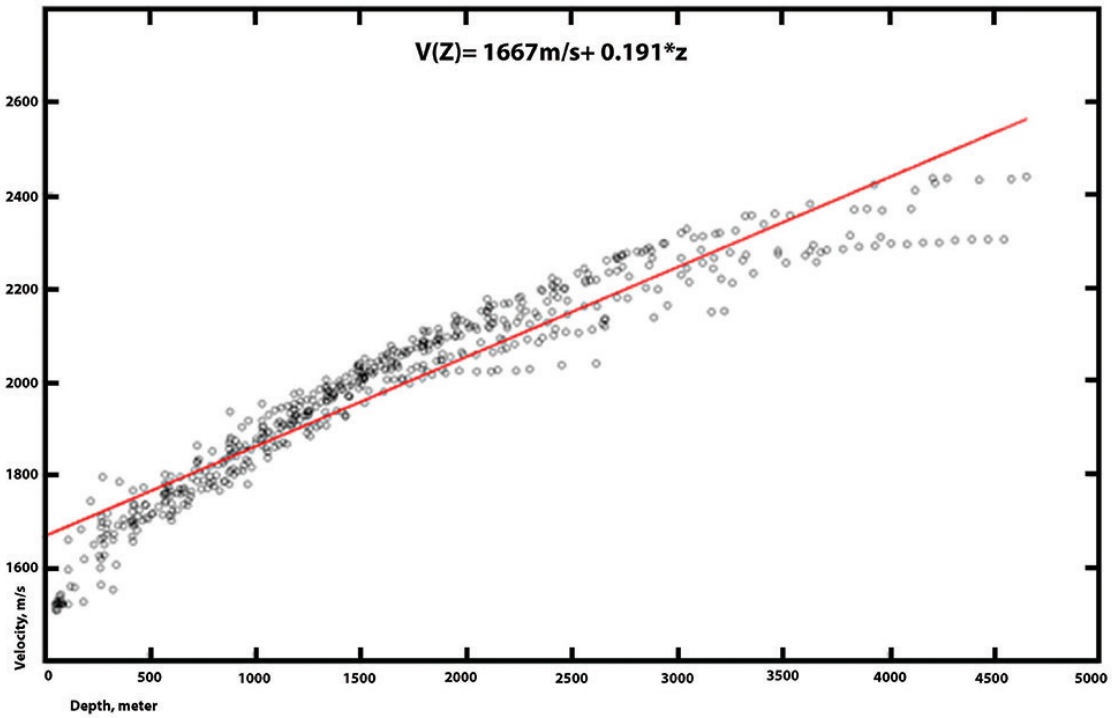

Fig 9: Velocity versus depth plot from 29 wells to be used for depth conversion of seismic data and velocity function.

Although well data show that velocity-depth values are best fit by a polynomial function, a linear velocity function is used for time-depth conversion. However, depth values are used to calculate displacement-length plots values at the first 3000 meters and time-depth conversion is suitable and accurate within this range.

3. Structural Interpretation

3.1 Sedimentation, Salt movement, and Structures

To help to understand the evolution of the study area 31 faults, 7 horizons, a top of salt, salt rollers, and salt welds were mapped. The fault systems in the study area consist of 25 concave basinward normal faults. Most of the faults sole into salt, a salt weld, or a salt roller. Three transgressive surfaces (Plac A (0.46Ma), Plac B (0.65 Ma), and Sm Gep (0.9 Ma)) and four horizons (Ozy 1, Ozy 2, Ozy 3, and Ozy 4) were interpreted. In the depositional/facies chapter, two more transgressive surfaces are interpreted. These are H. Sellii (1.27Ma) and C.mac (1.5Ma).

3.1.1 Salt, Salt Roller, and Salt Weld

Three types of salt structure were mapped within the boundaries of the seismic volume. These are a salt roller, a salt weld, and salt bodies. Roho term is defined by a number of authors. It is also called salt-evacuation surfaces or salt-withdrawal surfaces (Sumner et al., 1990; Diegel et al., 1995). Roho systems "*salt weld and salt roller*" cause the high-amplitude seismic reflection in seismic cross section (Jackson and Cramez, 1989). The developing deltas in the study area load sediment and mobilize the underlying salt, causing it to flow up-section, both laterally and vertically (Alexander and Fleming 1995; Rowan et al., 1998.)

Salt bodies and salt rollers were interpreted based on publicly available well data and their high-amplitude seismic reflection anomalies in the cross sections. This will be discussed in the interpretation of faults and horizons chapter.

3.1.2 Faults and Horizons

Interpretation of Faults:

Thirty-one faults were mapped within the study area. Fault interpretation was performed using IHS Kingdom software. Time-migrated seismic volume and depth-converted seismic volume were used to interpret faults in cross sections. Eight seismic amplitude cross sections were interpreted in this research to illustrate the relationship between salt movement, faulting, and deposition. A similarity attribute was created on this seismic volume to interpret faults in map view. Time slices with similarity based attribute were used to interpret major faults, and then minor faults. Five time slices were created to understand faults distribution in the study area. These are 0.5, 0.75, 1.0, 1.2, and 1.5 second time slices. Faults interpretation will be discussed in more detail in later chapters.

Interpretation of Horizons:

Ten horizons were mapped within the study area. Horizons interpretation was performed using IHS Kingdom software. Time-migrated seismic volume and depth-converted seismic volume were used to interpret horizons in cross sections. Interpretation of horizons (6 transgressive surfaces) was performed based on previously interpreted cross sections (Alexander and Fleming, 1995; Rowan et al., 1998). First of all, a ribbon map was created for each horizon. This interpretation was performed for every 10 inlines and crosslines. Then 3D seeker+ algorithm were used to construct the rest of the surfaces. These processes were performed for 6 horizons. A 3D view of these horizons is shown in figure 10. Horizons interpretation will be discussed in more detail in later chapters.

Ten horizons (Ozy 1, Ozy 2, Ozy 3, Plac A (0.46Ma), Ozy 4, Plac B (0.65), Sm Gep (0.9Ma), H. Sellii (1.27Ma), and C. Mac (1.5Ma) were interpreted for this study and time structure map of six horizons (Ozy 1, Ozy 2, Ozy 3, Plac A(0.46Ma), Ozy 4, and Plac B(0.65)) was performed (Figure 10).

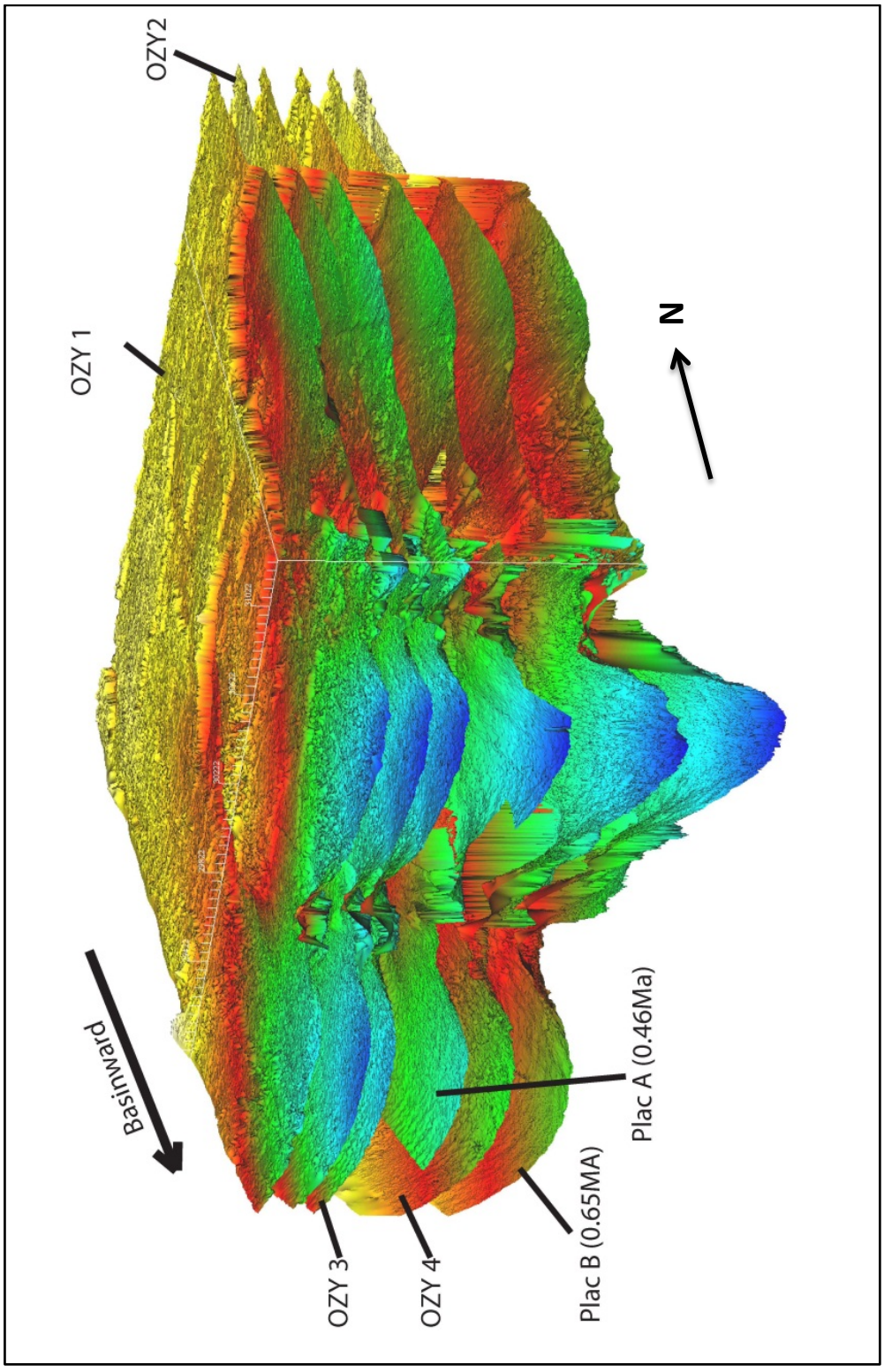

Figure 10: 3-D presentation of interpreted horizons in the study area.

3.1.2.1 Faults in Map View

In time slice 0.5 second, 23 faults are mapped (Figure 11). These are fault 1, fault 2, fault 2-a, fault 2-b, fault 2-c, fault 2-d, fault 2-e, fault 2-f, fault 3, fault 4, fault 5, fault 5-a, fault 5-c, fault 5-d, fault 6, fault 7, fault 8, fault 9, fault 10, fault 11, fault 12, fault 14, and fault 15. The fault systems in the 0.5 second time slice consists of 17 concave basinward normal faults and 6 counter-regional normal faults.

Fault 1, fault 2, fault 2-d, fault 2-e, fault 5, fault 8, and fault 15 dip south-southeast. Fault 2-a, fault 2-b, fault 2-c, fault 5-c, fault 11, and fault 12 dip south-southwest. Roller faults develop a concave-shaped fault array (Rowan et al., 1999), therefore these south-southeast and south-southwest dipping faults can be defined as roller fault families. The roller fault families can be divided into two groups in time slice 0.5, based on their dip direction, south-south- east dipping, and south-southwest dipping faults array.

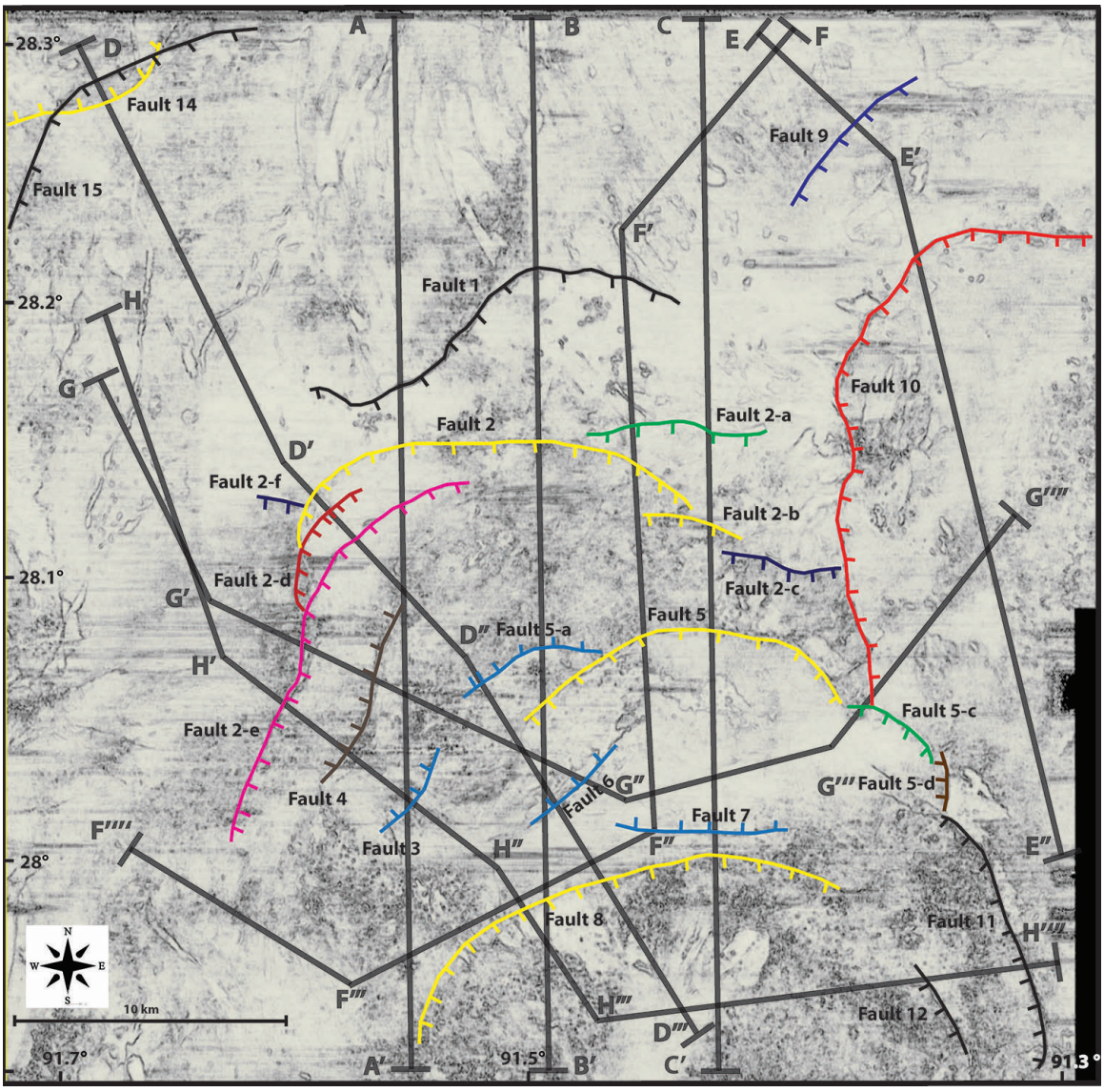

Figure 11: Fault interpretation in map view (0.5 second). Color lines represent faults. Ticks are on the hanging wall of these faults.

In time slice 0.75 second, 23 faults are mapped (Figure 12). These are fault 1, fault 2, fault 2-a, fault 2-b, fault 2-c, fault 2-d, fault 2-e, fault 2-f, fault 3, fault 4, fault 5, fault 5-a, fault 5-c, fault 5-d, fault 6, fault 7, fault 8, fault 9, fault 10, fault 11, fault 12, fault 14, and fault 15. The fault systems in the 0.75 second time slice consists of 17 concave basinward normal faults and 6 counter-regional normal faults.

Fault 1, fault 2, fault 2-d, fault 2-e, fault 5, fault 8, and fault 15 dip south-south east. Fault 2-a, fault 2-b, fault 2-c, fault 5-c, fault 11, and fault 12 dip south-southwest. The roller fault families can be divided into two groups in time slice 0.75, based on their dip direction, south-southeast dipping and south-southwest dipping faults array.

The difference between 0.5 second time slice and 0.75 second time slice is the length of the faults. Most of the faults length increase and dipping directions of faults is almost the same as the 0.75 second time slice.

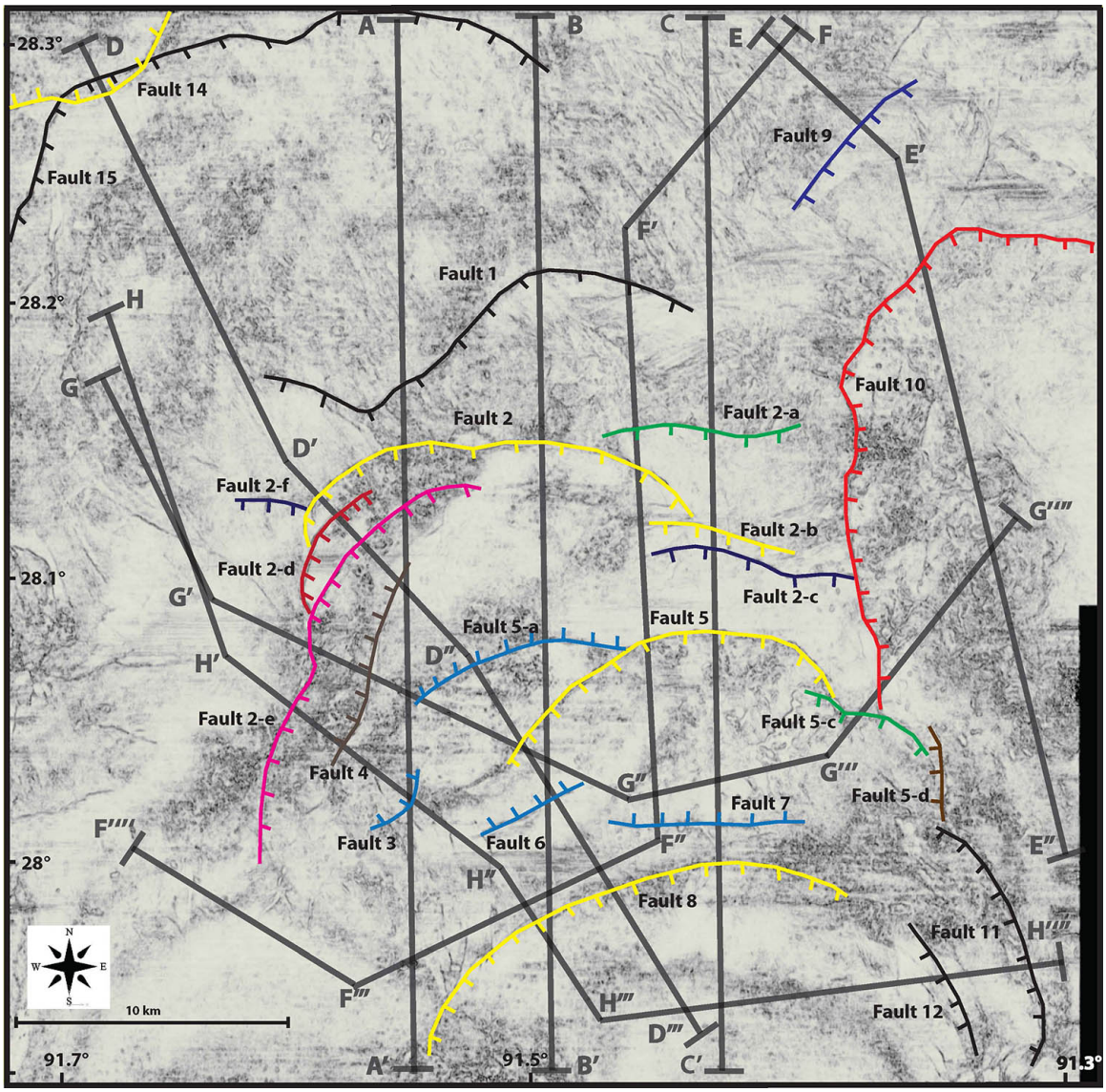

Figure 12: Fault interpretation in map view (0.75 second). Color lines represent faults. Ticks are on the hanging wall of these faults.

In time slice 1.0 second, 23 faults are mapped (Figure 13). These are fault 1, fault 2, fault 2-a, fault 2-b, fault 2-c, fault 2-d, fault 2-e, fault 2-f, fault 3, fault 4, fault 5, fault 5-a, fault 5-c, fault 5-d, fault 6, fault 7, fault 8, fault 9, fault 10, fault 11, fault 12, fault 14, and fault 15. The fault systems in the 1.0 second time slice consists of 17 concave basinward normal faults and 6 counter-regional normal faults.

Fault 1, fault 2, fault 2-d, fault 2-e, fault 5, fault 8, and fault 15 dip south-southeast. Fault 2-a, fault 2-b, fault 2-c, fault 5-c, fault 11, and fault 12 dip south-southwest. The roller fault families can be divided into two groups in time slice 1.0, based on their dip direction, south-southeast dipping and south-southwest dipping faults array.

The difference between 0.75 second time slice and 1.0 second time slice is the length of the faults. Most of the faults length increase and dipping directions of faults is almost the same as the 0.75 second time slice. The fault 2-f dips south-southwest in time slice 0.5 and 0.75 second but in time slice 1.0 second, the fault 2-f dips south-southeast.

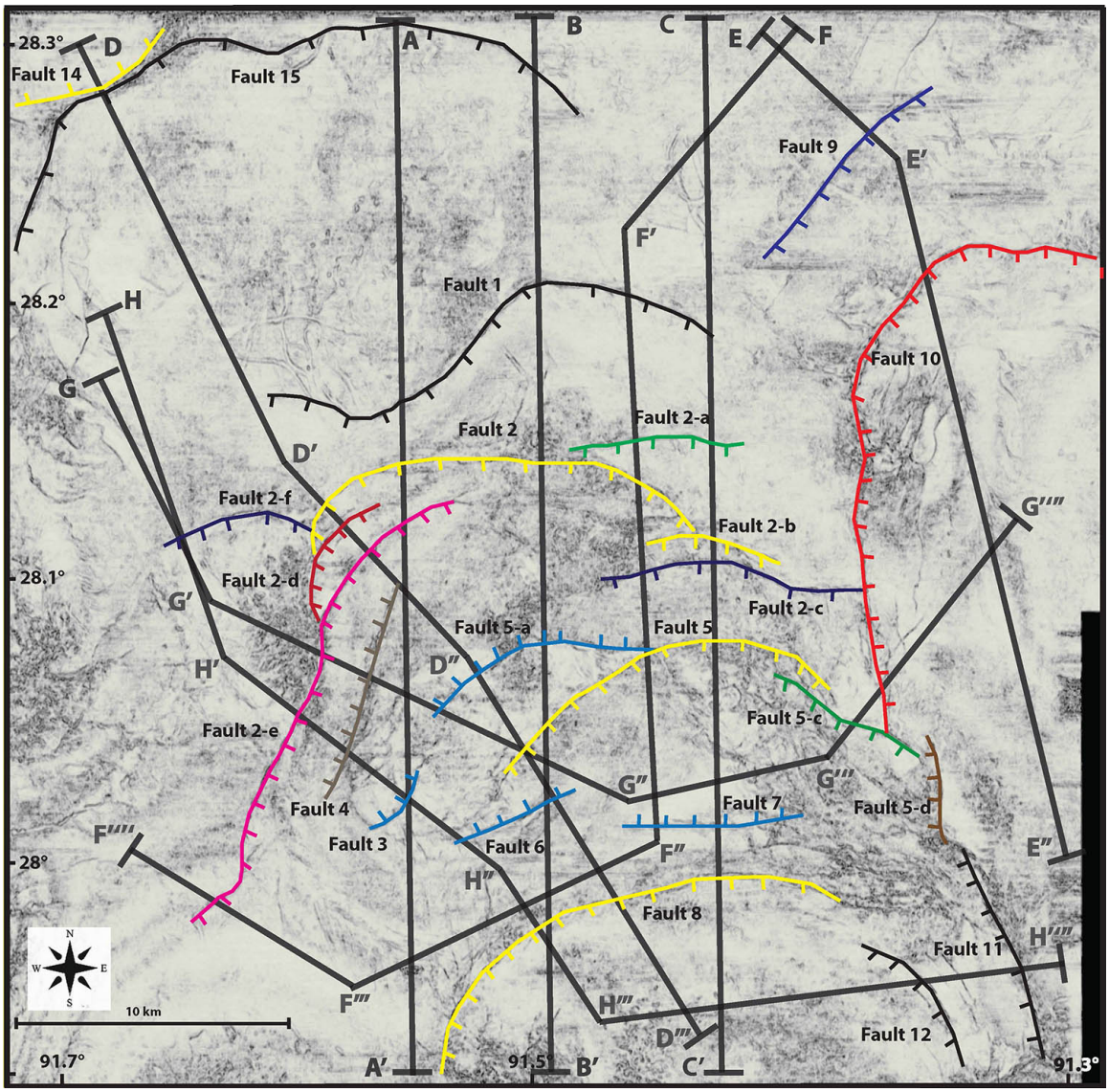

Figure 13: Fault interpretation in map view (1.0 second). Color lines represent faults. Ticks are on the hanging wall of these faults.

In time slice 1.2 second, 23 faults are mapped (Figure 14). These are fault 1, fault 1-a, fault1-b, fault 2, fault 2-a, fault 2-b, fault 2-c, fault 2-d, fault 2-e, fault 2-f, fault 3, fault 4, fault 5, fault 5-a, fault 5-c, fault 5-d, fault 6, fault 7, fault 8, fault 9, fault 10, fault 11, fault 12, fault 14, fault 15, and fault 16. The fault systems in the 1.2 second time slice consists of 20 concave basinward normal faults and 6 concave counter-regional normal faults.

Fault 1, fault 1-a, fault 1-b fault 2, fault 2-d, fault 2-e, fault 5, fault 8, and fault 15 dip south-south east. Fault 2-a, fault 2-b, fault 2-c, fault 5-c, fault 11, and fault 12 dip south-south-west. The roller fault families can be divided into two groups on time slice 1.0, based on their dip direction, south-southeast dipping and south-southwest dipping faults array.

The difference between 1.0 second time slice and 1.2 second time slice is the length of the faults. Most of the fault lengths increase and dipping directions of faults is almost the same as the 1.0 second time slices. In time slice 1.2 second, three more faults were interpreted. These are fault 1-a, fault 1-b and fault 16. These faults dip south-southeast.

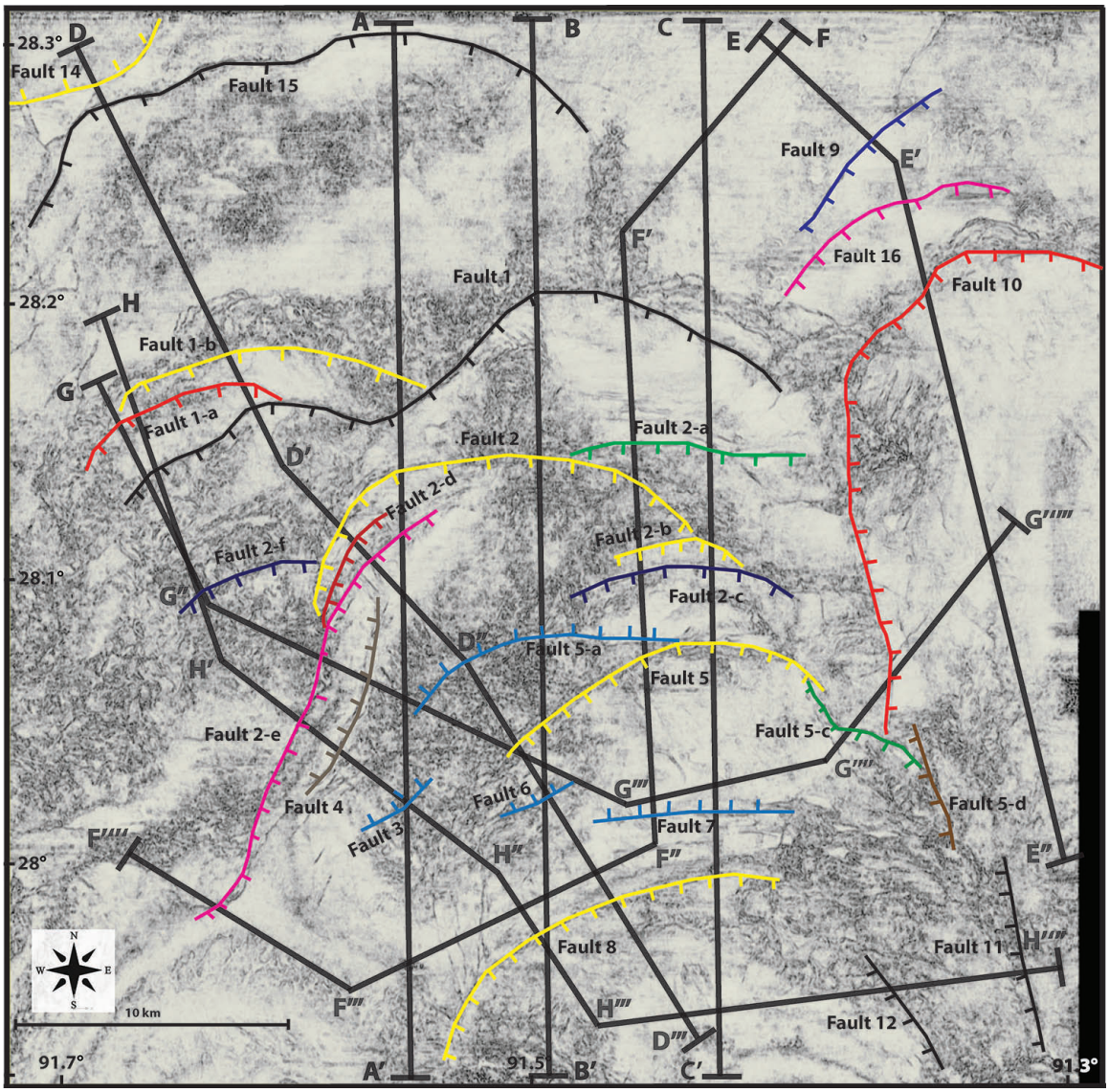

Figure 14: Fault interpretation in map view (1.2 second). Color lines represent faults. Ticks are on the hanging wall of these faults.

In time slice 1.5 second, 31 faults are mapped (Figure 15). These are fault 1, fault 1-a, fault 1-b, fault 2, fault 2-a, fault 2-b, fault 2-c, fault 2-d, fault 2-e, fault 2-f, fault 3, fault 4, fault 5, fault 5-a, fault 5-c, fault 5-d, fault 6, fault 7, fault 8, fault 9, fault 10, fault 11, fault 12, fault 14, fault 15, fault 15-a, fault 15-b, fault 15-c, fault 15-d, fault 15-e, and fault 16. The fault systems in the 1.5 second time slice consists of 25 concave basinward normal faults and 6 concave counter-regional normal faults.

Fault 1, fault 1-a, fault 1-b fault 2, fault 2-d, fault 2-e, fault 5, fault 8, and fault 15 dip south-southeast. Fault 2-a, fault 2-b, fault 2-c, fault 5-c, fault 11, and fault 12 dip south-south-west. The roller fault families can be divided into two groups in time slice 1.0, based on their dip direction, south-southeast dipping and south-southwest dipping faults array.

The difference between 1.2 second time slice and 1.5 second time slice is the length of the faults. Most of the fault lengths increase and dipping directions of faults is almost the same as the 1.2 second time slices. In time slice 1.5 second, five more faults were interpreted (15-a, fault 15-b, fault 15-c, fault 15-d, and fault 15-e), which dip south-southwest.

Moreover, the fault 2-b and the fault 2-c dipped south-southwest on the time slice 0.5 second but these faults dip direction turns slightly south-southeast on time slice 1.5 second.

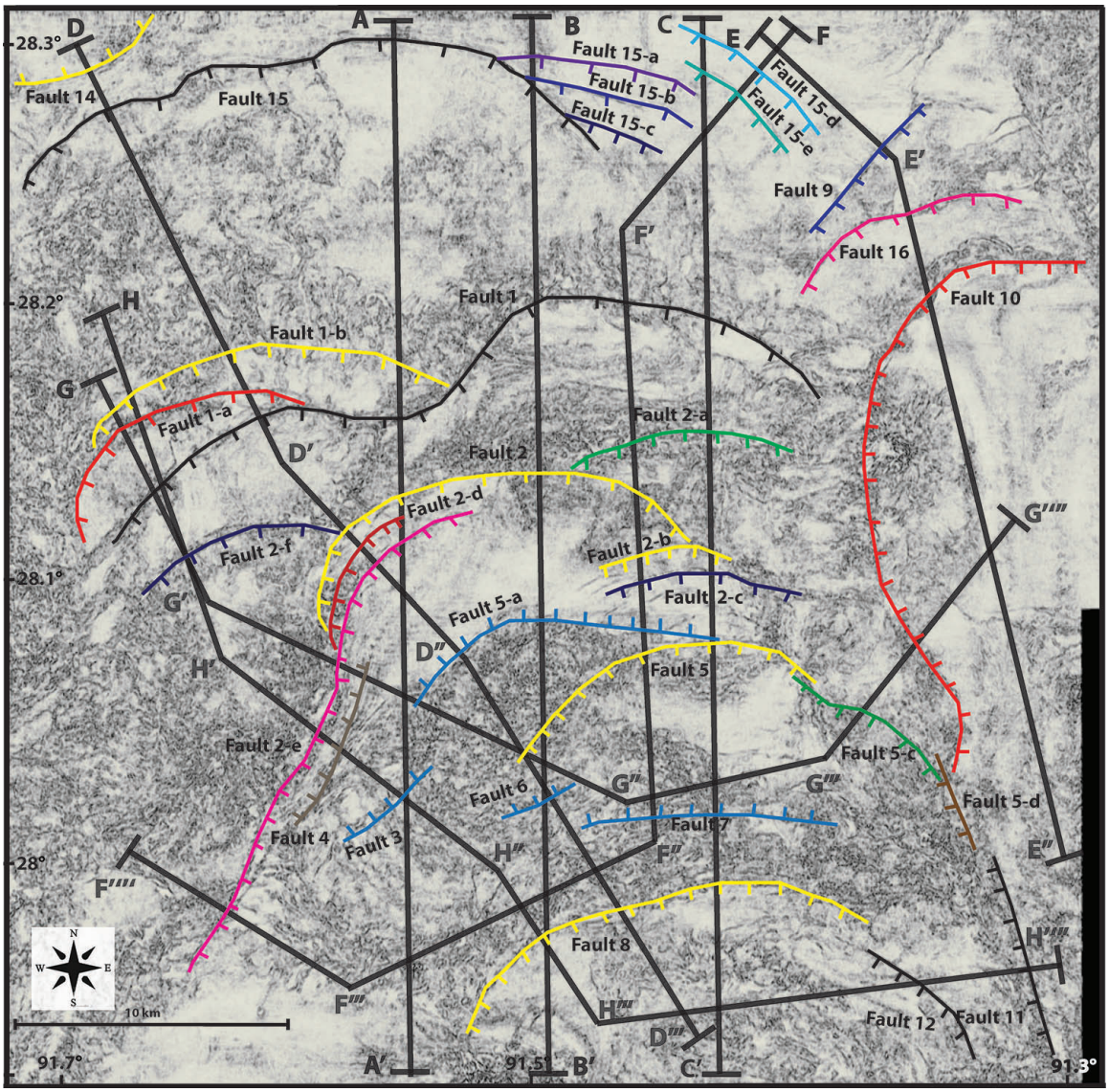

Figure 15: Fault interpretation in map view (1.5 second). Color lines represent faults. Ticks are on the hanging wall of these faults.

Summary of the Map View Interpretation:

In conclusion, 31 faults are interpreted in the study area. The fault systems in the study area consist of 25 concave basinward normal faults and 6 landward-dipping normal faults. At shallow levels, most faults have short lengths due to a decrease in displacement. With increasing depth, they tend to become longer in map view and are more often linked to other faults. The faults systems in the study area can be divided into two groups based on their dipping direction: south-southeast dipping and south-southwest dipping faults array.

3.1.2.2 Faults and Horizons in Cross Sections

Eight seismic amplitude cross sections are interpreted in this research to illustrate the relationship between salt movement, faulting, and deposition.

Salt welds and salt rollers cause the high amplitude seismic reflection in seismic cross sections (Jackson and Cramez, 1989). The interpretation of salt welds and salt rollers is based on this information and publicly available well data.

Uninterpreted and interpreted north-south-oriented seismic cross sections AA' can be seen in figures 16-17 (see figure 11-15 for location). This chapter will discuss the interpretation of the A-A' cross-section.

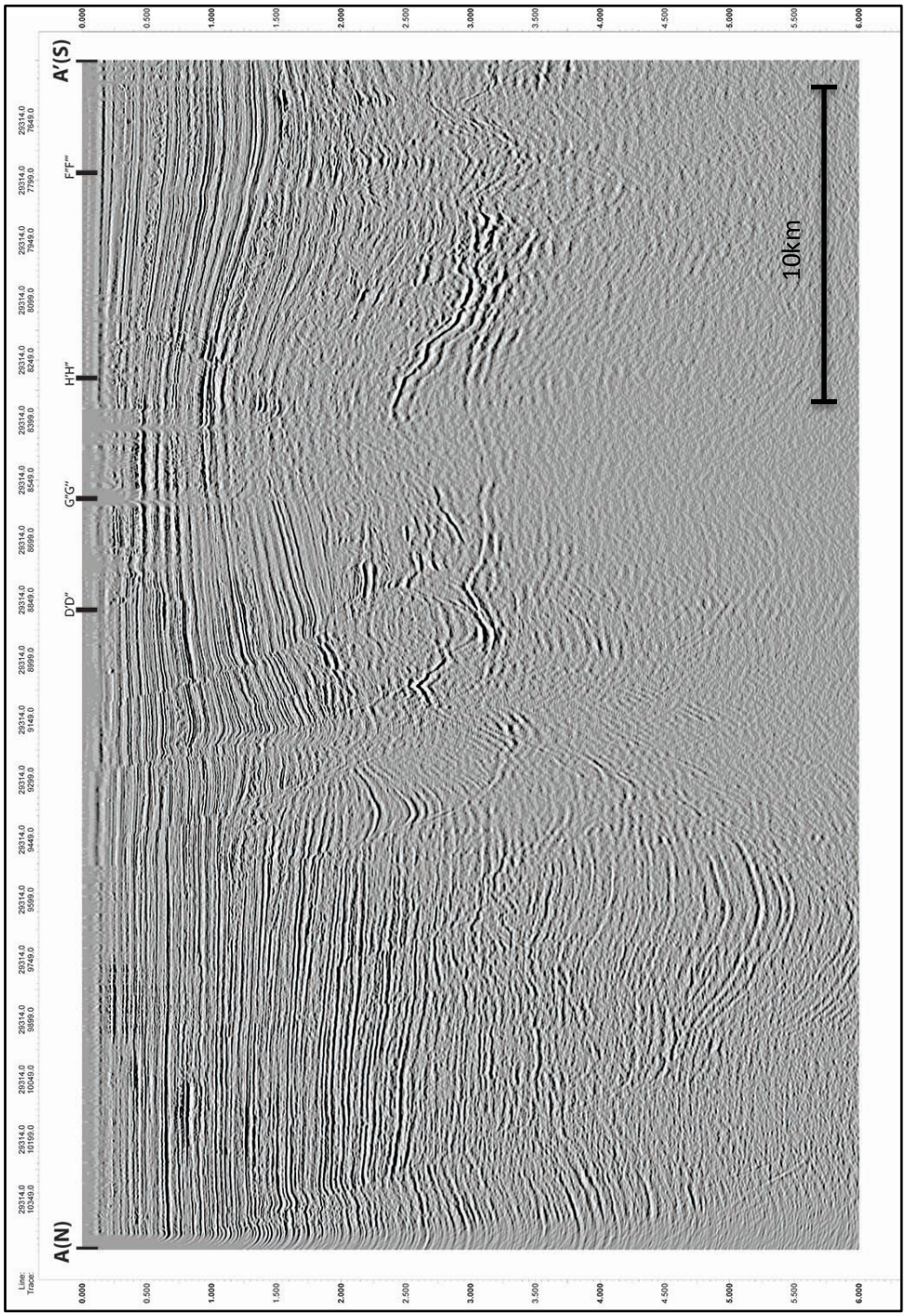

Figure 16: A-A' Cross section without interpretation. D'D'', G'G'', H'H'', and F''F''' are the intersecting point of other cross sections.

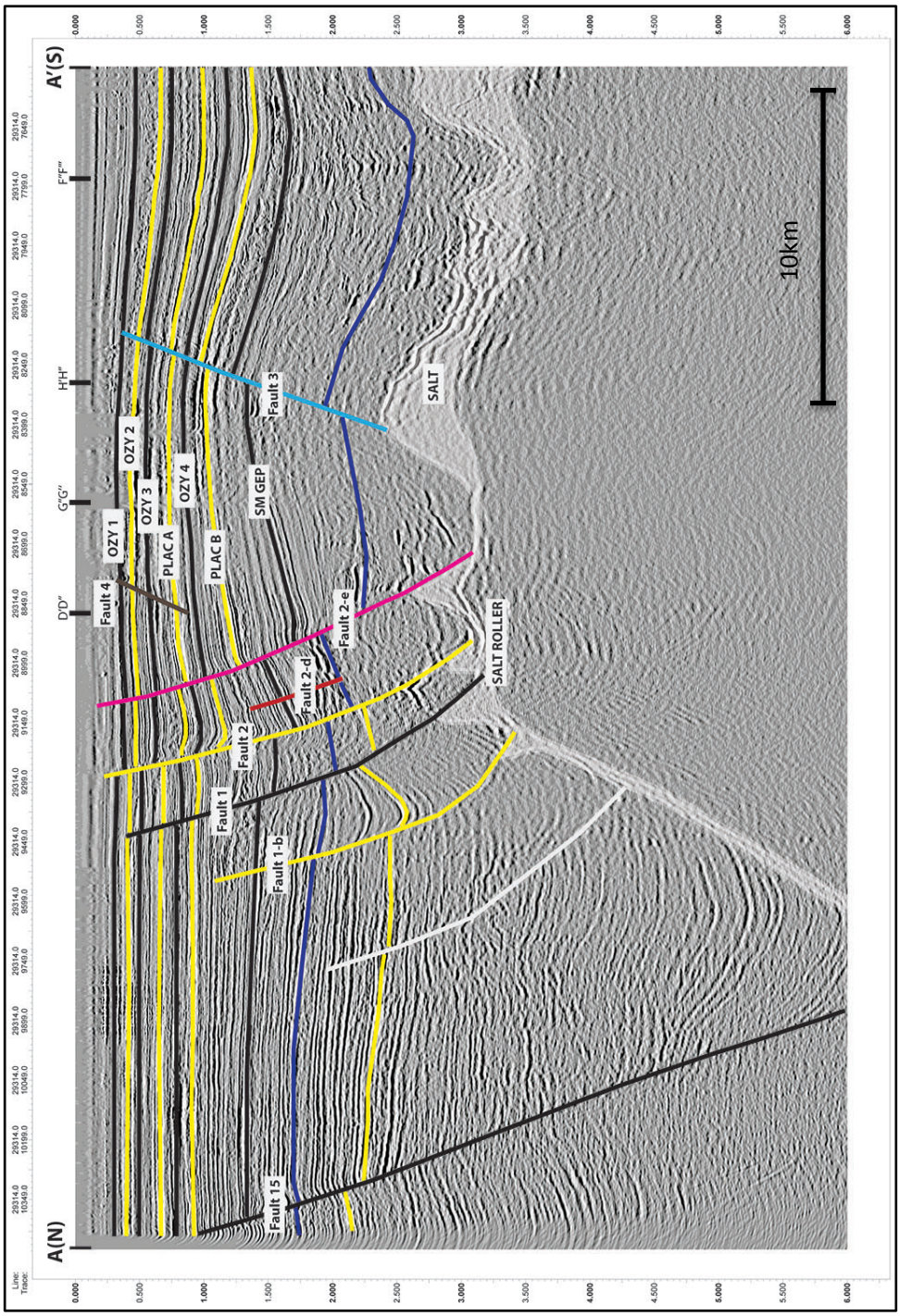

Figure 17: A-A' Cross section with faults and horizons. D'D'', G'G'', H'H'', and F''F''' are the intersecting point of other cross sections.

Horizon Interpretation:

Total sedimentary thickness increases from south to north in this cross section.

Horizons	Faults cutting horizon
OZY1	fault 2, fault 2-e, fault 4, fault 3
OZY2	fault 1, fault 2, fault 2-e, fault 4, fault 3
OZY3	fault 1, fault 2, fault 2-e, fault 4, fault 3
Plac A (0.46Ma)	fault 1, fault 2, fault 2-e, fault 4, fault 3
OZY4	fault 1, fault 2, fault 2-e, fault 3
Plac B (0.65Ma)	fault 1, fault 2, fault 2-e, fault 3
Sm Gep (0.9 Ma)	fault 15, fault 1, fault 2, fault 2-e, fault 3

Table 2: Table 2 shows horizon interpretation in cross section AA' from north to south direction.

Fault Interpretation:

Fault 15: This fault is a concave-basinward normal fault. The hanging wall of this fault contains a basinward-tilted inconspicuous rollover structure with growth section such that displacement slightly increases downward.

Fault 1-b: This fault is a concave-basinward normal fault. The hanging wall of this fault contains a landward-tilted prominent rollover structure with expanded growth section such that displacement increases downward and strata thicken landward. Fault 1-b soles into a salt roller. The age of growth strata in the fault 1-b hanging walls indicates that salt withdrawal occurred during the Pleistocene.

Fault 1: This fault is a concave-basinward normal fault. Fault 1 roots into a salt roller. Fault 1 consists of at least two major linked segments. Cross section AA' shows one of the linked points of this fault. A detailed interpretation will be done in the D*L plots chapter.

Fault 2: This fault is a concave-basinward normal fault. The hanging wall of this fault contains a landward-tilted prominent rollover structure with expanded growth section such that displacement increases downward and strata thickens landward. Fault 2 soles into a salt roller. The age of growth strata in the fault 2 hanging wall indicates that salt withdrawal occurred during the Pleistocene. Fault 2 consists of at least two major linked segments which will be interpreted in detail within the D*L plots chapter.

Fault 2-d: This fault is a concave-basinward normal fault that links fault 2 and fault 2-e. A detailed interpretation will be done in D*L plots chapter.

Fault 2-e: This fault is a concave-basinward normal fault. The hanging wall of this fault contains a landward-tilted prominent rollover structure with an expanded growth section such that displacement increases downward and strata thicken landward until the Sm Gap horizon. Fault 2-e soles into a salt roller. The age of growth strata in the normal fault hanging walls indicates that salt withdrawal occurred during the Pleistocene. Fault 2-e consists of at least two major linked segments that will be interpreted in detail in the D*L plots chapter.

Fault 4: This fault is a synthetic fault of fault 2-e.

Fault 3: This fault is a slightly concave counter-regional normal fault. This fault merges with a salt body. Between fault 2-e and fault 3, a dome-shaped structure is observed below the horizon Ozy 3. This dome-shaped structure is also observed in a 3D illustration of the Plac A horizon.

Salt Interpretation: The southern part of the salt body was interpreted based on publicly available well data and high amplitude seismic reflection. The fact that most of the faults in the study area sole into salt, implies that the kinematics of salt deformation are the same or at least similar to the kinematics of faulting.

Uninterpreted and interpreted north-south-oriented seismic cross sections BB' can be seen in figures 18-19 (see figure 11-15 for location). The BB' cross section interpretation will be discussed in this chapter.

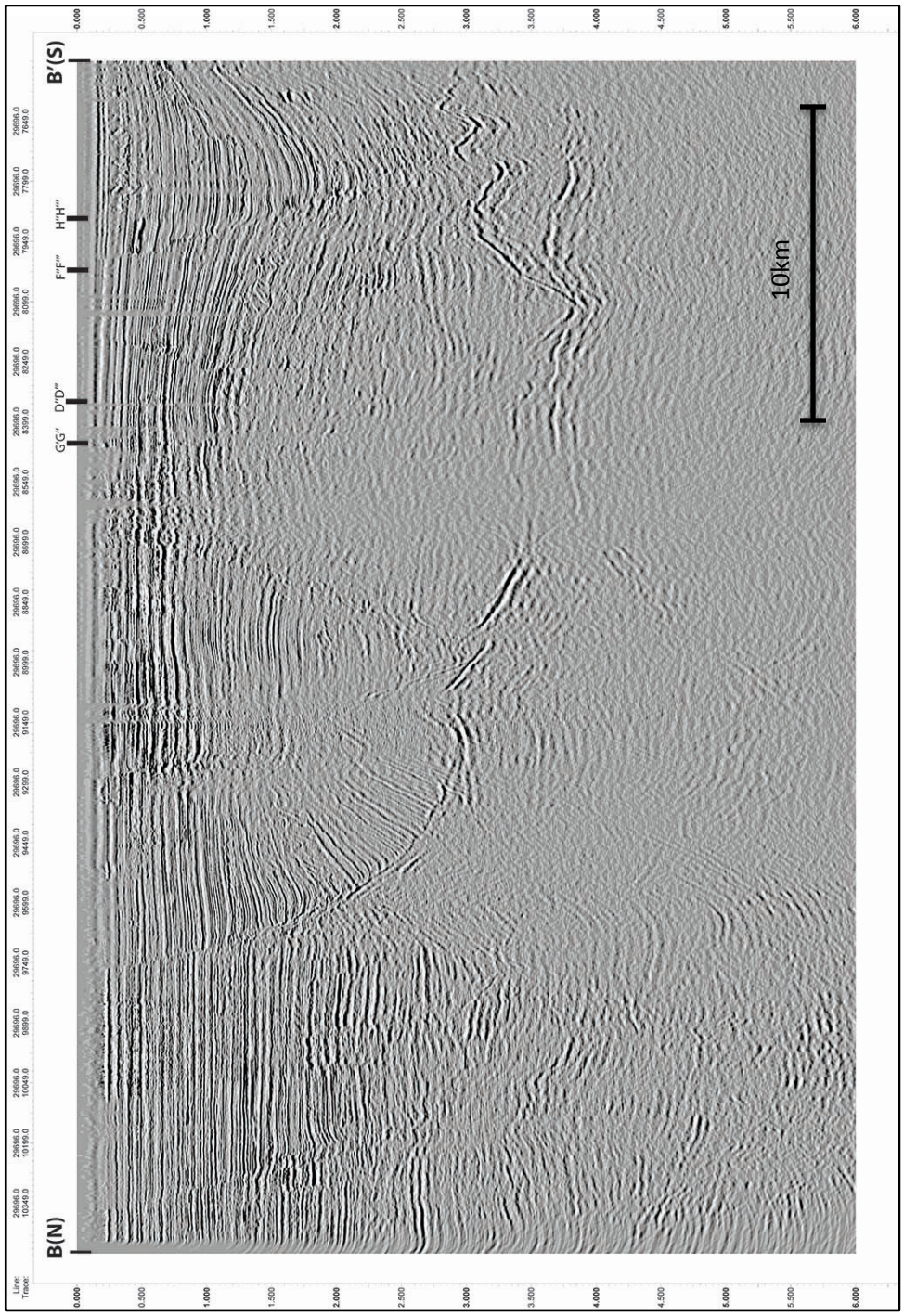

Figure 18: B-B' Cross section without interpretation. G'G'', D''D''', F''F''', and H''H''' are the intersecting point of other cross sections.

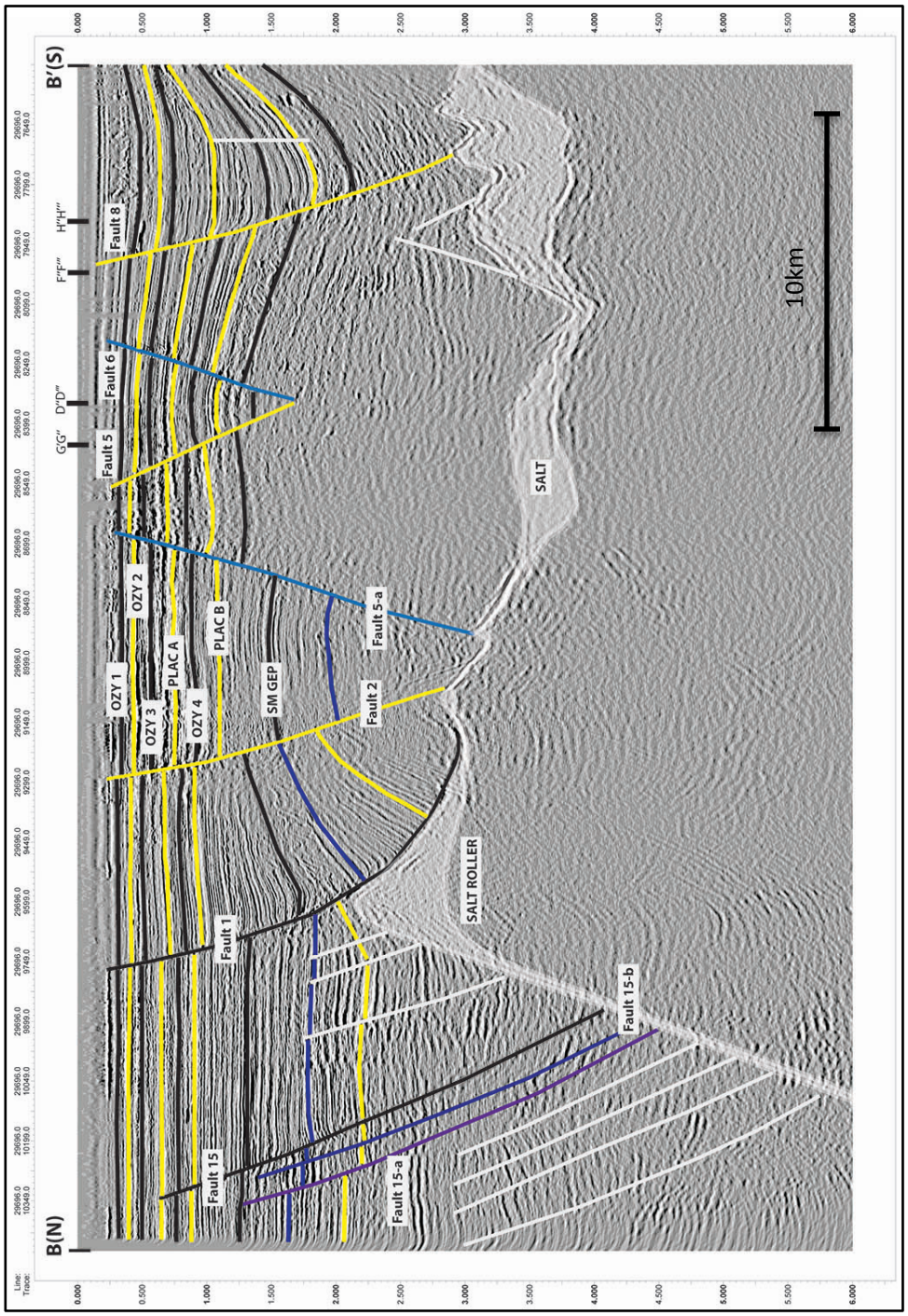

Figure 19: B-B' Cross section with faults and horizons. G'G'', D''D''', F''F''', and H''H''' are the intersecting point of other cross sections.

Horizon interpretation:

Total sedimentary thickness increases from south to north in this cross section.

Horizons	Faults cutting horizon
OZY1	fault 1, fault 2, fault 5-a, fault 6, fault 8
OZY2	fault 1, fault 2, fault 5-a, fault 6, fault 8
OZY3	fault 1, fault 2, fault 5-a, fault 6, fault 8
Plac A (0.46Ma)	fault 15, fault 1, fault 2, fault 5-a, fault 6, fault 8
OZY4	fault 15, fault 1, fault 2, fault 5-a, fault 6, fault 8
Plac B (0.65Ma)	fault 15, fault 1, fault 2, fault 5-a, fault 6, fault 8
Sm Gep (0.9 Ma)	fault 15, fault 1, fault 2, fault 5-a, fault 6, fault 8

Table 3: Table 3 shows horizon interpretation in cross section BB' from north to south direction.

Fault interpretation:

Fault 15-a: This fault is a slightly concave-basinward normal fault. The fault 15-a is one of the linked segments of fault 15.

Fault 15-b: This fault is a slightly concave-basinward normal fault. The fault 15-b is one of the linked segments of fault 15. Relationship between Fault 15, fault 15-a, and fault 15 b will be discussed in a later chapter.

Fault 15: This fault is a concave-basinward normal fault. The hanging wall of this fault contains a basinward-tilted inconspicuous roller structure with growth section.

Fault 1: This fault is a concave-basinward normal fault. The hanging wall of this fault contains a landward-tilted prominent rollover structure with an expanded growth section such that displacement increases downward and strata thickens landward. Fault 1 soles into a salt roller.

The age of growth strata in the fault 1 hanging walls indicates that salt withdrawal occurred during the Pleistocene. Detailed interpretation will be done in the D*L plots chapter.

Fault 2: This fault is a concave-basinward normal fault. Fault 2 soles into a salt weld. The growth strata of fault 2 could not be observed in this cross section. A detailed interpretation will be done in D*L plots chapter.

Fault 5-a: This fault is a counter-regional normal fault. Between fault 2 and fault 5-a, a dome-shaped structure is observed below the horizon Plac A. This dome-shaped structure is also observed on 3D illustration of the Plac A horizon (Figure 32).

Fault 5: This fault is a concave-basinward normal fault. The dome-shaped structure is also observed between fault 5 and fault 6 on the 3D illustration of Plac A horizon.

Fault 6: This fault is a planar counter-regional normal fault.

Fault 8: This fault is a concave-basinward normal fault. The hanging wall of this fault contains a landward-tilted prominent rollover monocline with expanded growth section such that displacement increases downward and strata thickens landward. Fault 8 merges with a salt body.

Salt interpretation: The southern part of the salt body was interpreted based on publicly available well data and high amplitude seismic reflection. The fact that most of the faults in the study area sole into salt, implies that the kinematics of salt deformation are the same or at least similar to the kinematics of faulting.

Uninterpreted and interpreted north-south-oriented seismic cross sections CC' can be seen in figures 20-21 (see figure 11-15 for location). The CC' cross section interpretation will be discussed in this chapter.

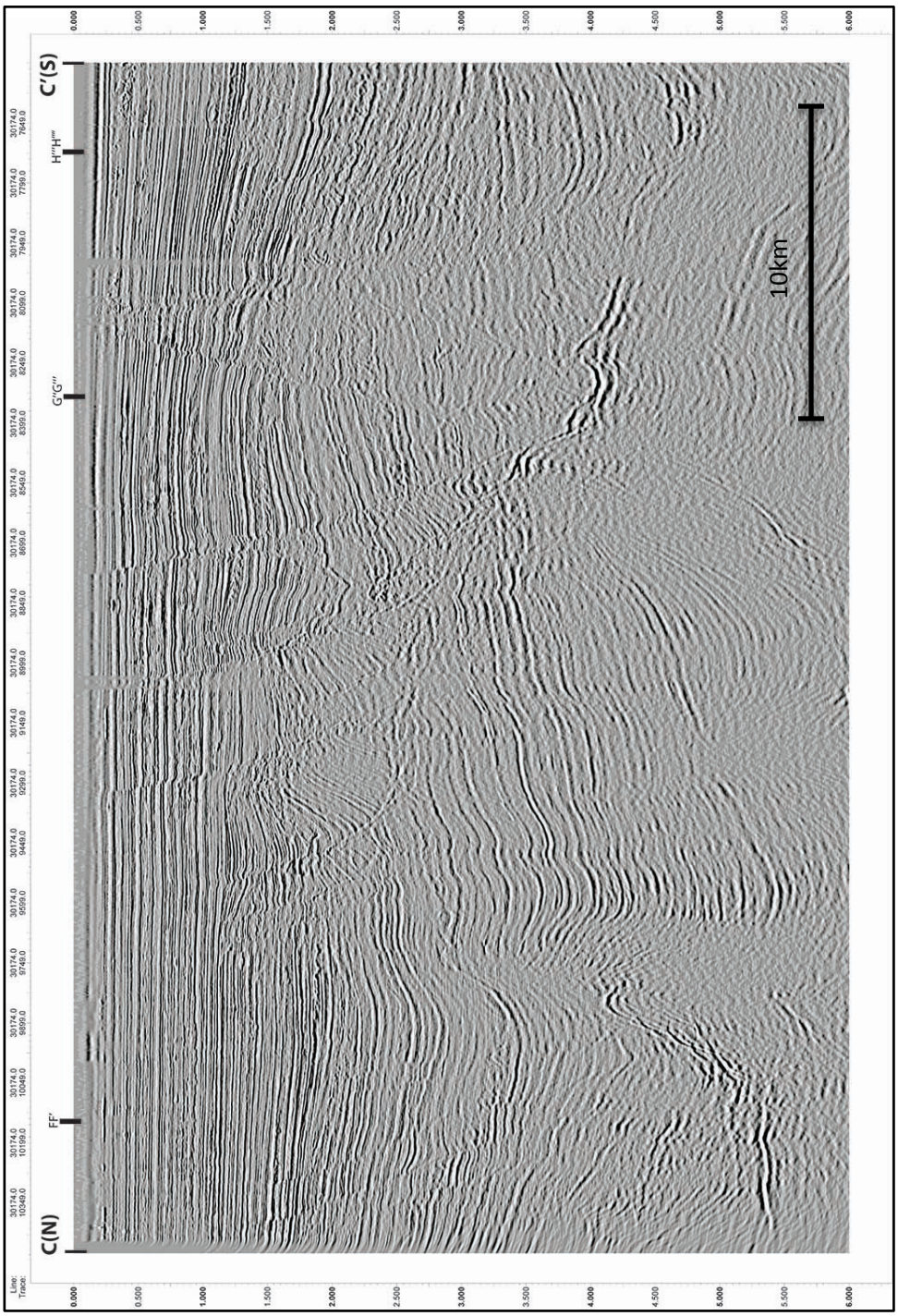

Figure 20: C-C' Cross section without interpretation. G'G'', F''F'',' and H''H''' are the intersecting point of other cross sections.

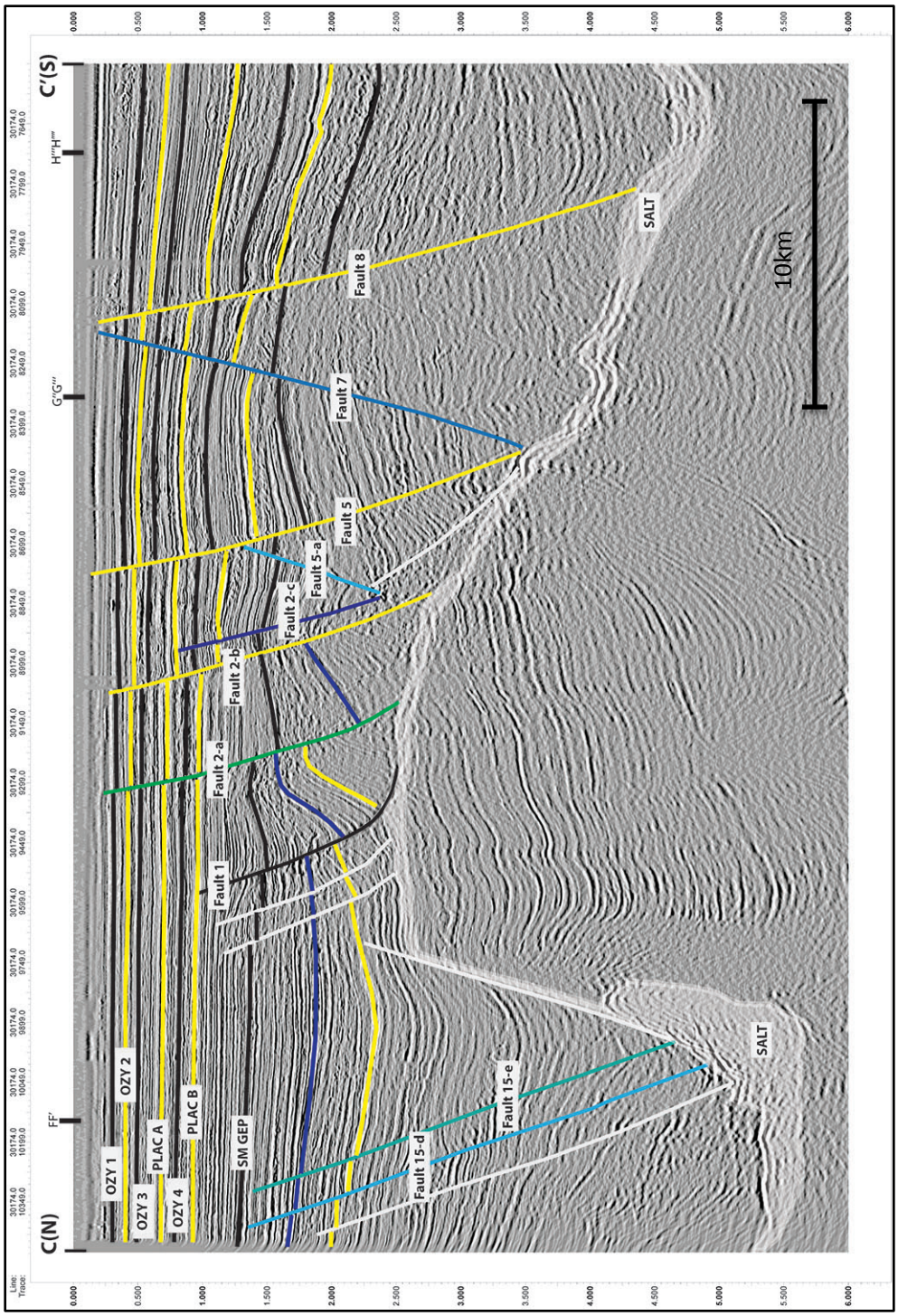

Figure 21: C-C' Cross section with faults and horizons. G'G'', F''F''', and H''H''' are the intersecting point of other cross sections.

Horizon interpretation:

Total sedimentary thickness increases from south to north in this cross section. Cross sections AA', BB' and CC' are parallel to each other's. The northern part of these cross sections shows that sediment thickness increases from east to west.

Horizons	Faults cutting horizon
OZY1	fault 2-a, fault 2-b, fault 5, fault 7, fault 8
OZY2	fault 2-a, fault 2-b, fault 5, fault 7, fault 8
OZY3	fault 2-a, fault 2-b, fault 5, fault 7, fault 8
Plac A (0.46Ma)	fault 2-a, fault 2-b, fault 2-c, fault 5, fault 7, fault 8
OZY4	fault 2-a, fault 2-b, fault 2-c, fault 5, fault 7, fault 8
Plac B (0.65Ma)	fault 1, fault 2-a, fault 2-b, fault 2-c, fault 5, fault 7, fault 8
Sm Gep (0.9 Ma)	fault 1, fault 2-a, fault 2-b, fault 2-c, fault 5-a, fault 5, fault 7, fault 8

Table 4: Table 4 shows horizon interpretation in cross section CC' from north to south direction.

Fault interpretation:

Fault 15-d and Fault 15-e: Fault 15-d and fault 15-e are slightly concave-basinward normal faults. They merge with a salt body. Time-structure map shows high interaction between fault 15, fault 15-a, fault 15-b, fault 15c, 15-d, and 15-e. It will be discussed in a later chapter.

Fault 1: This fault is a concave-basinward normal fault. The hanging wall of this fault contains a landward-tilted prominent rollover structure with expanded growth section such that displacement increases downward and strata thickens landward. Fault 1 soles into a salt roller. The age of growth strata in the fault 1 hanging wall indicates that salt withdrawal occurred during the Pleistocene.

Fault 2-a: This fault is a concave-basinward normal fault. The hanging wall of this fault contains a landward-tilted rollover structure with expanded growth section such that displacement increases downward and strata thicken landward. Fault 2-a merge with a salt weld.

Fault 2-b: This fault is a concave-basinward normal fault and merges with a salt weld.

Fault 2-c: This fault is a concave-basinward normal fault. The hanging wall of this fault contains basinward-tilted sediments.

Fault 5-a: This fault is a counter-regional normal fault.

Fault 5: This fault is a concave-basinward normal fault and merges with a salt weld. The hanging wall of the fault 5 contains a landward-tilted rollover structure with slightly expanded growth section such that displacement increases downward and strata thicken landward.

Fault 7: This fault is a counter-regional normal fault and merges with a salt weld**.** Hanging wall of this fault contains landward dipping sediments.

Fault 8: This fault is a concave-basinward normal fault and merges with a salt body. The hanging wall of this fault contains a basinward-dipping monocline.

Salt interpretation: The northern part of salt body acts as a salt feeder as seen in cross section CC'. The southern part of the salt body was interpreted based on publicly available well data and high amplitude seismic reflection. The fact that most of the faults in the study area sole into salt, implies that the kinematics of salt deformation are the same or at least similar to the kinematics of faulting.

Uninterpreted and interpreted northwest-southeast-oriented seismic cross sections DD''' can be seen in figure 22-23 (see figure 11-15 for location). DD''' cross section contains three arbitrary cross-lines (DD', D'D", and D"D'''), whose interpretation will be discussed in this chapter.

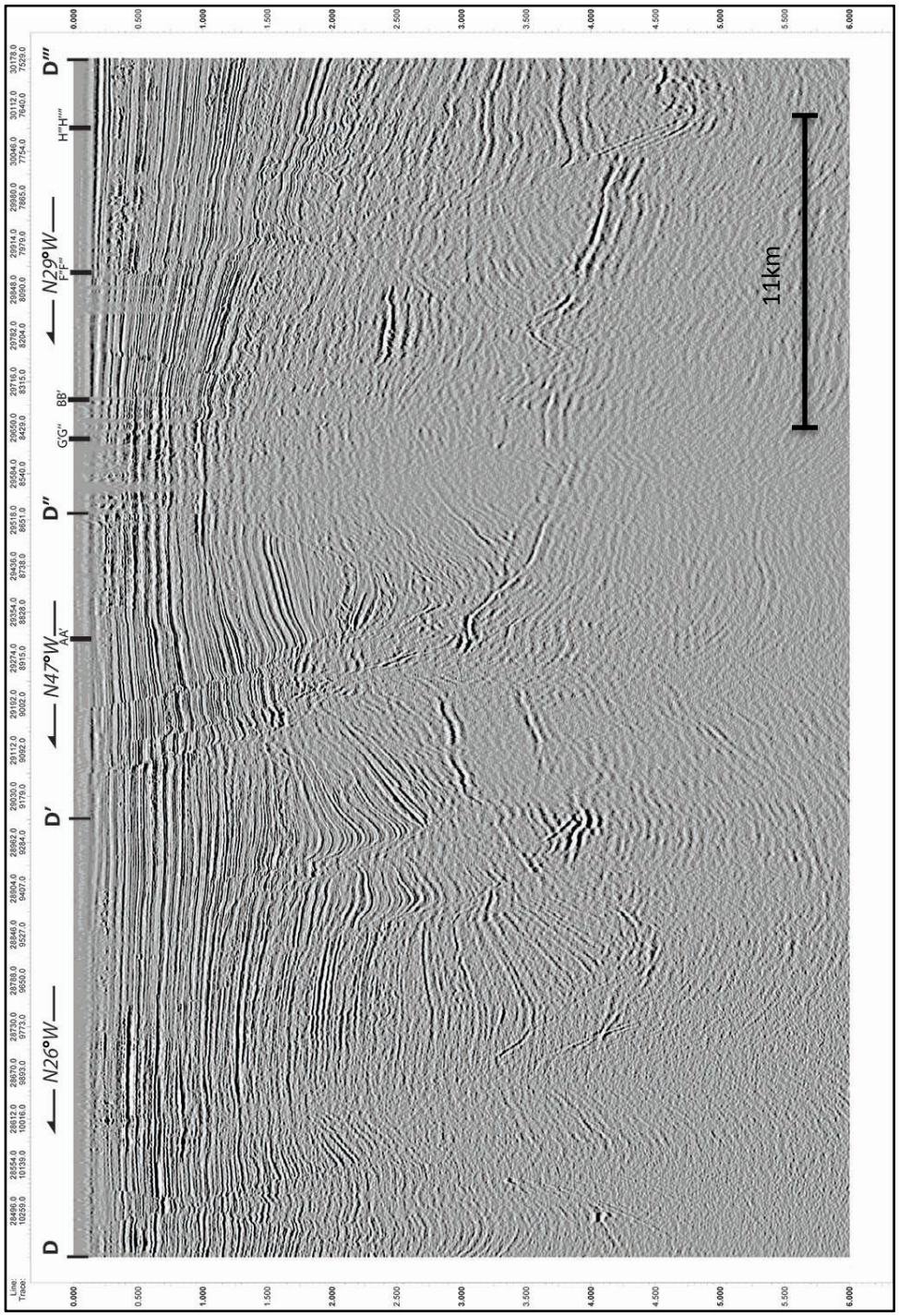

Figure 22: D-D''' Cross section without interpretation. G'G'', BB', F''F''', and H'''H'''' are the intersecting point of other cross sections.

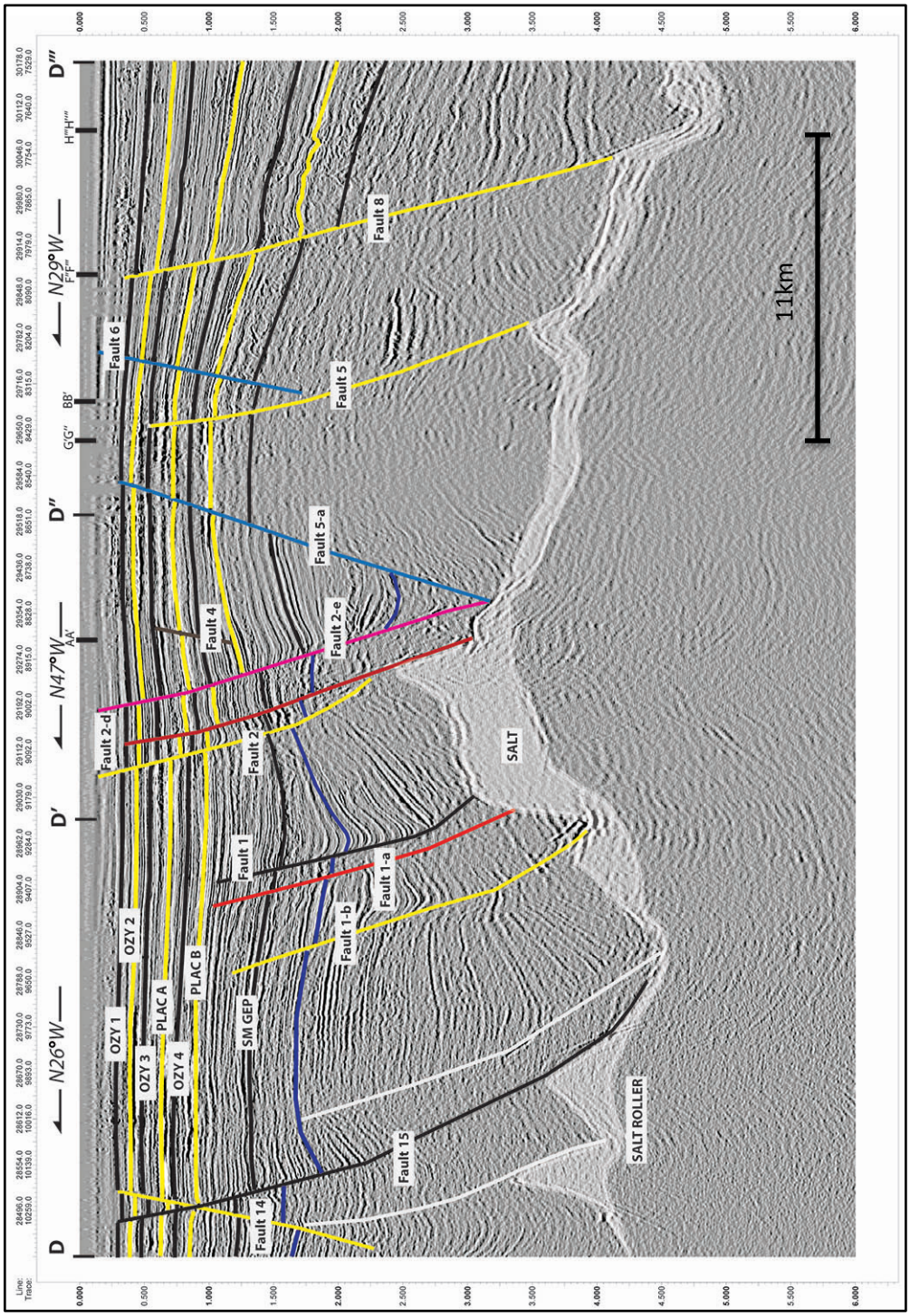

Figure 23: D-D''' Cross section with faults and horizons. G'G'', BB', F''F''', and H'''H'''' are the intersecting point of other cross sections.

Horizon interpretation:

Horizons	Faults cutting horizon
OZY1	fault 15, fault 14, fault 2, fault 2-d, fault 2-e, fault 5-a, fault 6, fault 8
OZY2	fault 15, fault 14, fault 2, fault 2-d, fault 2-e, fault 5-a, fault 6, fault 8
OZY3	fault 15, fault 14, fault 2, fault 2-d, fault 2-e, fault 4, fault 5-a, fault 6, fault 8
Plac A (0.46Ma)	fault 15, fault 14, fault 2, fault 2-d, fault 2-e, fault 4, fault 5-a, fault 6, fault 8
OZY4	fault 15, fault 14, fault 2, fault 2-d, fault 2-e, fault 4, fault 5-a, fault 5, fault 6, fault 8
Plac B (0.65Ma)	fault 15, fault 14, fault 2, fault 2-d, fault 2-e, fault 5-a, fault 5, fault 6, fault 8
Sm Gep (0.9 Ma)	fault 14, fault 15, fault 1-b, fault 1-a, fault 2, fault 2-d, fault 2-e, fault 5-a, fault 5, fault 6 fault 8

Table 5: Table 5 shows horizon interpretation in cross section DD''' from northwest to southeast direction.

Fault interpretation:

Fault 14: This fault is a concave counter-regional normal fault.

Fault 15: This fault is a concave-basinward normal fault. The hanging walls of this fault contain basinward-tilted roller structure with a growth section that starts after the Sm Gep horizon. This implies that this fault was active during Pleistocene age (0.9 Ma). Fault 15 soles into a salt roller.

Fault 1-b: This fault is a concave-basinward normal fault. The hanging wall of this fault contains a landward-tilted rollover structure with expanded growth section such that displacement increases downward and strata thickens landward. The fault 1-b soles into a salt roller

Fault 1-a: This fault is a concave-basinward normal fault and merges with a salt body. The fault 15-b is one of the linked segments of the fault 15.

Fault 1: This fault is a concave-basinward normal fault. The hanging wall of this fault contains a landward-tilted prominent rollover structure with an expanded growth section such that displacement increases downward and strata thickens landward. Fault 1 merges with a salt body. The age of growth strata in the fault 1 hanging walls indicates that salt withdrawal occurred during the Pleistocene. Detailed interpretation will be done in the D*L plots chapter.

Fault 2: This fault is a concave-basinward normal fault. Fault 2 merges with fault 2-d; a detailed interpretation will be done in the D*L plots chapter.

Fault 2-d: This fault is a concave-basinward normal fault. Fault 2-d soles into a salt body. Fault 2 and fault 2-e are linked by fault 2-d. A detailed interpretation will be done in the D*L plots chapter.

Fault 2-e: This fault is a concave-basinward normal fault and merges with a salt weld. The hanging walls of fault 2-e contains a landward-tilted rollover structure. A detailed interpretation will done in the D*L plots chapter.

Fault 4: This fault is a synthetic fault of fault 2-e.

Fault 5-a: This fault is a counter-regional normal fault. Between fault 2 and fault 5-a, a dome-shaped structure is observed below the Plac A horizon. This dome-shaped structure is also observed on 3D illustration of Plac A horizon (Figure 32). Fault 5-a merges with a salt weld.

Fault 5: This fault is a concave-basinward normal fault and merges with a salt weld. The dome-shaped structure is also observed between fault 5 and fault 6 on the 3D illustration of Plac A horizon (Figure 32).

Fault 6: This fault is a planar counter-regional normal fault.

Fault 8: This fault is a concave-basinward normal fault and merges with a salt weld. The hanging wall of this fault contains basinward-dipping sedimentation.

Salt interpretation: The middle part of the salt body was interpreted based on publicly available well data and high amplitude seismic reflection. The fact that most of the faults in the study area sole into salt, implies that the kinematics of salt deformation are the same or at least similar to the kinematics of faulting.

Uninterpreted and interpreted northwest-southeast-oriented seismic cross sections EE'' can be seen in figure 24-25 (see figure 11-15 for location). EE" cross section contains 2 arbitrary cross-lines, EE' and E'E", whose interpretation will be discussed in this chapter.

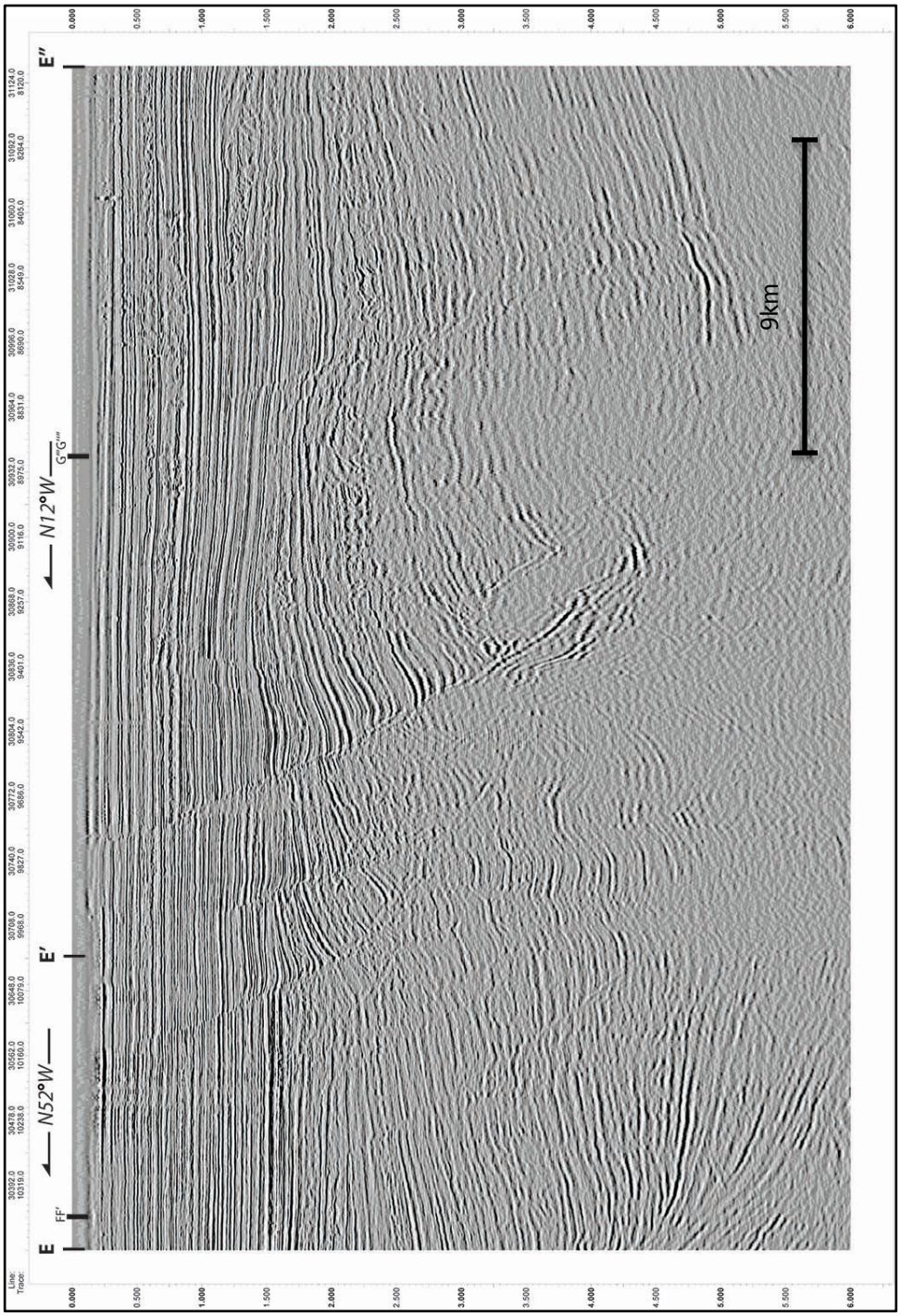

Figure 24: E-E'' Cross section without interpretation. FF', and G'''G'''' are the intersecting point of other cross sections.

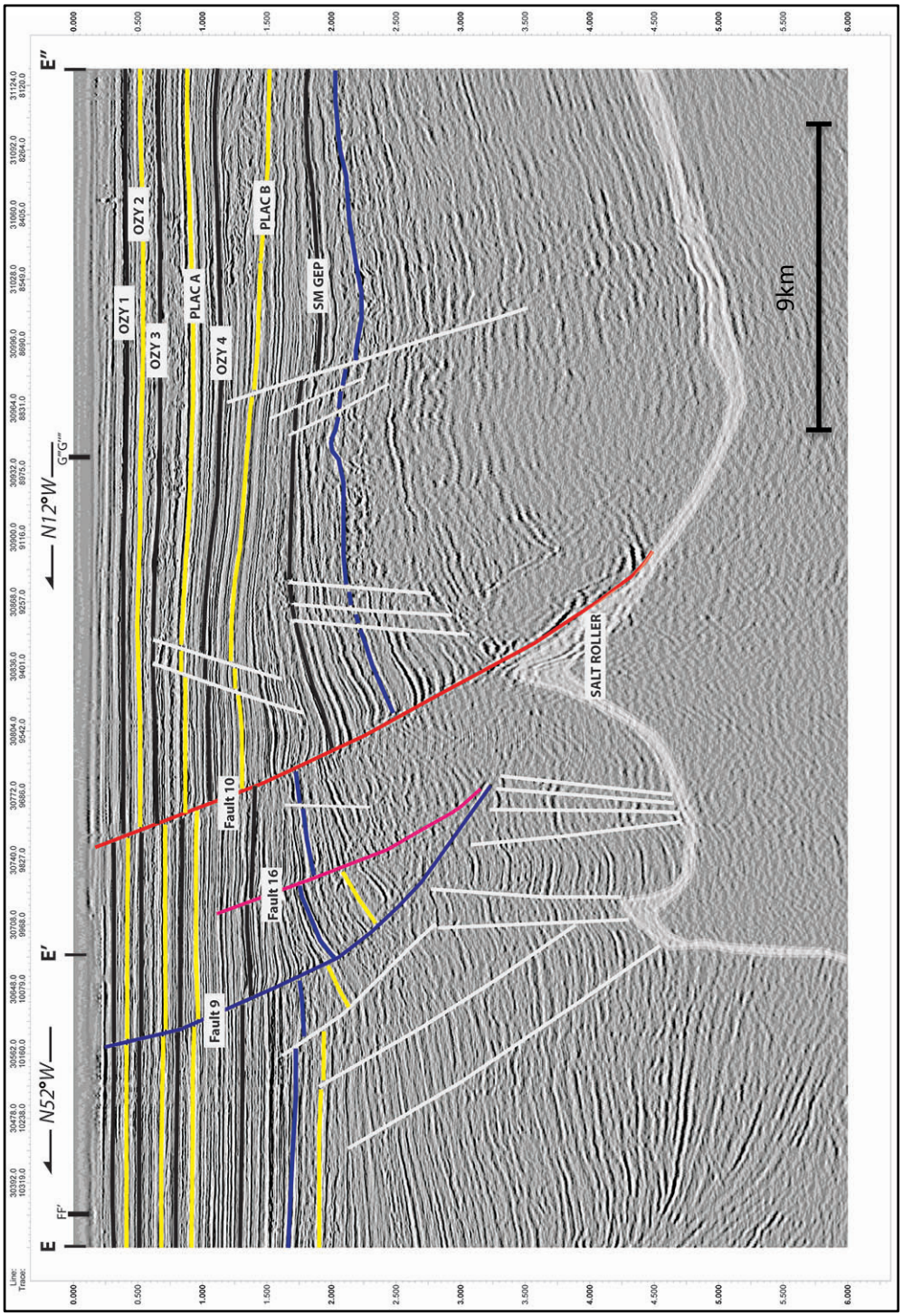

Figure 25: E-E'' Cross section with faults and horizons. FF', and G'''G'''' are the intersecting point of other cross sections.

Horizon interpretation:

Total sedimentary thickness increases from south to north in this cross section.

Horizons	Faults cutting horizon
OZY1	fault 9, fault 10
OZY2	fault 9, fault 10
OZY3	fault 9, fault 10,
Plac A (0.46Ma)	fault 9, fault 10
OZY4	fault 9, fault 10,
Plac B (0.65Ma)	fault 9, fault 10
Sm Gep (0.9 Ma)	fault 9, fault 16, fault 10

Table 6: Table 6 shows horizon interpretation in cross section EE'' from north to south direction.

Fault interpretation:

Fault 9: This fault is a slightly concave-basinward normal fault. The hanging walls of this fault contain a basinward-tilted roller structure with growth section that starts after the Sm Gep horizon. This implies that this fault was active during Pleistocene age (0.9 Ma).

Fault 16: This fault is a concave-basinward normal fault. The hanging wall of this fault contains a slightly landward-tilted rollover structure with expanded growth section such that displacement increases downward and strata thicken landward.

Fault 10: This fault is a concave-basinward listric normal fault. The hanging walls of this fault contain basinward-tilted roller structures with a growth section. The hanging wall of fault 10 has a rollover fault family with dip directions antithetic to fault 10. Also, rollover strata and roller

fault have the same dip direction. In cross section, they are planar and they do not reach downward into salt.

Salt interpretation: Fault 10 has a triangular salt roller in its footwall.

Uninterpreted and interpreted north-south-oriented seismic cross sections FF’’’ can be seen in figure 26-27 (see figure 11-15 for location). FF’’’ cross section contains four arbitrary cross-lines (FF’, F’F’’, F’’F’’’, and F’’’F’’’’). The FF’’’ cross section interpretation will be discussed in this chapter.

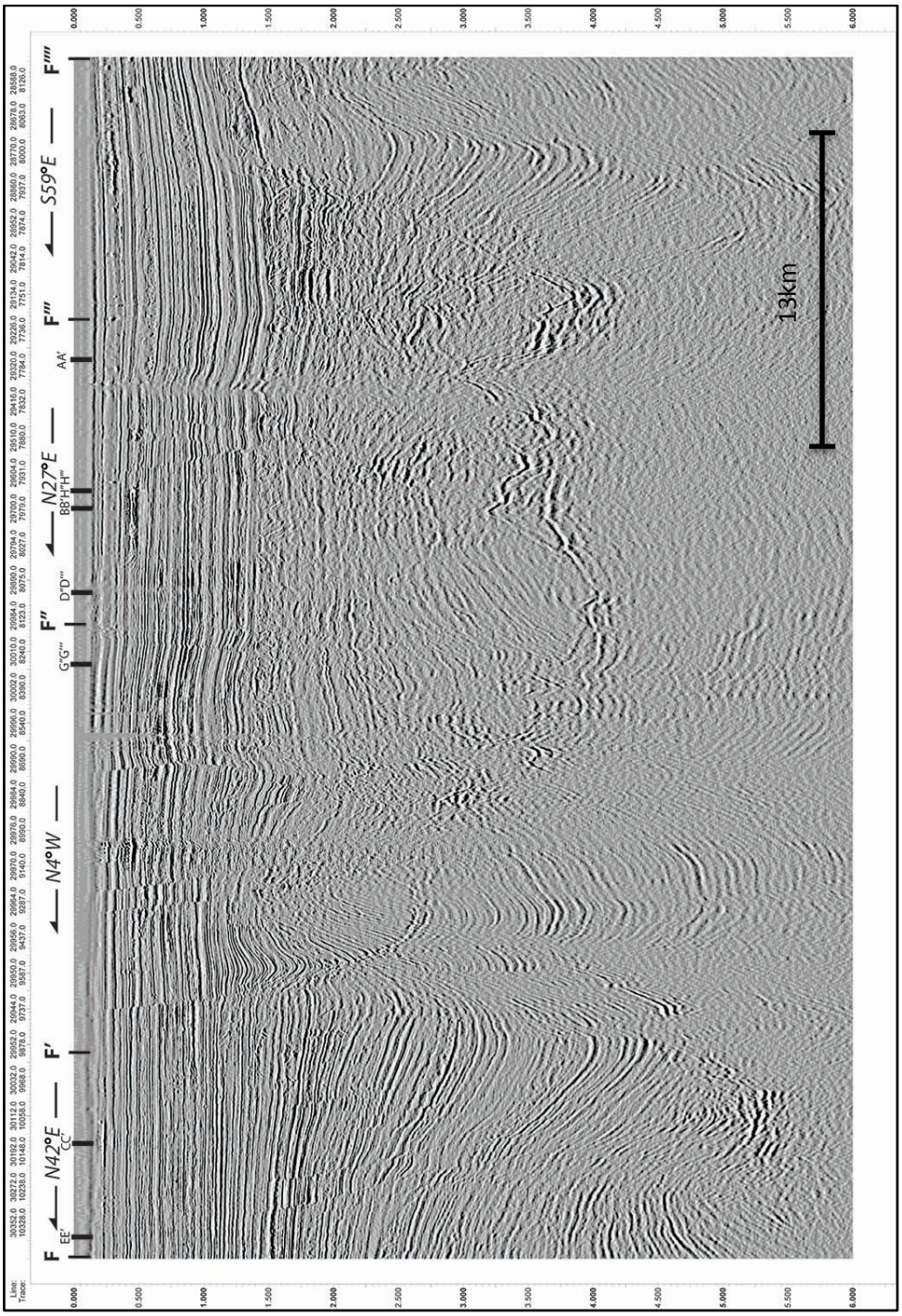

Figure 26: F-F’’’’ Cross section without interpretation. EE’, CC’, D’’D’’’, BB’, H’’H’’’, and AA’ are the intersecting point of other cross sections.

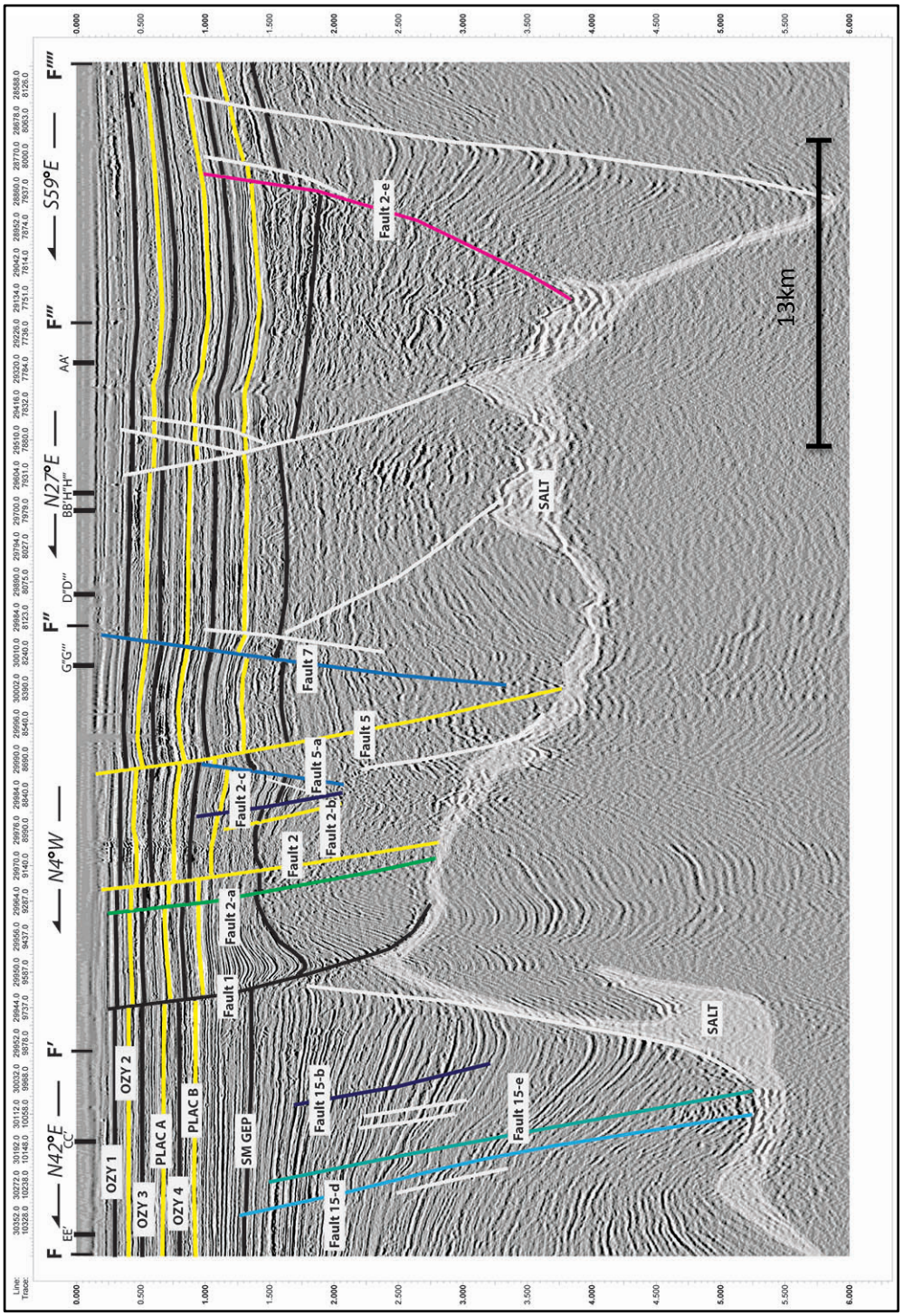

Figure 27: F-F'''' Cross section with faults and horizons. EE', CC', D''D''', BB', H''H''', and AA' are the intersecting point of other cross sections.

Horizon interpretation:

Horizons	Faults cutting horizon
OZY1	fault 1, fault 2-a, fault 2, fault 5, fault 7
OZY2	fault 1, fault 2-a, fault 2, fault 5, fault 7
OZY3	fault 1, fault 2-a, fault 2, fault 5, fault 7
Plac A (0.46Ma)	fault 1, fault 2-a, fault 2, fault 5, fault 7
OZY4	fault 1, fault 2-a, fault 2, fault 5, fault 7, fault 2-e
Plac B (0.65Ma)	fault 1, fault 2-a, fault 2, fault 2-c fault 5-a, fault 5, fault 7 fault 2-e
Sm Gep (0.9 Ma)	fault 15-d, fault 1, fault 2-a, fault 2, fault 2-b fault 2-c, fault 5-a, fault 5, fault 7, fault 2-e

Table 7: Table 7 shows horizon interpretation in cross section FF'''' from north to south direction.

Fault interpretation:

Fault 15-d and Fault 15-e: The fault 15-d and fault 15-e is a slightly concave-basinward normal fault. These faults merge with a salt body. The time-structure map shows high interaction between fault 15, fault 15-a, fault 15-b, fault 15c, 15-d, and 15-e. It will be discussed in later chapter.

Fault 15-b: This fault is a slightly concave-basinward normal fault. The fault 15-b is one of the linked segments of the fault 15.

Fault 1: This fault is a concave-basinward normal fault. The hanging wall of this fault contains a landward-tilted prominent rollover structure with expanded growth section such that displacement increases downward and strata thickens landward. Fault 1 soles into a salt roller. The age of growth strata in the fault 1 hanging wall indicates that salt withdrawal occurred during the Pleistocene. Detailed interpretation will be done in the D*L plots chapter.

Fault 2-a: In this cross section, the fault 2-a is a planar-basinward normal fault and merges with a salt weld.

Fault 2: In this cross section, fault 2 is a planar-basinward normal fault. Fault 2 merges with a salt weld. Detailed interpretation will be discussed in the D*L plots chapter.

Fault 2-b: In this cross section, the fault 2-b is a planar-basinward normal fault.

Fault 2-c: In this cross section, the fault 2-c is a planar-basinward normal fault.

Fault 5-a: In this cross section, the fault 5-a is a planar-landward normal fault.

Fault 5: In this cross section, the fault 5 is a planar-basinward normal fault and merges with a salt weld.

Fault 7: The fault 7 is a planar-landward normal fault.

Fault 2-e: This fault is a concave-basinward normal fault. The hanging wall of this fault contains a landward-tilted prominent rollover structure with expanded growth section such that displacement increases downward and strata thicken landward. Fault 2-e merges with a salt body.

Salt interpretation: Northern part of salt body acts as a salt feeder in cross section FF’’’. Salt bodies and a salt weld were interpreted based on publicly available well data and high amplitude seismic reflections. The fact that most of the faults in the study area sole into salt, implies that the kinematics of salt deformation are the same or at least similar to the kinematics of faulting.

Uninterpreted and interpreted west-east-oriented seismic cross sections GG’’’ can be seen in figure 28-29 (see figure 11-15 for location). GG’’’ cross section contains four arbitrary cross-lines (GG’, G’G’’, G’’G’’’, and G’’’G’’’). The GG’’’ cross section interpretation will be discussed in this chapter.

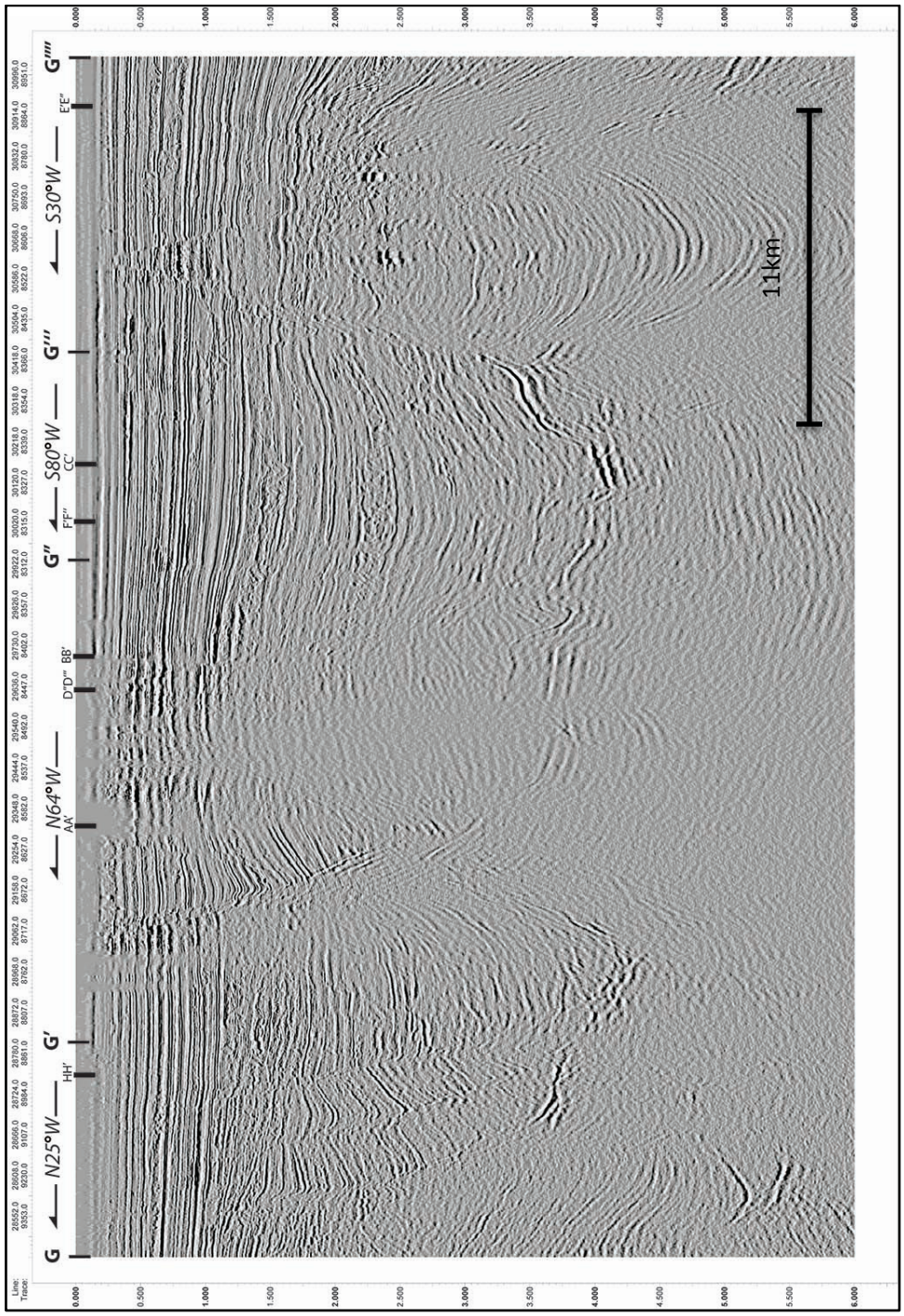

Figure 28: G-G'''' Cross section without interpretation. EE', CC', D''D''', BB', H''H''', and AA' are the intersecting point of other cross sections.

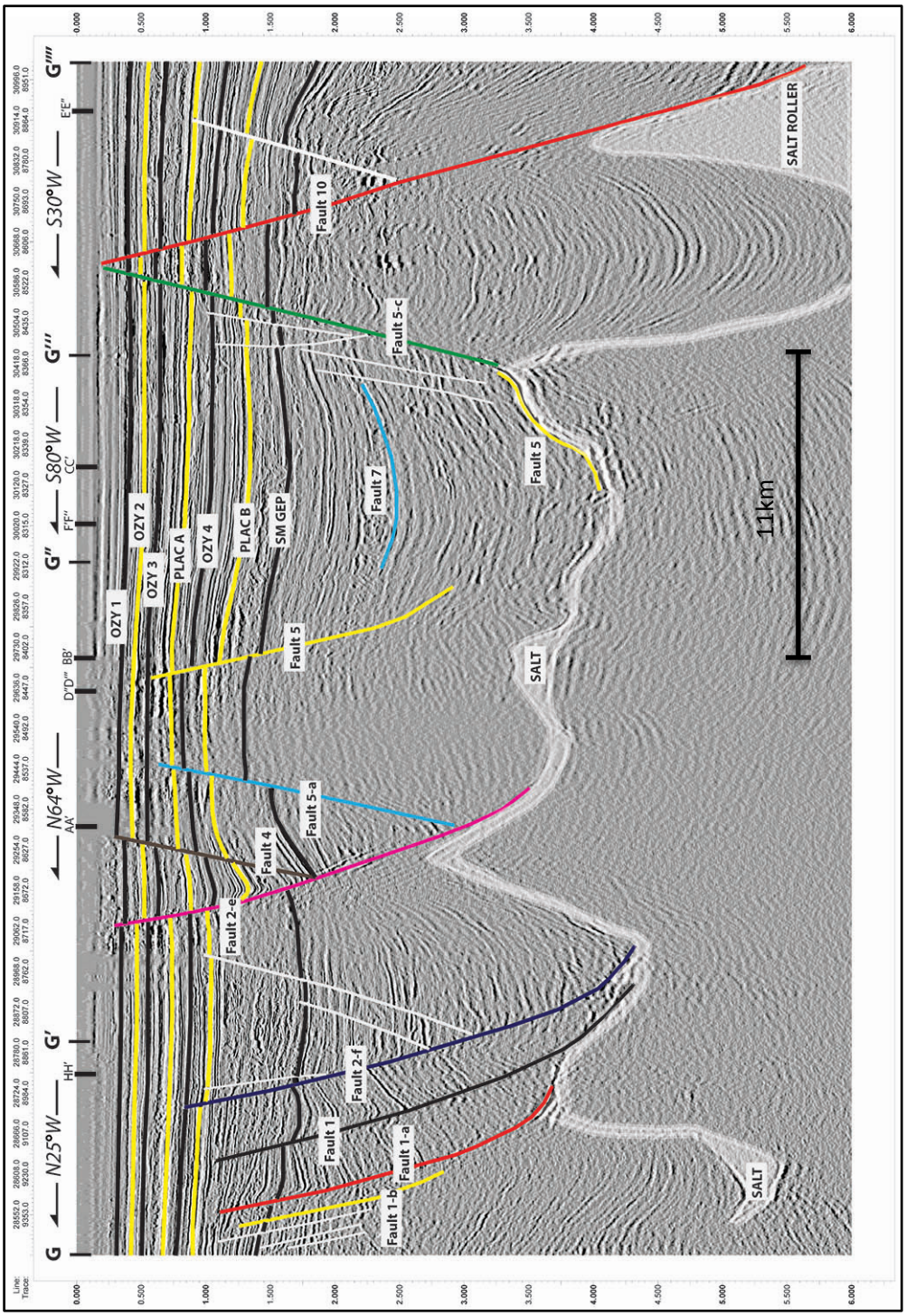

Figure 29: G-G'''' Cross section with faults and horizons. EE', CC', D''D''', BB', H''H''', and AA' are the intersecting point of other cross sections.

Horizon interpretation:

Total sedimentary thickness increases from south to north in this cross section.

Horizons	Faults cutting horizon
OZY1	fault 2-e, fault 4, fault 5-c, fault 10
OZY2	fault 2-e, fault 4, fault 5-c, fault 10
OZY3	fault 2-e, fault 4, fault 5-c, fault 10
Plac A (0.46Ma)	fault 2-e, fault 4, fault 5-a, fault 5, fault 5-c, fault 10
OZY4	fault 2-e, fault 4, fault 5-a, fault 5, fault 5-c, fault 10
Plac B (0.65Ma)	fault 2-f, fault 2-e, fault 4, fault 5-a, fault 5, fault 5-c, fault 10
Sm Gep (0.9 Ma)	fault 1-b, fault 1-a, fault 1, fault 2-f, fault 2-e, fault 5-a, fault 5, fault 5-c, fault 10

Table 8: Table 8 shows horizon interpretation in cross section GG'''' from west to east direction.

Fault interpretation:

Fault 1-b: This fault is a concave-basinward normal fault. The hanging wall of this fault contains a landward-tilted rollover structure.

Fault 1-a: This fault is a concave-basinward normal fault. The hanging wall of this fault contains a landward-tilted rollover structure with expanded growth section such that displacement increases downward and strata thickens landward. The age of growth strata in fault 1-a's hanging wall indicates that salt withdrawal occurred during the Pleistocene. Fault 1-a soles into a salt weld.

Fault 1: This fault is a concave-basinward normal fault. The hanging wall of this fault contains a landward-tilted prominent rollover structure with an expanded growth section such that displacement increases downward and strata thicken landward. The fault 1 soles into a salt

weld. The age of growth strata in the fault 1 hanging walls indicates that salt withdrawal occurred during the Pleistocene. Detailed interpretation will be done in the D*L plots chapter.

Fault 2-f: This fault is a concave-basinward normal fault. The fault 2-f soles into a salt roller. The hanging wall of this fault contains one synthetic and two antithetic faults.

Fault 2-e: This fault is a concave-basinward listric normal fault that into a salt roller. The hanging wall of this fault contains a landward-tilted rollover structure with an expanded growth section such that displacement increases downward and strata thicken landward**.** Between fault 2-e and fault 4 a graben structure was observed.

Fault 4: This fault is a landward normal fault that merges with fault 2-e.

Fault 5-a: This fault is a landward normal fault that merges with fault 2-e.

Fault 5: This fault is a concave-basinward normal fault. G''-G''' is an arbitrary line that passes through fault 5 and fault 7 in parallel. This causes fault surfaces to be observable parallel to horizons.

Fault 5-c: This fault is a basinward normal fault that merges with a salt weld. The hanging wall of this fault contains one synthetic and one antithetic fault.

Fault 10: This fault is a concave-basinward listric normal fault that soles into a salt roller. The hanging wall of this fault contains an antithetic fault.

Salt interpretation: The salt body, a salt roller, and a salt weld were interpreted based on publicly available well data and high amplitude seismic reflection. The fact that most of the faults in the study area sole into salt, implies that the kinematics of salt deformation are the same or at least similar to the kinematics of faulting.

Uninterpreted and interpreted west-east-oriented seismic cross sections HH’’’’ can be seen in figure 30-31 (see figure 11-15 for location). HH’’’’ cross section contains four arbitrary cross-lines (HH’, H’H’’, H’’H’’’, and H’’’H’’’’). The HH’’’’ cross section interpretation will be discussed in this chapter.

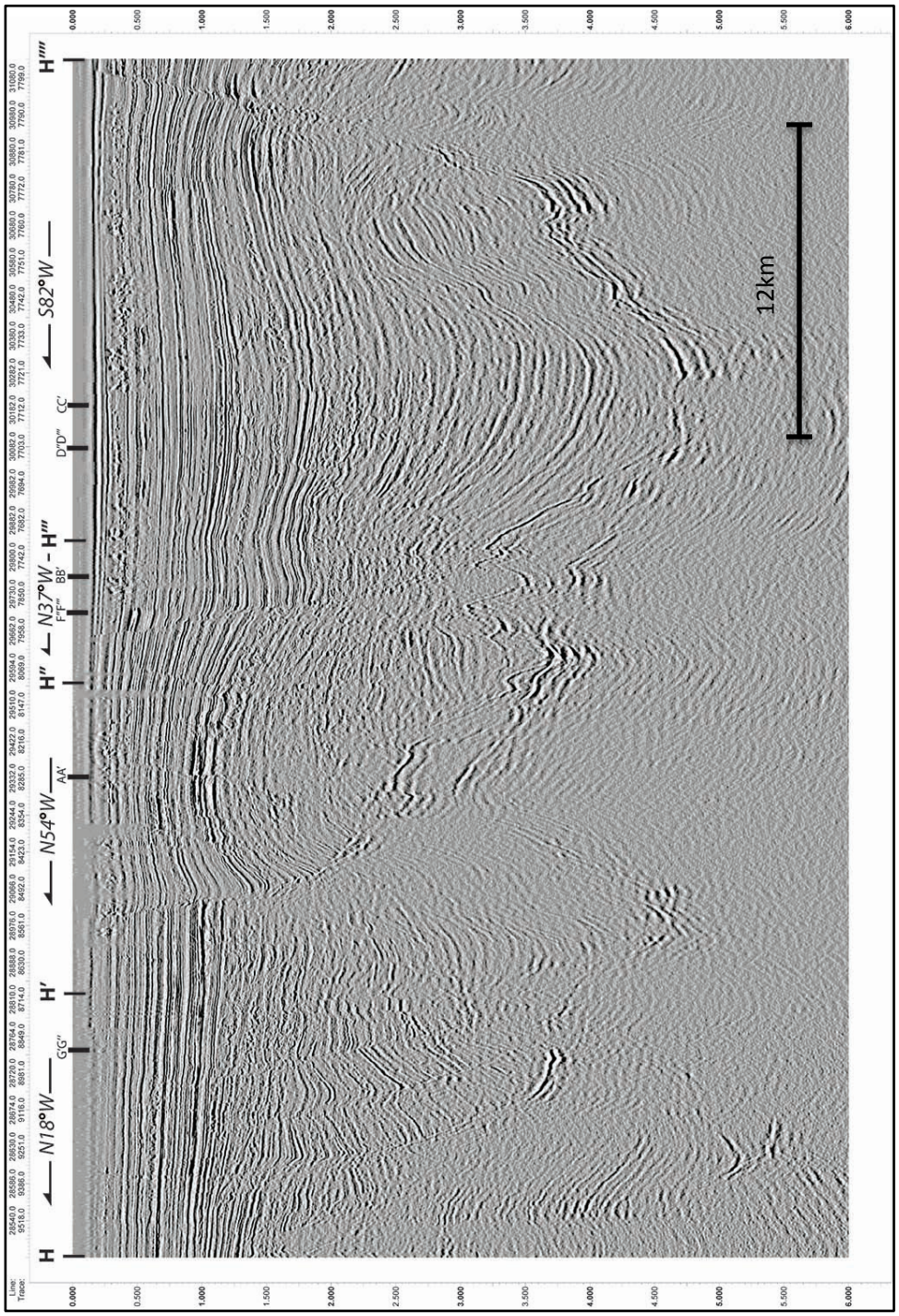

Figure 30: H-H’’’’ Cross section without interpretation. G’G’’, AA’, F’’F’’’, BB’, D’’D’’’, and CC’ are the intersecting point of other cross sections.

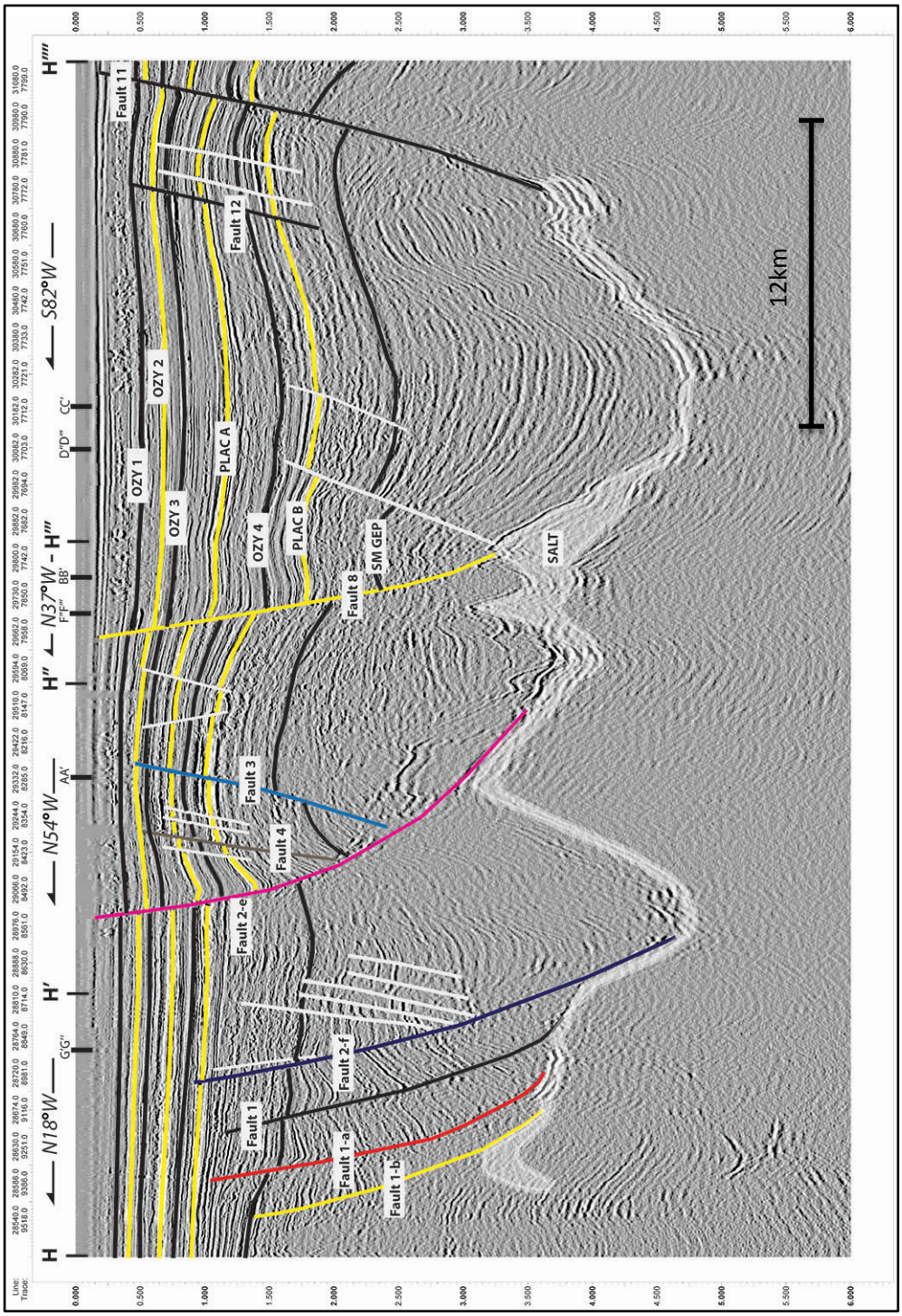

Figure 31: H-H'''' Cross section with faults and horizons. G'G'', AA', F''F''', BB', D''D''', and CC' are the intersecting point of other cross sections.

Horizon interpretation:

Horizons	Faults cutting horizon
OZY1	fault 2-e, fault 8, fault 11,
OZY2	fault 2-e, fault 8, fault 12, fault 11
OZY3	fault 2-e, fault 4, fault 3, fault 8, fault 12, fault 11
Plac A (0.46Ma)	fault 2-e, fault 4, fault 3, fault 8, fault 12, fault 11
OZY4	fault 2-e, fault 4, fault 3, fault 8, fault 12, fault 11
Plac B (0.65Ma)	fault 2-f, fault 2-e, fault 4, fault 3, fault 8, fault 12, fault 11
Sm Gep (0.9 Ma)	fault 1-b, fault 1-a, fault 1, fault 2-f, fault 2-e, fault 4, fault 3, fault 8, fault 11

Table 9: Table 9 shows horizon interpretation in cross section HH'''' from northwest to southeast direction.

Fault interpretation:

Fault 1-b: This fault is a concave-basinward normal fault. The hanging wall of this fault contains a landward-tilted rollover structure.

Fault 1-a: This fault is a concave-basinward normal fault. The hanging wall of this fault contains a landward-tilted rollover structure with expanded growth section such that displacement increases downward and strata thickens landward. The age of growth strata in the fault 1-a hanging wall indicates that salt withdrawal occurred during the Pleistocene. Fault 1-a soles into a salt weld.

Fault 1: This fault is a concave-basinward normal fault. The hanging wall of this fault contains a landward-tilted prominent rollover structure with an expanded growth section such that displacement increases downward and strata thicken landward. Fault 1 soles into a salt weld.

The age of growth strata in the fault 1 hanging walls indicates that salt withdrawal occurred during the Pleistocene. Detailed interpretation will be done in the D*L plots chapter.

Fault 2-f: This fault is a concave-basinward normal fault. The fault 2-f soles into a salt roller. The hanging wall of this fault contains one synthetic and five antithetic faults.

Fault 2-e: This fault is a concave-basinward listric normal fault. The fault 2-e soles into a salt roller. The hanging wall of this fault contains a landward-tilted rollover structure with expanded growth section such that displacement increases downward and strata thicken landward**.** Between fault 2-e and fault 4 a graben structure was observed.

Fault 4: This fault is a landward normal fault and merges with a salt weld.

Fault 3: This fault is a landward normal fault and merges with the fault 2-e.

Fault8: This fault is a concave-basinward normal fault that merges with a salt body. The hanging wall of this fault contains basinward-dipping sedimentation.

Fault 12: This fault is a basinward normal fault.

Fault 11: This fault is a basinward normal fault.

Salt interpretation: The fact that most of the faults in the study area sole into salt, implies that the kinematics of salt deformation are the same or at least similar to the kinematics of faulting.

Summary of Cross Sections Interpretation:

Most of the faults offset Pleistocene-age horizons and root into salt, a salt weld, or a salt roller. A majority of them dip south-southeast. Faults consist of synthetic splay and antithetic faults in both the hanging wall and footwall. All faults have variable range from planar to slightly listric in cross sections.

Highest extensions strain is located in block 319, 320, 325, 326, 327, 341, and 350. We interpret that normal faulting occurs above a region of salt withdrawal. The age of growth strata in the normal fault hanging walls indicates that salt withdrawal occurred during the Pleistocene.

The fact that most of the faults in the study area sole into salt, implies that the kinematics of salt deformation are the same or at least similar to the kinematics of faulting.

3.1.2.3 Time-structure Maps

A time-structure map (Figure 32) shows traces of interpreted faults between 0.494 and 1.348 seconds two-way travel time (TWT) in the horizon Plac A (0.49Ma). Initially isolated faults with varying orientations propagate towards each other until their fault tips overlap, giving rise to relay ramps and eventually transfer faults that link these faults. High levels of interaction were observed between fault 2, fault 2-d, and fault 2-e in this horizon, where a relay ramp is present between those 3 faults (Figure 32). Relay ramps are also observed between fault 2 and the fault 2-a, and between fault 2-b and the fault 2-c.

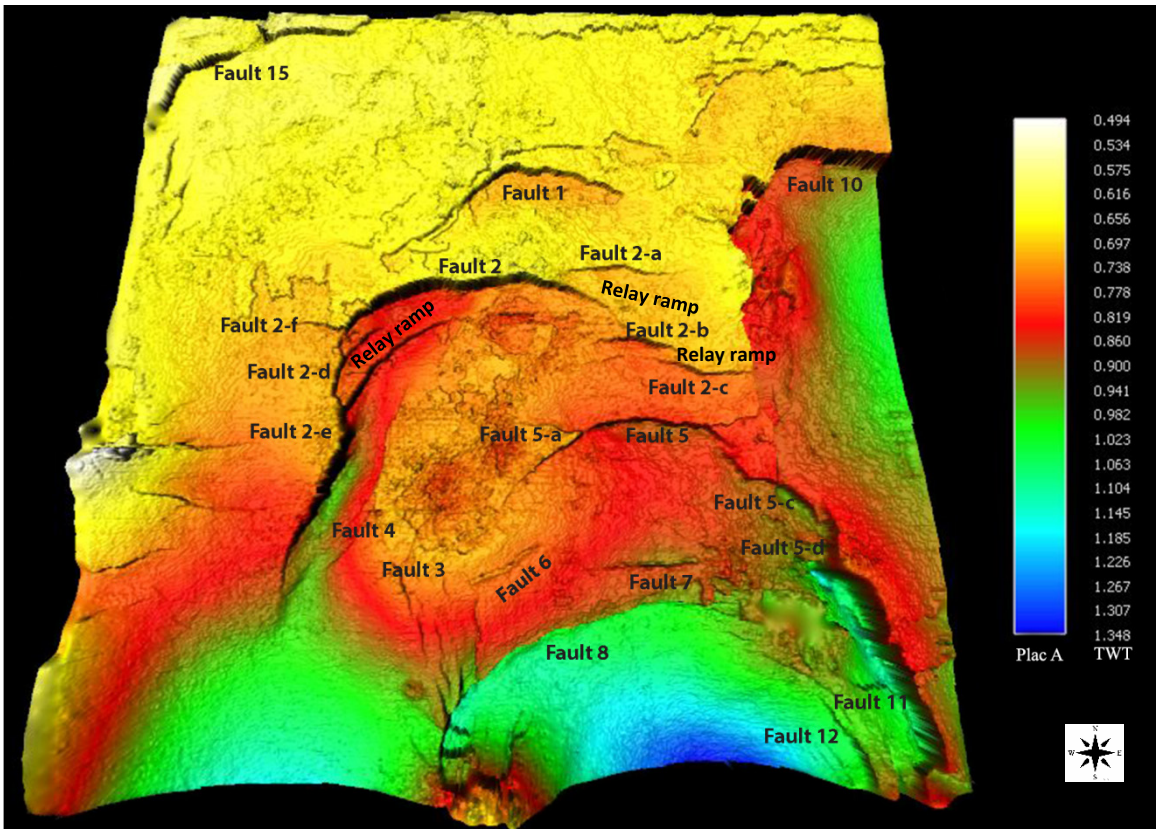

Figure 32: 3D Time-structure Map of Plac A horizon (0.46 Ma).

A time-structure map (Figure 33) shows the traces of interpreted faults between 1.452 and 2.108 seconds TWT. High levels of interaction are observed between fault 15, fault 15-a, fault 15-b, and fault 15-c in this horizon where a relay ramp is present between those 3 faults (Figure 33). Also, the fault 15-d and the fault 15-e overlap, which is noticeable on the time-structure map, where the relay ramp is present between those 2 faults.

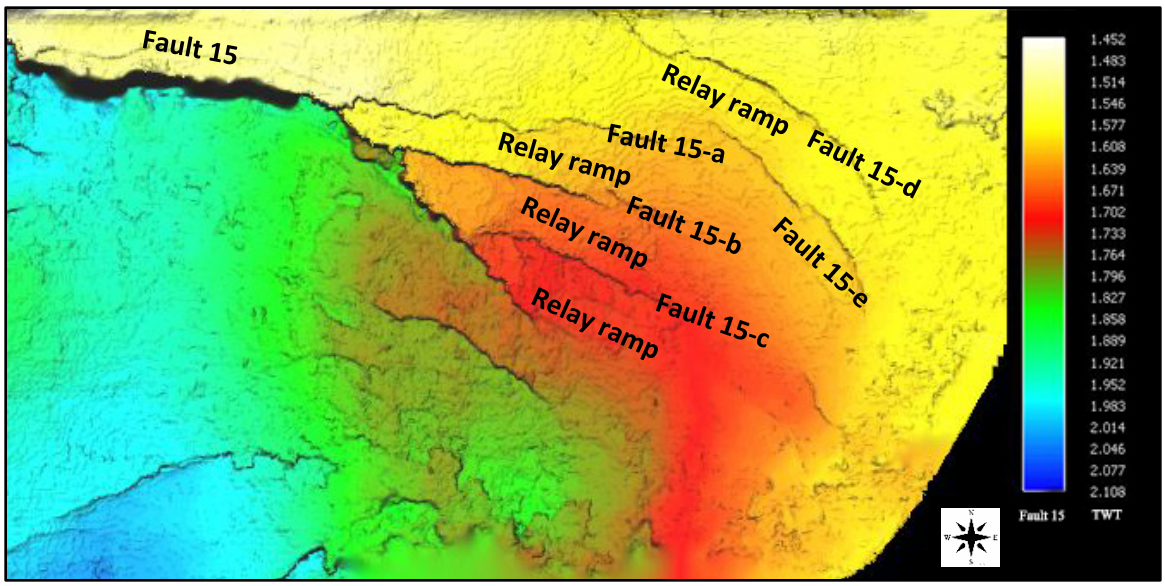

Figure 33: 3D Time-structure map for Fault 15, Fault 15-a, Fault 15-b, Fault 15-c, Fault 15-d, and Fault 15-e.

3.1.3 Sedimentation, Depositional/ Facies in Study Area

To understand depositional systems and sediment supplies in the study area, two river systems are interpreted based on similarity attribute. To visualize the whole river system in one map, four different time slices are merged with each other's. First river systems were recognized by using 0.8, 0.816, 0.840 and 0.860 second time slice maps (Figure 34-35).

Incised valleys form by fluvial erosion during a drop of a relative base level and fill with sediment as relative base-level rises (Dalrymple et al., 1994). Interpretations of the incised valley are discussed in this chapter.

The incised valley is at least 10.45 km long in map view, and 273 m wide in cross section X-X'. The incised valley formed between Plac A and Plac B transgressive surfaces, indicating the age of the incised valley is between 0.49 Ma and 0.65 Ma.

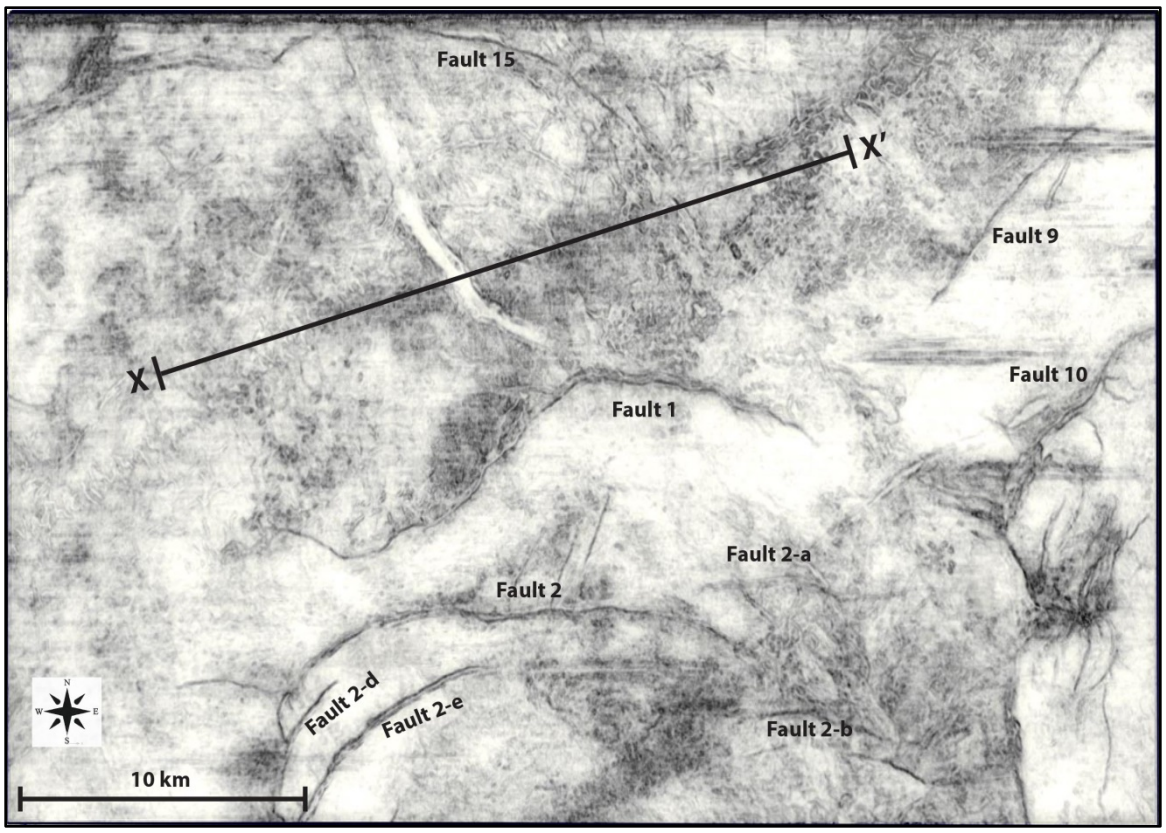

Figure 34: Combination of 0.8, 0.816, 0.840, and 0.860 seconds similarity time slices without interpretation.

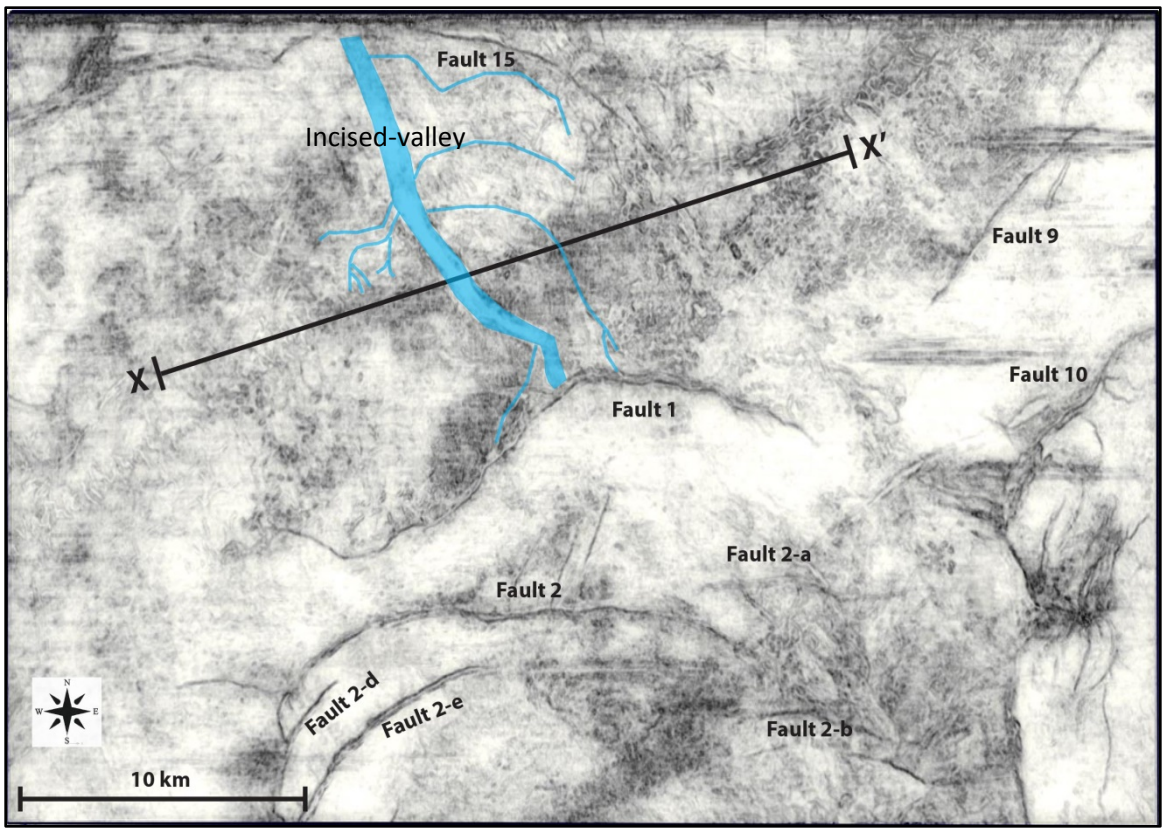

Figure 35: Combination of 0.8, 0.816, 0.840, and 0.860 seconds similarity time slices. Blue lines illustrate submarine channels.

To visualize the all river systems in one map, five different time slices are merged together. The second river system was recognized by using 0.94, 0.96, 0.98, 1.0 and 1.02 second time slice maps (Figure 36-37).

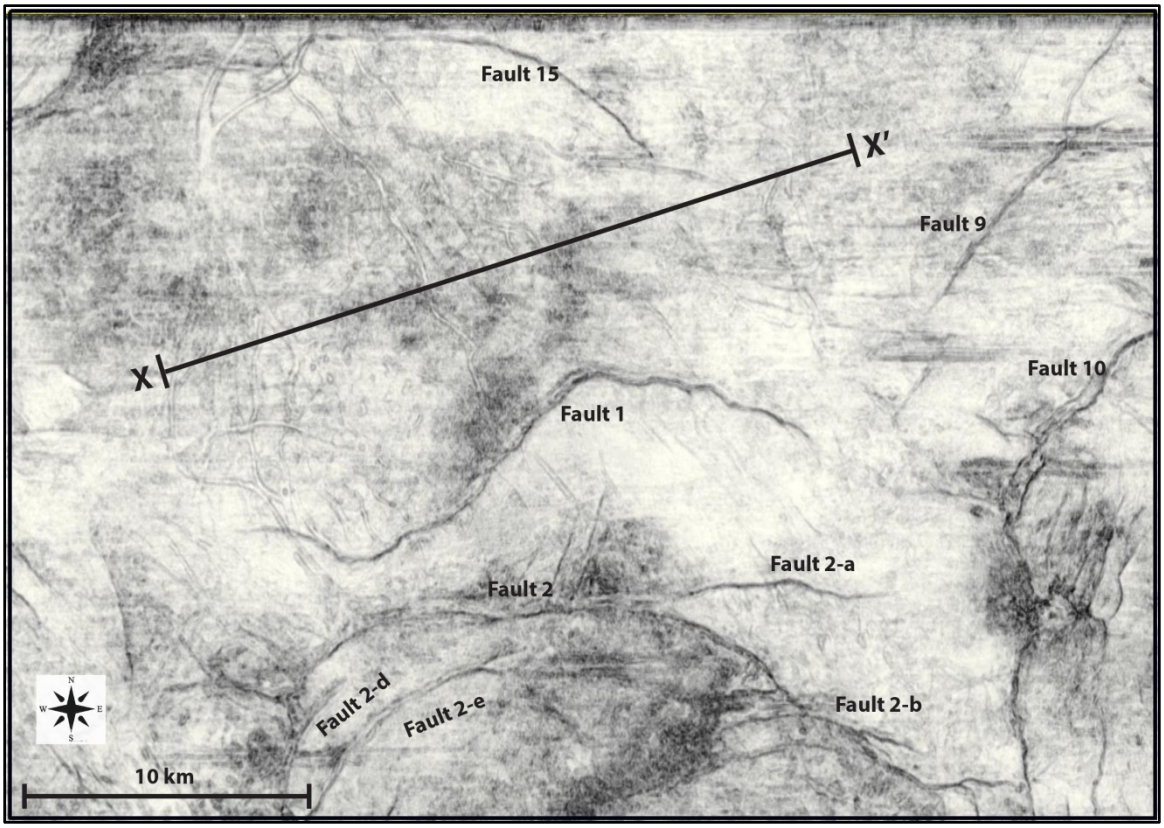

Figure 36: Combination of 0.94, 0.96, 0.98 and 0.86, 1.0, and 1.02 seconds similarity time slices without interpretation.

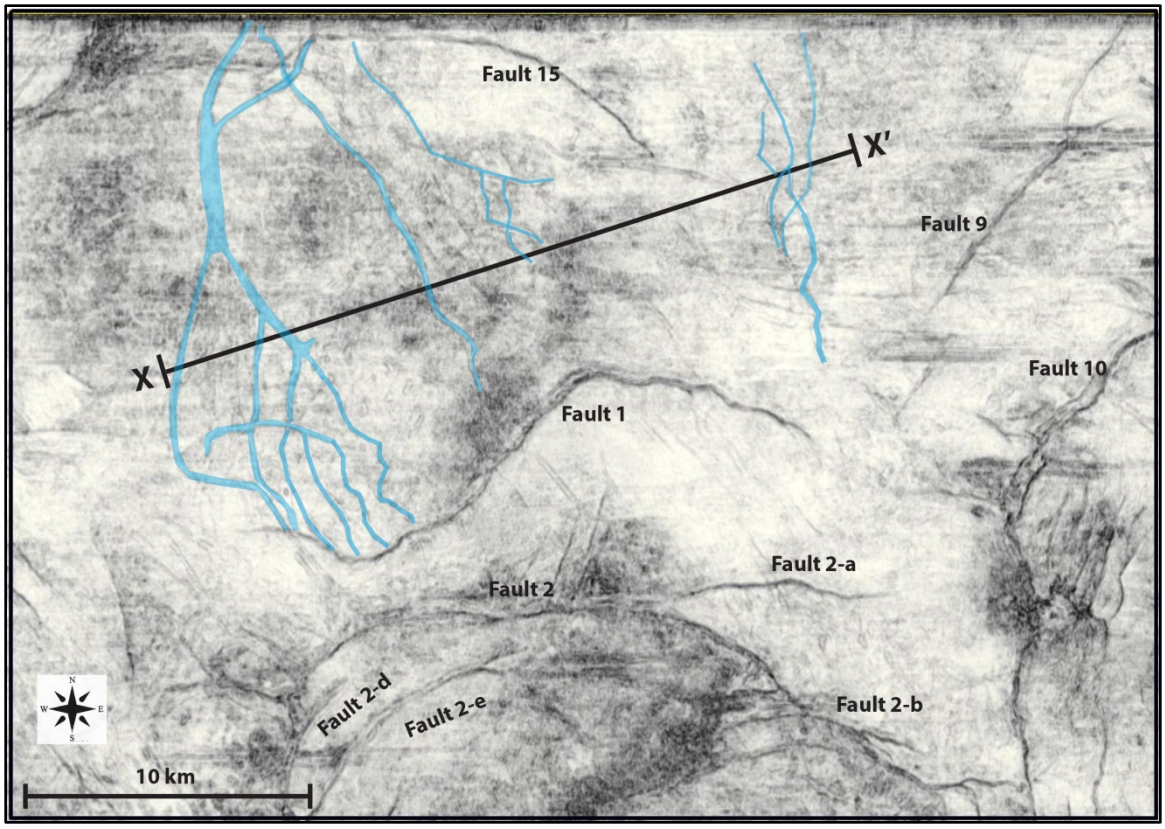

Figure 37: Combination of 0.94, 0.96, 0.98, 1.0, and 1.02 seconds similarity time slices. Blue lines illustrate channel networks.

Sedimentary rocks can be classified by their specific characteristics such as color, composition, geometry, lithology, sedimentary structures, and fossil content. In seismic data, depositional environments or seismic facies can be defined with different seismic parameters such as amplitude, continuity, phase, and frequency (Vail et al., 1977).

To understand of the evolution of the study area, five transgressive surfaces (Plac A 0.46Ma, Plac B 0.65Ma, Sm Gep 0.9Ma, H. Sellii 1.27Ma, and C. Mac 1.5Ma) and six sand bodies (CA, DA, EA, EA-2, GA, and JD) were constructed (Figure 38). The interpretation was performed based on previous studies (Holland et al., 1990; Alexander and Fleming, 1995; Rowan et., al 1998).

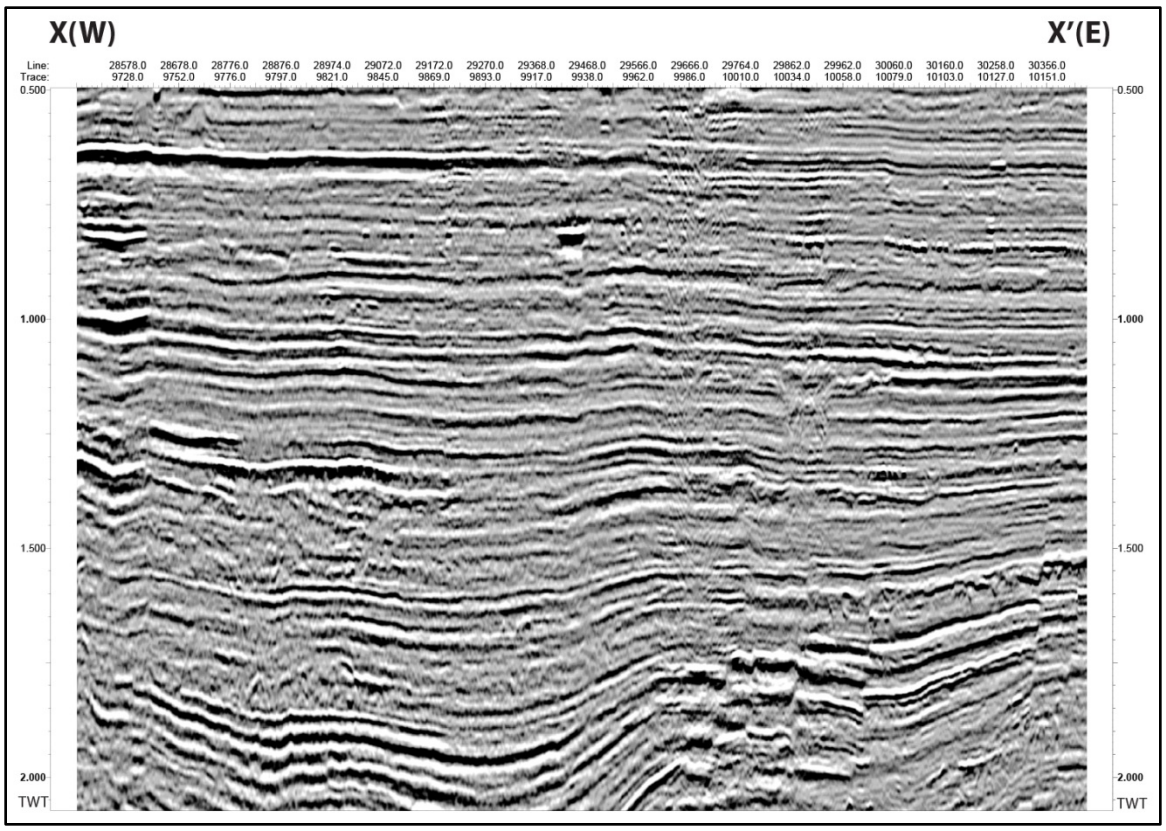

Figure 38: Uninterpreted west-east cross section.

Plac B to Plac A: Between those two intervals, two main sand bodies are interpreted (CA and DA). These are incised-valley fill deposits. A sedimentary deposit of material transported by or suspended in a river (0-1.0 Ma) consisting of shallow marine deltaic and fluvial deposition.

Sm Gep to Plac B: Between those two intervals, two main sand bodies are interpreted (EA and EA-2). EA is a deltaic sand and EA-2 is an incised-valley fill deposit. Four channels are interpreted above the EA-2 incised valley deposit.

H. Sellii to Sm Gep: Between these two intervals, one main sand body is interpreted (GA). GA is a fluvial-deltaic deposit. A channel is also observed below the EA-2 deposit.

C. Mac to H. Sellii: Between those two intervals, one main sand body is interpreted (JD). It is deltaic sand.

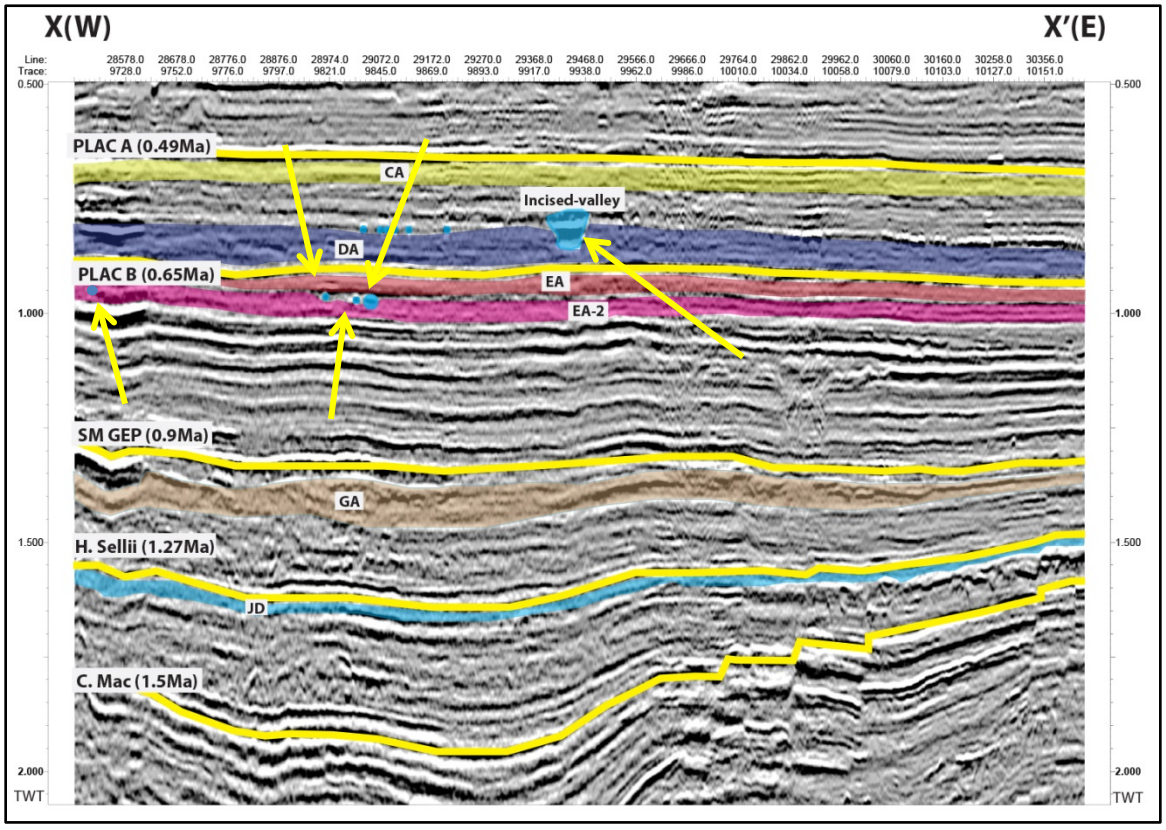

Figure 39: The West-East cross section illustrates interpreted transgressive horizons (yellow solid lines) and main sand bodies of the study area see figure 33, 34, 35, and 36 for location. Yellow arrows show location of interpreted rivers and the incised valley.

3.1.3.1 Isopach Maps

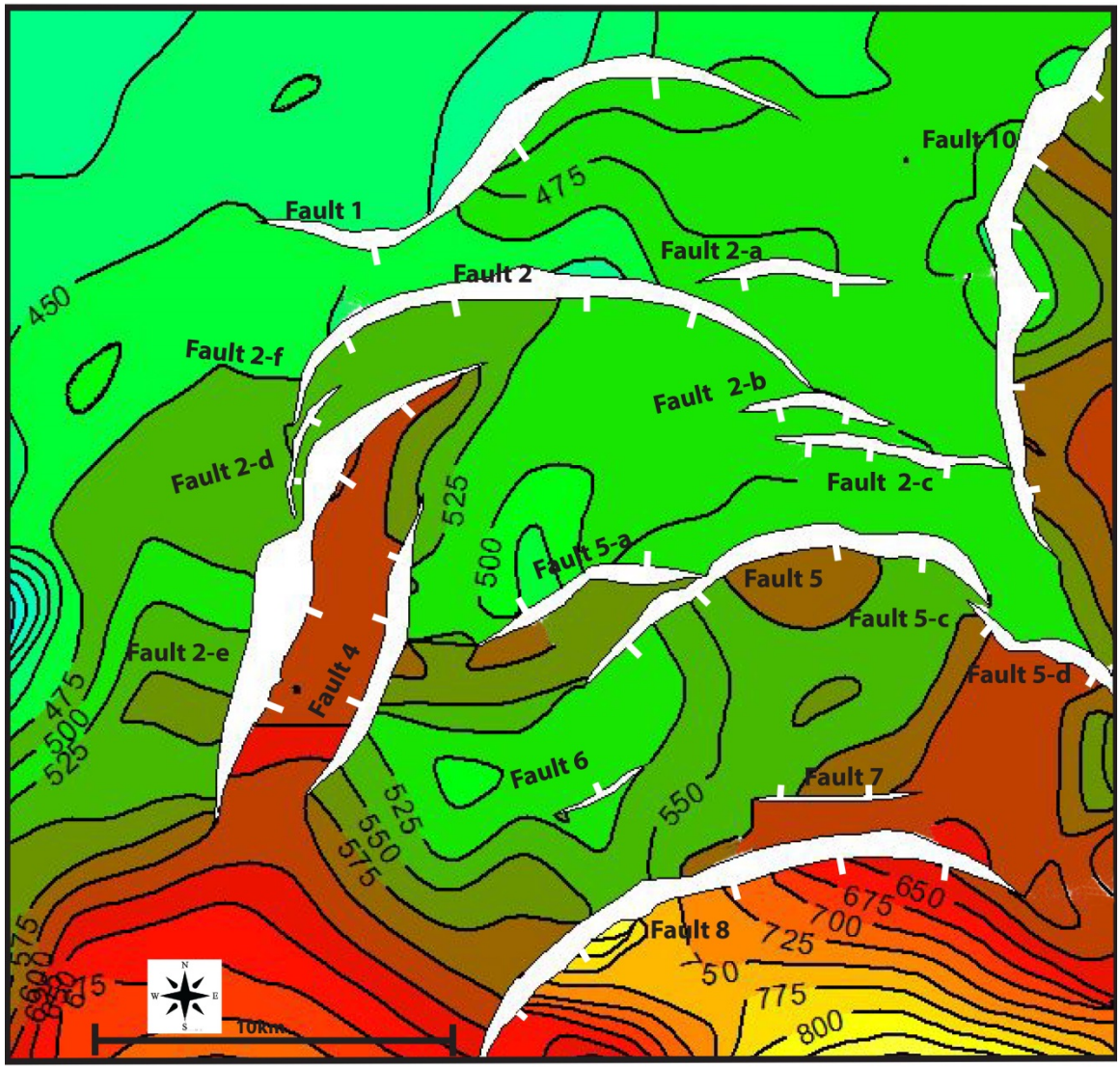

Figure 40: Isopach map, in meter, of the intervals between the mapped surfaces; this map represents the horizon Plac A-Ozy 1. Red areas represent the thick accumulations and green areas correspond to relatively thinner section of strata.

Isopach maps represent the sedimentary thickness between two interpreted horizons. Figure 40 shows the sedimentary thickness between horizon Plac A (0.65Ma) and Ozy 1 (the youngest interpreted horizon in this research). Sedimentary thickness is around 400 meters at the northern part and reaches 800 meters at the southern part of the study area.

Sedimentary thickness between fault 2-e and fault 4 is around 600 meters in this interval (Figure 40). The sedimentary thickness decreases towards the northern tips of fault 2-e and fault 4 and, increases towards the southern part of the fault tips that may result from deposition via a submarine channel system in the northern portion of the study area (Figure 37). The sedimentary thickness increases towards the southwest and reaches maximum of 700 meters. Since there is no faulting in the southernmost depocenter this can be explained by local salt-withdrawal.

A depocenter is located at the hanging wall of the fault 5 and thickness is around 600 meters at the center of the fault. The sedimentary thickness decreases towards to fault tips.

The thickest depocenter is located the southeastern part of the study area that sedimentary thickness reaches the maximum 800 meters. The sedimentary thickness is decreasing toward to fault tips. This depocenter is controlled by the fault 8 and local salt-withdrawal.

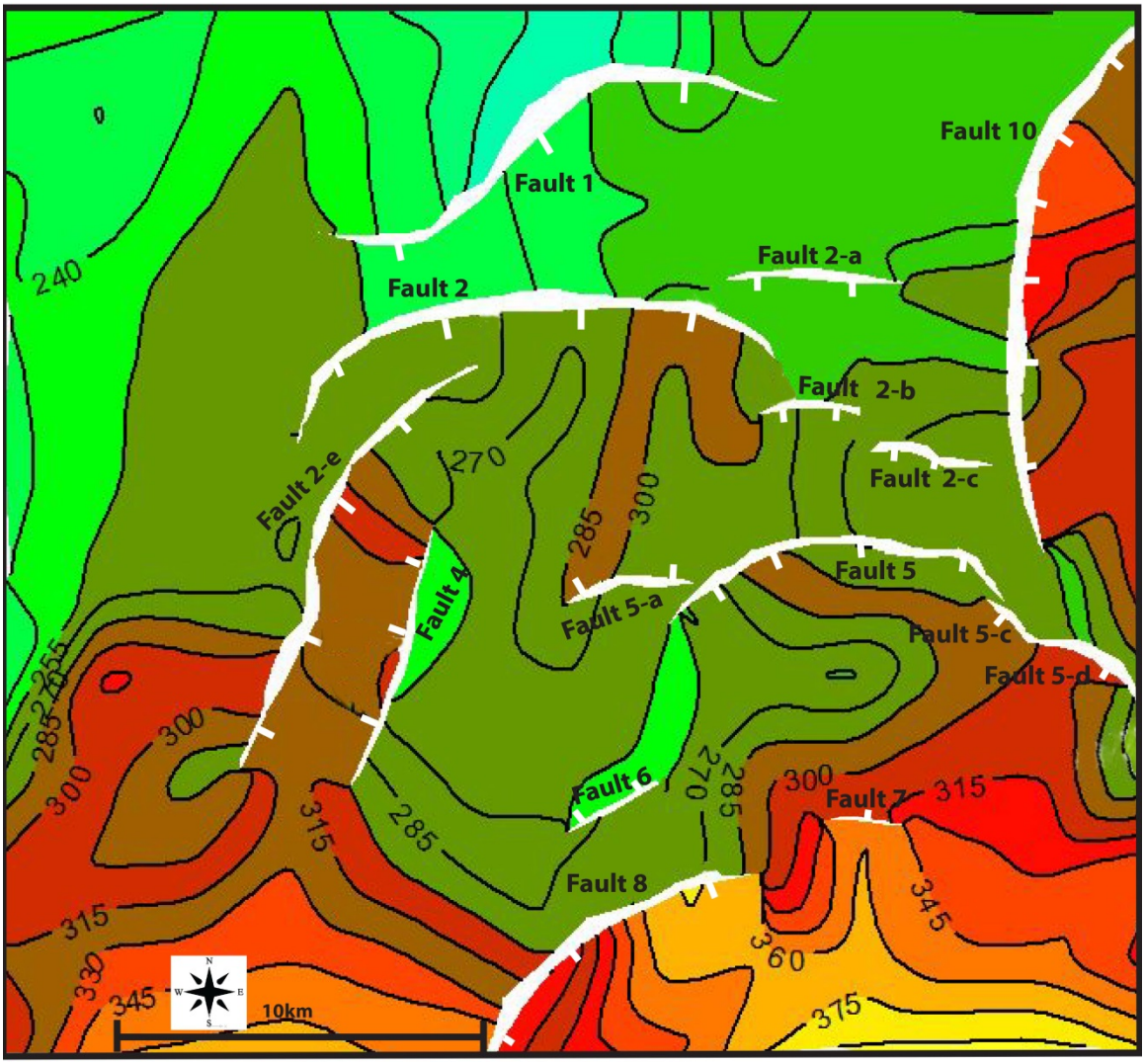

Figure 41: Isopach map, in meter, of the intervals between the mapped surfaces; this map represent the horizon Ozy 3-Ozy 1. Red areas represent the thick accumulations and green areas correspond to relatively thinner section of strata.

Figure 41 shows that sedimentary thickness between horizon Ozy 3 and Ozy 1. Sedimentary thickness is around 240 meters at the northern part and reaches maximum of 390 meters at the southern part of the study area. Based on Isopach maps, the age of faulting increases towards the south.

Sedimentary thickness between fault 2-e and fault 4 is around 300 meters in this interval (Figure 41). The sedimentary thickness decreases towards the northern tips of fault 2-e and fault 4 and, increases towards the southern part of the fault tips. The sedimentary thickness increases towards the southwest and reaches maximum of 360 meters. Since there is no faulting in the southernmost depocenter this can be explained by local salt-withdrawal.

The thickest depocenter is located the southeastern part of the study area that sedimentary thickness reaches the maximum 390 meters. The sedimentary thickness is decreasing toward to fault tips. This depocenter is controlled by the fault 8 fault 7 and local salt-withdrawal.

4. Structural Analysis of faults

4.1 Purpose and Goals of the Analysis

Displacement-Length (D*L) plots are commonly used in investigating displacement distributions along the faults (e.g. Morley and Wonganan, 2000; Peacock 2002; Morley et al., 2007). In this research D*L plots provide information on fault relationships (linkage and interaction), fault growth intervals and displacement distribution along faults (Figure 42).

In order to investigate the strain distribution in the study area, D*L plots were performed for four faults. Plots were created for six interpreted horizons.

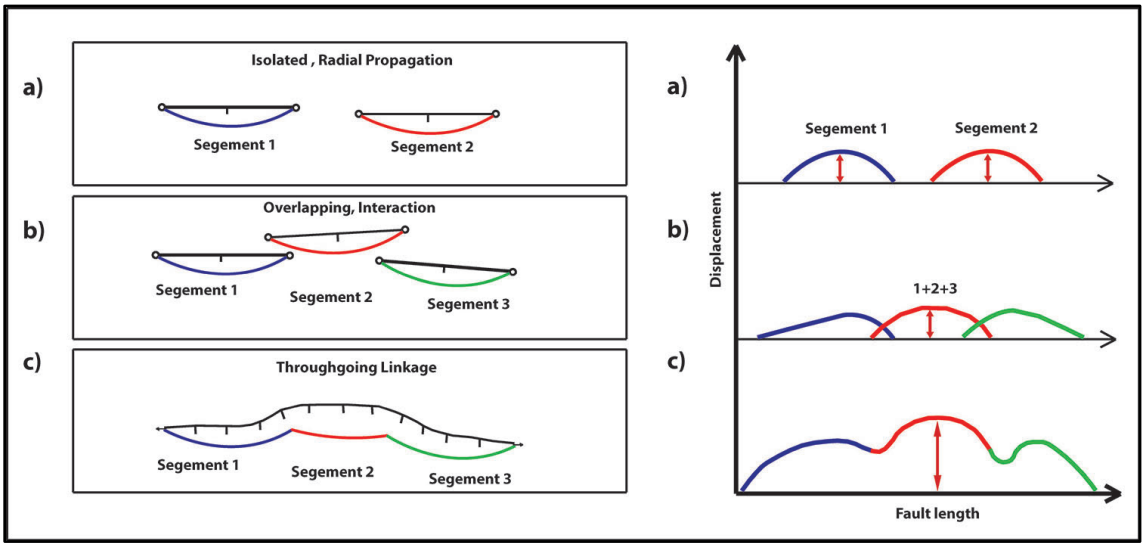

Figure 42: Illustration of D*L plot for isolated, overlapping, and linked faults (modified from Cartwright et al., 1995).

4.2 Displacement length plots

Workflow

Fault displacement and length measurements were made based on structural interpretation of faults and horizons in the study area. Faulted horizons were built in IHS-Kingdom software based on horizon point-sets and interpreted faults. Displacements values were calculated along the faults with 250 m intervals.

A result of calculating displacement values for six interpreted horizons that has been cut by faults is that six sets of displacement values were created for four faults. Manually calculated displacement values were digitized using Excel spreadsheets.

Interpretation

Displacement vs. Length calculation of fault 1 was performed from the western fault tip where displacement is zero in horizon Plac B (for location see figure 43 and 44). The fault 1 has displacement histories below the horizon Plac B but this could not be calculated because of the resolution problem. Fault 1 reaches the horizon Plac B at 8400 meters from the western fault tip (for location see figure 44).

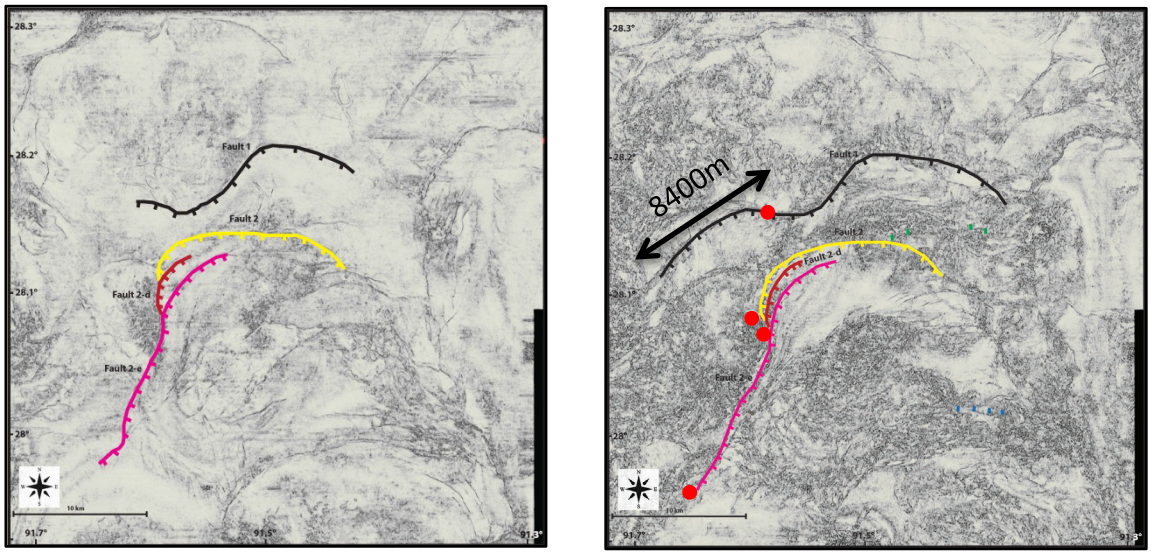

Figure 43-44: Similarity attribute time slices, respectively, 1.0 second and 1.5 second. Black, yellow, dark red and pink lines represent the fault 1, fault 2, fault 2-d, and fault 2-e. Ticks are on the hanging wall of these faults. Red points show the beginning point of D*L plots interpretation.

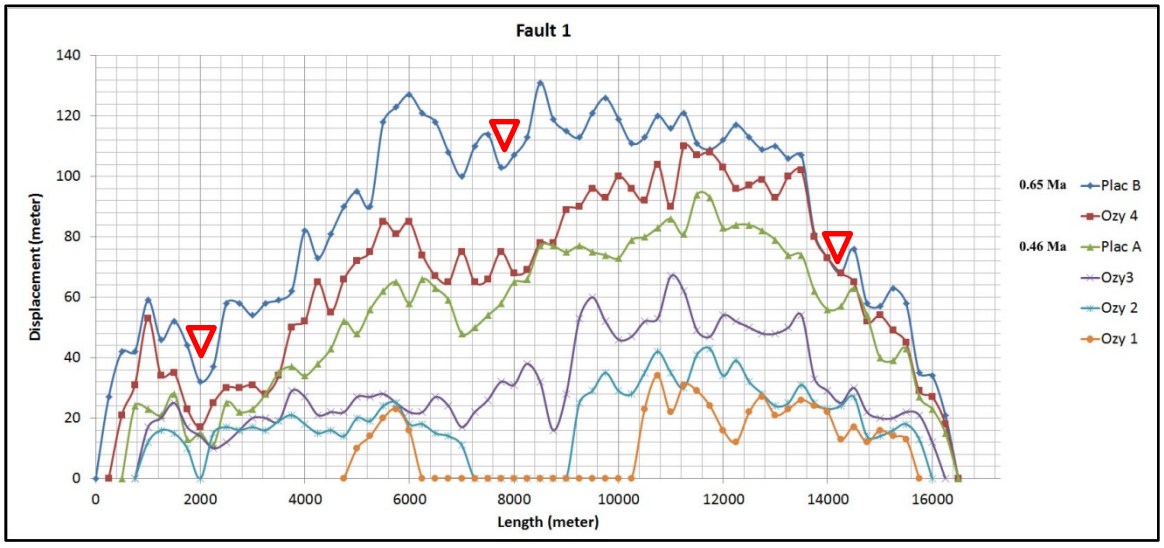

Figure 45: Displacement versus Length plot for the fault 1. Plac B, Ozy 4, Plac A, Ozy 3, Ozy 2, and Ozy 1 are interpreted horizon names that are represented by different color profiles. The vertical axis is displacement along the fault 1, and the horizontal axis is length of fault along the horizons. Red triangular shapes points to a potential linkage points.

Four major growth cycles can be identified for Fault 1 based on the above graph. Fault 1 is interpreted as a growth fault that has been active throughout at least the last 0.65 Ma (the age of deepest horizon, Plac B). Fault 1 is interpreted to grow by lengthening until it overlaps other faults as shown in figure 40 b-c. Then, displacement rises enough that overlapped faults are breached and the isolated segments link to form a larger fault. The linkages of fault 1 are also interpreted both laterally and in the dip direction (Figure 45).

Detail interpretation of D*L plot for the fault 1 (Figure 43):

OZY 1: Fault 1 is interpreted to consist of at least three major segments that cut Ozy 1 horizon. The first segment occurs between 4750 m and 6250 m. Displacement increases north-northeastward along strike from 0 m to a maximum of 23 m. Then displacement decreases from 23 m to 0 m. The second segment occurs between 10250 m and 12250 m. Displacement increases north-northeastward along strike from 0 m to a maximum of 31 m then decreases slightly to 12 m. The third segment occurs between 12250 m and 15750 m. Displacement increases eastward along the strike from 12 m to a maximum 27m than decreases gradually to 0 m.

As a result, the first segment can be interpreted as an isolated segment. Segment 2 and segment 3 can also be interpreted as a through-going linkage based on their displacement histories.

OZY 2: Fault 1 is interpreted to consist of at least three major segments that cut Ozy 2 horizon. The first segment occurs between 750 m and 2000 m. This segment was not observed at the horizon Ozy 1. Displacement increases eastward along strike from 0 m to a maximum of 16 m. Then displacement decreases from 16 m to 0 m. The second segment occurs between 2000 m and 7250 m. Displacement increases north-northeastward along strike from 0 m to a maximum

of 25 m. Then displacement decreases from 25 m to 0 m. The third segment occurs between 9000 m and 16000 m. Displacement increases eastward along strike from 0m to a maximum of 43 m. Then displacement decreases from 43 m to 0 m.

As a result, the first segments can be interpreted as an isolated segment. Also, the second segment can be interpreted as a through-going linkage based on their displacement history. The third segment has a complex displacement history to contain more than one segment. Because of this the third segment can be interpreted as a thoroughgoing linkage based on their displacement histories.

OZY 3: Fault 1 is interpreted to consist of at least four major segments that cut Ozy 3 horizon. The first segment occurs between 750 m and 2250 m. Displacement increases eastward along strike from 0 m to a maximum of 25 m. Then displacement decreases from 25 m to 10 m. The second segment occurs between 2250 m and 7000 m. Displacement increases north-northeastward along strike from 10 m to a maximum of 29 m. Then displacement decreases slightly to 17 m. The third segment occurs between 7000 m and 8750 m. Displacement increases north-northeastward along strike from 17 m to a maximum of 38 m, and then decreases from 38 m to 16 m. The fourth segment occurs between 8750 m and 16250 m. Displacement increases eastward along strike from 16 m to a maximum of 67 m. Then displacement decreases slightly from 67 m to 0 m.

As a result, fault 1 consist of at least four major segments that cut the horizon Ozy 3 ; can be identified as a through-going linkage based on their displacement histories.

Plac A (0.46Ma): The Plac A horizon is one of the transgressive surfaces in the study area which has been dated as Pleistocene (0.46Ma). Fault 1 is interpreted to consist of at least three major segments that cut Plac A horizon. The first segment occurs between 500 m and 2250 m.

Displacement increases eastward along strike from 0 m to a maximum 28 m. Then displacement decreases from 28 m to 11 m. The second segment occurs between 2250 m and 7000 m. Displacement increases north-northeastward along strike from 0 m to a maximum of 66 m. Then displacement decreases slightly to 48 m. The third segment occurs between 7000 m and 16500 m. Displacement increases eastward along strike from 48 m to a maximum of 94 m. Then displacement decreases eastward along strike from 94 m to 0 m.

As a result, fault 1 consists of at least three major segments that cut the Plac A horizon; these segments can be identified as a through-going linkage based on their displacement histories.

OZY 4: The fault 1 is interpreted to consist of least three major segments that cut Ozy 4 horizon. The first segment occurs between 250 m and 2000 m. Displacement increases eastward along strike from 0m to a maximum of 53 m. Then displacement decreases from 53 m to 17 m. The second segment occurs between 2000 m and 7250 m. Displacement increases north-northeastward along strike from 17 m to a maximum of 85 m. Then displacement decreases slightly to 65m. The third segment occurs between 7250 m and 16500 m. Displacement increases eastward along strike from 65 m to a maximum of 110 m. Then displacement decreases eastward along strike from 110 m to 0 m.

As a result, fault 1 consists of at least three major segments that cut the Ozy 4 horizon; these segments can be identified as a through-going linkage based on their displacement histories.

Plac B (0.65Ma): The horizon Plac B is one of the transgressive surfaces in the study area that the age of this horizon is Pleistocene (0.65Ma). Fault 1 is interpreted to consist of at least three major segments that cut Plac B horizon. The first segment occurs between 0 m and 2000 m.

Displacement increases eastward along strike from 0 m to a maximum of 59 m. Then displacement decreases from 59 m to 32 m. The second segment occurs between 2000 m and 7000 m. Displacement increases north-northeastward along strike from 32 m to a maximum of 127 m. Then displacement decreases slightly to 100 m. The third segment occurs between 7000 m and 16500 m. Displacement increases eastward along strike from 100 m to a maximum of 131 m. Then displacement decreases slightly eastward along strike from 131 m to 0 m.

As a result, fault 1 consists of at least three major segments that cut the Plac B horizon; these segments can be identified as a through-going linkage based on their displacement histories.

	Ozy 1	HD	Ozy 2	HD	Ozy 3	HD
Segment 1	4750m-6250m	23m	750m-2250m	16m	750m-2250m	25m
Segment 2	10250m-12250m	31m	2000m-7250m	23m	2250m-7000m	29m
Segment 3	12250m-15750m	27m	9000m-16000m	43m	7000m-8750m	38m
Segment 4					8750m-16500m	67m
	Plac A	HD	Ozy 4	HD	Plac B	HD
Segment 1	500m-2250m	28m	250m-2000m	53m	0m-2000m	59m
Segment 2	2250m-7000m	66m	2000m-7250m	85m	2000m-7000m	127m
Segment 3	7000m-16500m	94m	7250m-16500m	110m	7000m-16500m	131m

Table 10: Summary of segmentations for interpreted horizons along the fault 1. HD= Highest displacement.

A summary of displacement histories can be seen in table 10. The first segment of all horizons (except Ozy 1) was interpreted as the western fault tip and all of them support each other based on their displacement histories. The Ozy 1 is cut by three segments and two gaps along fault 1.

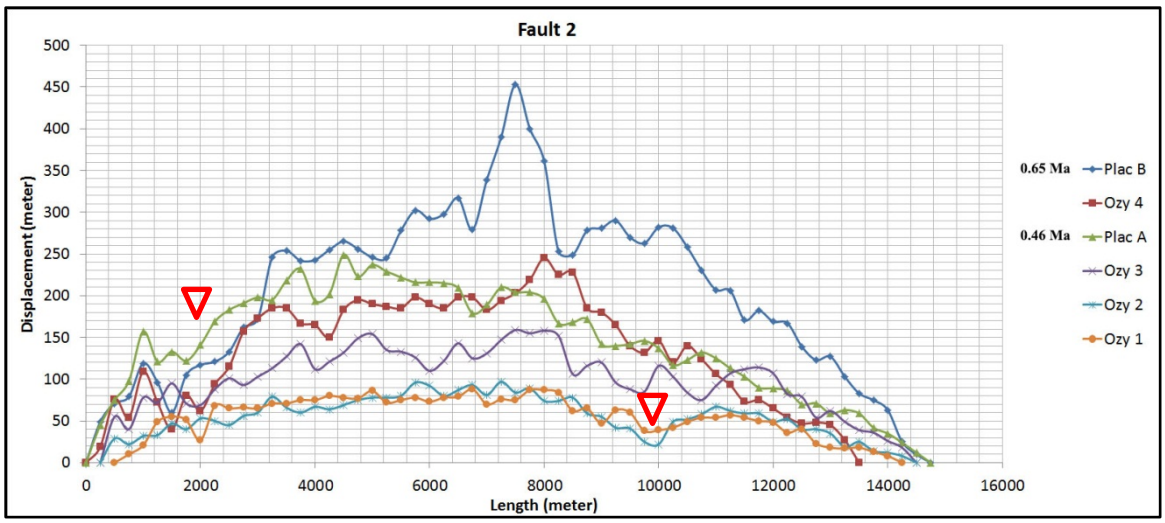

Figure 46: Displacement versus Length plot for the fault 2. Plac B, Ozy 4, Plac A, Ozy 3, Ozy 2, and Ozy 1 are interpreted horizon names that are represented by different color. The vertical axis is displacement along the fault 2, and the horizontal axis represents length of the fault along the horizons. Red triangular shapes points to a potential linkage points.

Fault 2 is interpreted as a growth fault from the western tip between 0 m to 8000 m. After 8000 m fault 2 turns into a planar fault. However, displacement of horizons still increases with depth on the hanging wall of the fault 2. The displacement history of fault 2 is interpreted both laterally and in the dip direction (Figure 46).

Detailed interpretation of D*L plot for the fault 2 (Figure 46):

For fault 2, a D*L calculation was performed from the western fault tip where displacement is 0 m and increases eastward along strike to maximum of 453 m then decreases to the eastern fault tip where displacement is 0m.

OZY 1: Fault 2 is interpreted to consist of at least three major segments that cut Ozy 1 horizon. The first segment occurs between 500 m and 2000 m. Displacement increases north-northeastward along strike from 0 m to a maximum of 55 m. Then displacement decreases from 55 m to 27 m. The second segment occurs between 2000 m and 9750 m. Displacement increases from west to east along strike from 27 m to a maximum of 88 m then decreases slightly to 38 m.

The third segment occurs between 9750 m and 14250 m. Displacement increases eastward along the strike from 38 m to a maximum 57 m then decreases slightly to 0 m.

OZY 2: Fault 2 is interpreted to consist of at least two major segments that cut Ozy 2 horizon. The first segment occurs between 250 m and 10000 m. Displacement increases from the western fault tip where displacement is 0 m and increases eastward along strike to a maximum of 97 m. Then displacement decreases from 97 m to 22 m. The second segment occurs between 10000 m and 14750 m. Displacement here increases eastward along strike to maximum 67m then decreases slightly to 0m.

As a result, fault 2 consists of at least two major segments that cut Ozy 2 horizon, and can be identified as a through-going linkage based on their displacement histories.

OZY 3: Fault 2 is interpreted to consist of at least four major segments that cut Ozy 3 horizon. The first segment occurs between 250 m and 2000 m. Displacement increases eastward along strike from 0 m to a maximum of 95 m then displacement decreases to 69 m. The second segment occurs between 2000 m and 6000 m. Displacement increases eastward along strike from 69 m to a maximum of 154 m. Then displacement decreases slightly to 110 m. The third segment occurs between 6000 m and 10750 m. Displacement increases eastward along strike from 110 m to a maximum of 158 m. Then displacement decreases from 158 m to 75 m. The fourth segment occurs between 10750 m and 14500 m. Displacement increases eastward along strike from 75 m to a maximum 114 m. Then displacement decreases slightly from 114 m to 0 m.

As a result, fault 2 consists of at least four major segments that cut Ozy 3 horizon, and can be identified as a through-going linkage based on their displacement histories.

Plac A (0.46Ma): The horizon Plac A is one of the transgressive surfaces in the study area and is Pleistocene (0.46Ma) in age. Fault 2 consists of at least three major segments that cut Plac A horizon. The first segment occurs between 0 m and 1750 m. Displacement increases eastward along strike from 0 m to a maximum of 157 m. Then displacement decreases from 157 m to 122 m. The second segment occurs between 1750 m and 4000 m. Displacement increases eastward along strike from 122 m to a maximum of 232 m. Then displacement decreases sharply from 232 m to 194 m. The third segment occurs between 4000 m and 14750 m. Displacement increases eastward along strike from 194 m to a maximum of 249 m. Then displacement decreases slightly from 249 m to 0 m.

As a result, fault 2 consists of at least three major segments that cut the Plac A horizon, and can be identified as a through-going linkage based on their displacement histories.

OZY 4: Fault 2 consists of at least three major segments that cut the Ozy 4 horizon. The first segment occurs between 0 m and 1500 m. Displacement increases eastward along strike from 0 m to a maximum of 109 m. Then displacement decreases from 109 m to 40 m. The second segment occurs between 1500 m and 4250 m. Displacement increases eastward along strike from 40 m to a maximum of 185 m. Then displacement decreases slightly to 150 m. The third segment occurs between 4250 m and 13500 m. Displacement increases eastward along strike from 150 m to a maximum of 245 m. Then displacement decreases eastward along strike from 245 m to 0 m.

As a result, fault 2 consists of least three major segments that cut the Ozy 4 horizon, and can be identified as a through-going linkage based on their displacement histories.

Plac B (0.65Ma): The horizon Plac B is one of the transgressive surfaces in the study area which is Pleistocene (0.65Ma) in age. Fault 2 consists of at least two major segments that cut the Plac B horizon. The first segment occurs between 0 m and 1500 m. Displacement increases eastward along strike from 0 m to a maximum of 119 m. Then displacement decreases from 119m to 60m. The second segment occurs between 1500 m and 14750 m. Displacement increases eastward along strike from 60 m to a maximum of 453 m. Then displacement decreases from 453 m to 0 m.

As a result, the fault 2 consists of at least two major segments that cut the Plac B horizon, and can be identified as a through-going linkage based on their displacement histories.

The fault 2 has a different anomaly between 6750 m and 8250 m; this will be explained in the summary part of the D*L interpretation.

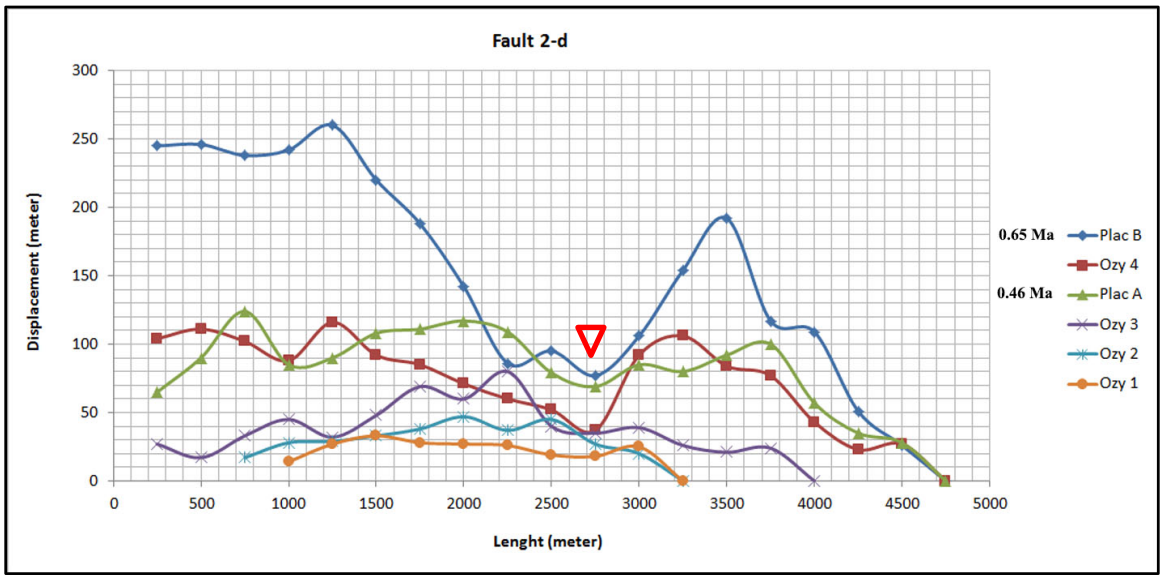

Figure 47: Displacement versus Length plot for the fault 2-d. Plac B, Ozy 4, Plac A, Ozy 3, Ozy 2, and Ozy 1 are interpreted horizon names that are represented by different colors. The vertical axis is displacement along the fault 2-d, and the horizontal axis presents length of the fault along the horizons. Red triangular shape points to a potential linkage point.

The displacement history of fault 2 is interpreted both laterally and in the dip direction (Figure 47).

Detailed interpretation of D*L plot for the fault 2-d (Figure 47):

Fault 2-d is located between fault 2 and fault 2-e. For fault 2-d, a D*L calculation was performed from the southern part of the fault to the northern fault tip.

OZY 1: Fault 2-d is 2250 m long at the horizon Ozy 1. A D*L calculation was performed from the southern part of the fault 2-d where displacement is 14 m. Displacement increases slightly from 14 m to 33 m. Then displacement decreases slightly from 33 m to 18 m at the 1750th m of this fault, which it is an important anomaly. A similar anomaly was observed for every interpreted horizon. At the end of the fault 2-d, displacement increases from 18 m to 25 m then decreases to 0m.

OZY 2: Fault 2-d is 2500 m long at the horizon Ozy 2. A D*L calculation was performed from the southern part of the fault 2-d where displacement is 17 m. Displacement increases slightly from 17 m to 47 m. Then displacement decreases slightly from 47 m to 37 m at 1500th m of this fault. At the end of the fault 2-d, displacement increases from 37 m to 45 m then decreases to 0m.

OZY 3: Fault 2-d is 3750 m long at the horizon Ozy 3. D*L calculation was performed from the southern part of the fault 2-d where displacement is 27 m. Displacement increases slightly from 27 m to 80 m. Then displacement decreases slightly from 80 m to 35 m at the 2500th m (same point with the horizon Ozy 1) of this fault. At the end of the fault 2-d, displacement increases from 35 m to 39 m, then decreases to 0 m.

Plac A (0.46Ma): The horizon Plac A is one of the transgressive surfaces in the study area that is Pleistocene (0.46Ma) in age. Fault 2-d is 4500 m at the horizon Plac A. A D*L calculation was

performed from the southern part of the fault 2-d where displacement is 65 m. Displacement increases sharply from 65 m to 124 m. Then displacement decreases sharply from 124 m to 85 m. After this point displacement increases slightly from 85 m to 117 m than decreases again to 69 m at the 2750th m (same point with the horizon Ozy 1 and Ozy 3) of this fault. At the end of the fault 2-d, displacement increases from 59 m to 100 m then decreases to 0m.

OZY 4: Fault 2-d is 4500 m long at the horizon Ozy 4. A D*L calculation was performed from the southern part of the fault 2-d where displacement is 104 m. Displacement increases slightly from 104 m to 111 m, then decreases smoothly from 111 m to 88 m. After this point displacement increases sharply from 88 m to 116 m, than decreases again to 37 m at the 2750th m (same point with the horizon Ozy 1, Ozy 3 and Plac A) of this fault. At the end of the fault 2-d, displacement increases from 37 m to 106 m then decreases to 0m.

Plac B (0.65Ma): The horizon Plac B is one of the transgressive surfaces in the study area that is Pleistocene (0.65Ma) in age. Fault 2-d is 4500 m long at the horizon Plac A. D*L calculation was performed from southern part of the fault 2-d where displacement is 245 m. Displacement increases slightly from 245 m to 260 m. Then displacement decreases sharply from 260 m to 77 m at the 2750th m (same point with the horizon Ozy 1, Ozy 3, Plac A, and Ozy 4) of this fault. After this point displacement increases sharply from 77 m to 192 m, then decreases to 0 m.

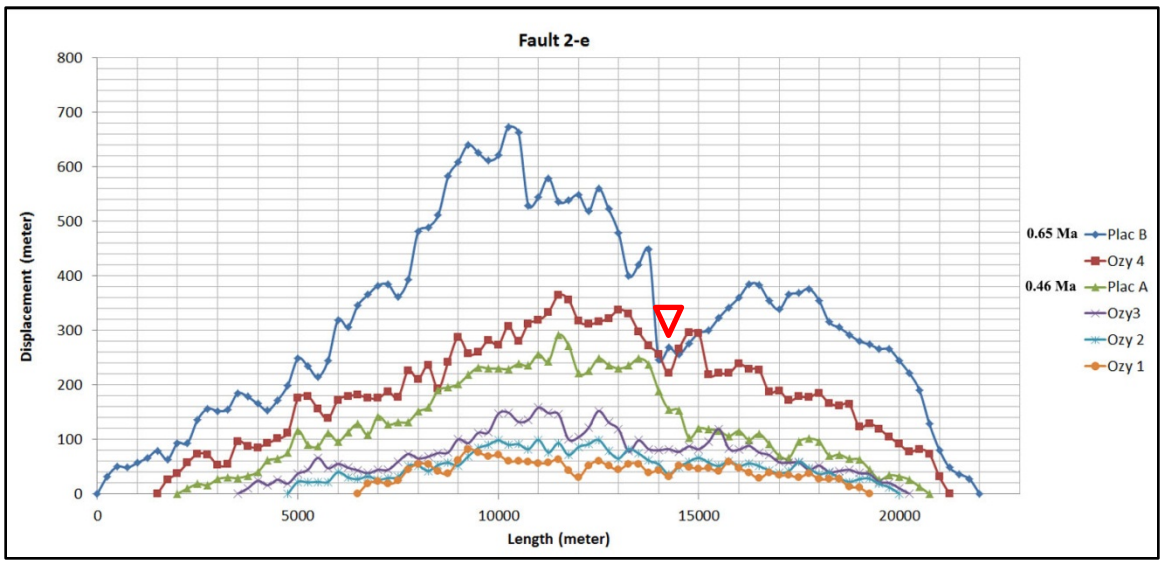

Figure 48: Displacement Length plot for the fault 2-e. Plac B, Ozy 4, Plac A, Ozy 3, Ozy 2, and Ozy 1 are interpreted horizon names that are represented by different colors. The vertical axis is displacement along the fault 2-e, and the horizontal axis represents length of the fault along the horizons. Red triangular shapes points to a potential linkage points.

Two major growth cycles can be identified for fault 2-e based on the above graph. Fault 2-e is interpreted as growth fault that has been active throughout at least the last 0.65 Ma (age of the deepest, Plac B, horizon). Fault 2-e is interpreted to grow by lengthening until it overlaps other faults as shown in figure 40 b-c. Then, displacement rises enough that overlapped faults are breached and the isolated segments link to form a larger fault. The linkages of the fault 2-e are also interpreted both laterally and in the dip direction (Figure 48).

Detailed interpretation of D*L plot for the fault 2-e (Figure 48):

For fault 2-e, a D*L calculation was performed from the southern fault tip where displacement is 0 m and increases northward along strike to a maximum of 673 m then decreases toward the northern fault tip where displacement is 0 m.

OZY 1: The fault 2-e is interpreted to consist of at least five major segments that cut Ozy 1 horizon. The first segment occurs between 6500 m and 8750 m. Displacement increases north-eastward along strike from 0 m to a maximum of 55 m. Then displacement decreases from 55 m to 37 m. The second segment occurs between 8750 m and 12000 m. Displacement increases north-northeastward along strike from 37 m to a maximum 82 m, and then decreases to 30 m. The third segment occurs between 12000 m and 14250 m. Displacement increases north-eastward along strike from 30 m to a maximum of 50 m than decreases slightly to 32 m. The fourth segment occurs between 14250 m and 16500 m. Displacement increases north-eastward along strike from 32 m to a maximum of 59 m than decreases slightly to 28 m. The fifth segment occurs between 16500 m and 19250 m. Displacement increases north-eastward along strike from 28 m to maximum 37 m then decreases slightly to 0 m.

As a result, fault 2-e consists of at least five major segments that cut the Ozy 1 horizon; these segments can be identified as a through-going linkage based on their displacement histories.

OZY 2: Fault 2-e is interpreted to consist of at least three major segments that cut Ozy 2 horizon. The first segment occurs between 4750 m and 7000 m. Displacement increases north-eastward along strike from 0 m to a maximum of 40 m. Then displacement decreases from 40 m to 26 m. The second segment occurs between 7000 m and 14250 m. Displacement increases north-northeastward along strike from 26 m to a maximum of 99 m then decreases to 36 m. The third segment occurs between 14250 m and 20000 m. Displacement increases north-eastward along strike from 30 m to a maximum of 66 m than decreases slightly to 0 m.

As a result, the fault 2-e consists of at least three major segments that cut the Ozy 2 horizon; these segments can be identified as a through-going linkage based on their displacement histories.

OZY 3: Fault 2-e is interpreted to consist of at least four major segments that cut Ozy 3 horizon. The first segment occurs between 3500 m and 6750 m. Displacement increases north-eastward along strike from 0 m to a maximum of 66 m. Then displacement decreases from 66 m to 38 m. The second segment occurs between 6750 m and 11750 m. Displacement increases north-northeastward along strike from 38 m to a maximum of 158 m then decreases to 100 m. The third segment occurs between 11750 m and 13250 m. Displacement increases sharply north-eastward along strike from 100 m to a maximum of 152 m than decreases sharply to 78 m. The forth segment occurs between 13250 m and 20250 m. Displacement increases north-eastward along strike from 78 m to a maximum of 119 m than decreases slightly to 0 m.

As a result, the fault 2-e consists of at least four major segments that cut the Ozy 3 horizon; these segments can be identified as a through-going linkage based on their displacement histories.

Plac A (0.46Ma): The horizon Plac A is one of the transgressive surfaces in the study area that is Pleistocene (0.46Ma) in age. Fault 2-e consists of at least three major segments that cut Plac A horizon. The first segment occurs between 2000 m and 14750 m. Displacement increases north-eastward along strike from 0 m to a maximum of 291 m. Then displacement decreases from 291 m to 103 m. The second segment occurs between 14750 m and 17250 m. Displacement increases slightly north-northeastward along strike from 103 m to a maximum of 115 m then decreases to 66 m. The third segment occurs between 17250 m and 20750 m. Displacement increases north-eastward along strike from 66 m to a maximum of 101 m than decreases to 0 m.

As a result, fault 2-e consists of at least three major segments that cut the Ozy 3 horizon; these segments can be identified as a through-going linkage based on their displacement histories.

OZY 4: Fault 2-e consists of at least two major segments that cut Ozy 4 horizon. The first segment occurs between 1500 m and 14250 m. Displacement increases north-eastward along strike from 0 m to a maximum of 364 m. Then displacement decreases from 364 m to 221 m. The second segment occurs between 14250 m and 21250 m. Displacement increases sharply north-northeastward along strike from 221 m to a maximum of 296 m then decreases slightly to 0 m.

As a result, fault 2-e consists of at least two major segments that cut Ozy 4 the horizon; these segments can be identified as a through-going linkage based on their displacement histories.

Plac B (0.65Ma): The horizon Plac B is one of the transgressive surfaces in the study area that is Pleistocene (0.65Ma) in age. Fault 2-e consists of at least two major segments that cut Plac B horizon. The first segment occurs between 0 m and 14000 m. Displacement increases north-eastward along strike from 0 m to a maximum of 673 m. Then displacement decreases from 673 m to 245 m. The second segment occurs between 14000 m and 22000 m. Displacement increases north-northeastward along strike from 245 m to a maximum of 383 m then decreases slightly to 0 m.

As a result, fault 2-e consists of at least two major segments that cut the Plac B horizon; these segments can be identified as a through-going linkage based on their displacement histories.

5. Discussion

5.1 Relay Ramp and Example of Linkage

Fault linkage and relay ramp geometry are common in extensional basins, where they can facilitate hydrocarbon migration. Relay ramps may also create hydrocarbon traps, which are significant for petroleum systems (Rowan et al., 1998; Peacock 2002).

In this study, fault linkage and relay ramps are observed in time-structure maps, as well as in D*L plot interpretations. Examination of D*L plots for the fault 2-e, fault 2-d, and fault 2 shows high interaction between those three faults (Figure 49).

5.1.2 Interpretation

Summary of the Fault 2, Fault 2-d, and Fault 2-e:

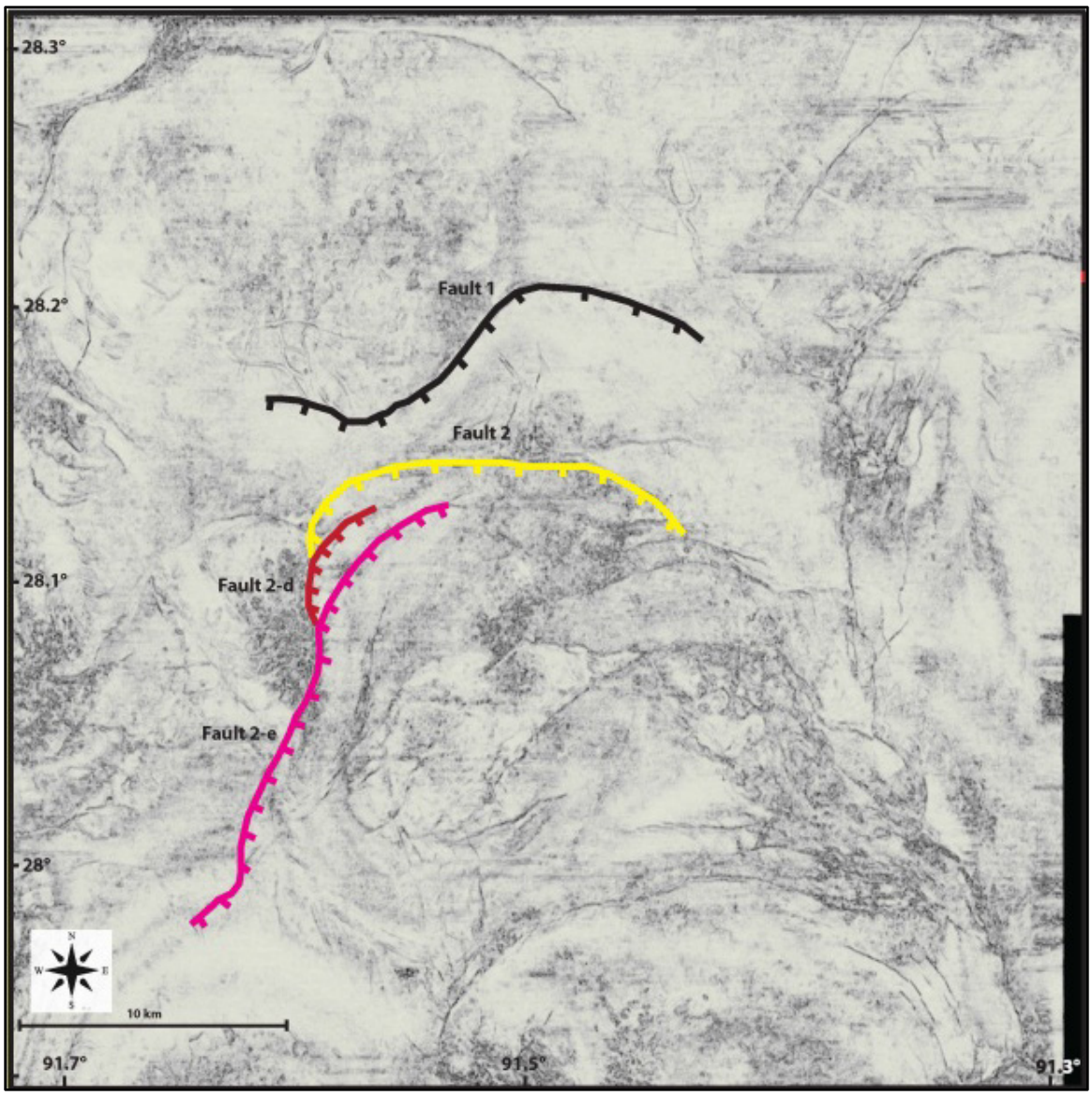

Figure 49: Similarity attribute time slice (1.0 second) illustrates fault 1, fault 2-e, fault 2-d, and fault 2 in the map view

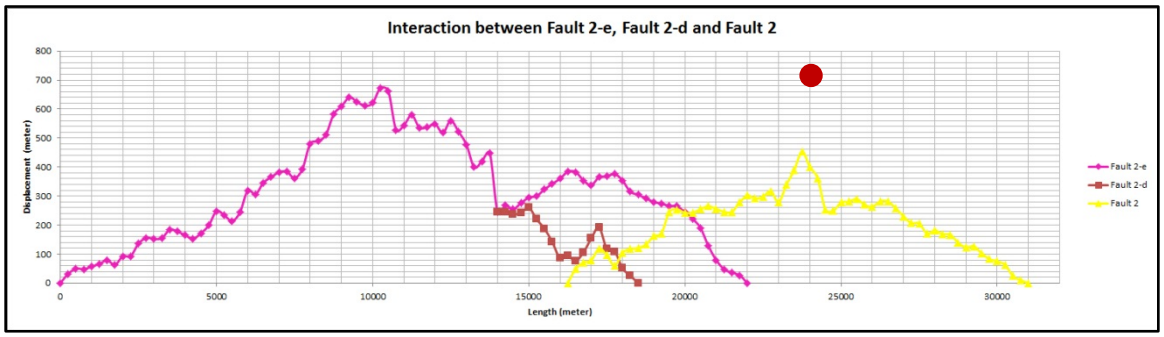

Figure 50: Displacement versus Length plot for the fault 2-e, fault 2-d, and fault 2 in the horizon Plac B. Red point is the end point of growth strata for the fault 2.

For fault 2-e, the D*L calculation was performed from southern fault tip where displacement is 0m and increases northward along strike to a maximum of 673 m (Figure 50). The length of this fault is around 22000 m; displacement decreases sharply from 448 m to 245 m at 14000th m. This point corresponds to starting point of the fault 2-d, where displacement starts with 245 m, thus indicating that the beginning of fault 2-d is also a possible linkage point between fault 2-e and 2-d. Moreover, displacement decreases progressively after 1300 m of fault 2-d until it meets with fault 2 at 2500th m of fault 2-d (Figure 51).

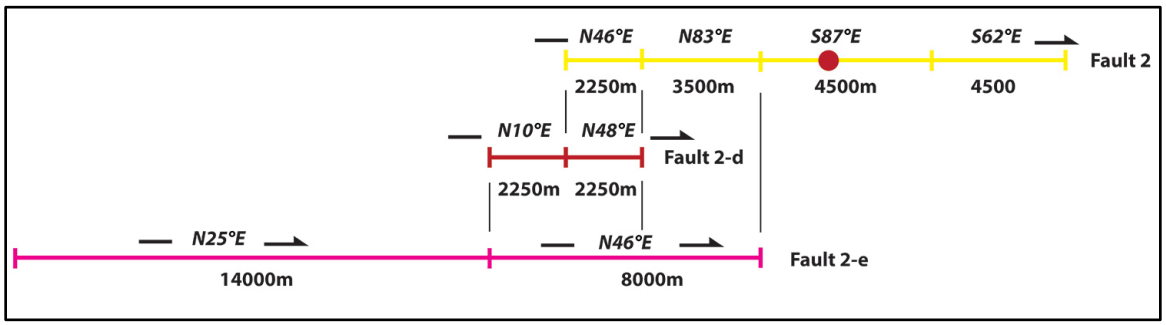

Figure 51: Summary of interaction between the fault 2-e, the fault 2-d, and the fault 2. Pink, red, and yellow lines illustrate faults. Red point is the end point of growth strata for the fault 2. (Length of the faults corresponds to the horizon Plac B).

For fault 2, the D*L calculation was performed from the western fault tip where displacement is 0 m and increased eastward along strike to max 453 m. The beginning point of the fault 2 affects fault 2-d and fault 2-e in that both of the fault's displacement decreases slightly.

Displacement increases abruptly after 5500 m of fault 2, which corresponds with the end point of fault 2-e. Moreover, displacement decreases sharply at the 7500th m of fault 2 that

corresponds to the end point of growth strata for fault 2. Most of the horizons support these displacement histories and interactions between fault 2-e, fault 2-d, and fault 2.

Although the geometries of salt-related faults can be highly complex, the evolution of overlap and fault linkages are observed between those three faults.

6. Summary and Conclusion

In conclusion, the fault systems in the study area consist of 25 concave basinward normal faults which consist of roller fault families and rollover fault families. All of the faults offset Pleistocene-age horizons. A majority of them dip south-southeast. All faults root into salt, a salt weld, or a salt roller.

The highest extension strain is located in block 319, 320, 325, 326, 327, 341, and 350. We interpret that normal faulting occurs above a region of salt withdrawal. The age of growth strata in the normal fault hanging walls indicates that salt withdrawal occurred during the Pleistocene. We calculate displacement-length (D*L) plots based on faults and horizons interpretation.

We observed fault linkage and relay ramp in 3D seismic data, as well as in D*L plot interpretation. For fault 2-e, a D*L calculation was performed from the southern fault tip where displacement is 0 m and increases northward along strike to a maximum of 673 m. The length of this fault is around 23000m and displacement decreases sharply from 448 m to 245 m at 13750 m. For fault 2-d, a D*L calculation was performed from the southern part of this fault where displacement is 245m, thus indicating that the beginning point of fault 2-d is also a possible linkage point for fault 2-e and 2-d. Moreover, displacement decreases progressively after 1300 m of fault 2-d until it meets with fault 2. When we look at the D*L plot for fault 2, an abrupt increase after 6000 m can be explained with the end point of fault 2-e. The D*L plots show high interaction between fault 2, fault 2-d and fault 2-e.

My research shows that faults in the study area are kinematically linked and act as a system which accommodates north-south extension, mostly affecting Pliocene and Pleistocene strata. The fact that most of the fault in the study area sole into salt implies that the kinematics of salt deformation is the same or at least similar to the kinematics of faulting.

This study is important because fault linkage as well as relay ramp geometry are common in an extensional basin, where they can facilitate hydrocarbon migration. Also, relay ramps may create hydrocarbon traps which are significant for petroleum system.

7. Limitation of this Study

The limitations of this research include un-available well data and interpretation uncertainty. Transgressive surfaces and sand bodies were interpreted based on previous studies in adjacent areas and characteristic of seismic amplitude. If well data had been available with lithology information, these interpretations would be more accurate.

Moreover, interpretations could not be carried out below the Plac B horizon in 3D because of resolution problems. If sonic, density, gamma ray and velocity information had been available for a couple of wells, we could have created synthetic to interpret below the horizon Plac B.

8. References

Alexander. L., & Flemings, P. B. (1995). Geologic evolution of a Plio-Pleistocene salt withdrawal Minibasin: Eugene Island Block330, offshore Louisiana. Bulletin of the American Association of Petroleum Geologists, v. 79, 1737-1756.

Cartwright, J. A., Trudgill, B. D., Mansfield, C. S., 1995, Fault growth by segment linkage: an explanation for scatter in maximum displacement and trace length data from the Canyon lands Grabens of SE Utah, Journal of Structural Geology, v. 17, No. 9, p. 1319-1326.

Barry C. McBride., Mark G. Rowan., and Paul Weimer., (1998). The evolution of allochthonous salt system, Northern Green Canyon and Ewing Bank (offshore Louisiana), Northern Gulf of Mexico: American Association of Petroleum Geologists Bulletin, v. 82, No.5B, p.1013-1036

Bird, D.E., Burke, K., Hall, S.A., and Casey, J.F., 2005, Gulf of Mexico tectonic history: Hotspot tracks, crustal boundaries, and early salt distribution: American Association of Petroleum Geologists Bulletin, v. 89, p. 311–328.

Dalrymple, R. W., R. Boyd, and B. A. Zaitlin,1994, History of research, types and internal organization of incised-valley systems: Introduction to the volume, in R. W. Dalrymple, R. Boyd, B. Zaitlin, and P. A. Scholle, eds., Incised-valley systems: Origin and sedimentary sequences: SEPM Special Publication v. 51, p. 3– 10.

Diegel, F. A., J. F. Karlo, D. C. Schuster, R. C. Shoup, and P. R. Tauvers, 1995, Cenozoic structural evolution and Tectono-stratigraphic framework of the northern Gulf Coast continental margin, in M. P. A. Jackson, D. G. Roberts, and S. Snelson, eds., Salt tectonics: A global perspective: AAPG Memoir v. 65, p. 109–151.

Ebeniro, J. O., Y. Nakamura, D. S. Sawyer, and W. P. O'Brien, Jr., 1988, Sedimentary and crustal structure of the northwestern Gulf of Mexico: Journal of Geophysical Research, v. 93, p. 9075– 9092.

Galloway, W.E., 2005b, Gulf of Mexico basin depositional record of Cenozoic drainage basin evolution, *in* Blum, M.D., Marriott, S.B., and Leclair, S.F., Fluvial sedimentology VII: Malden Massachusetts, International Association of Sedimentologists Special Publication v. 35, p. 409–423.

Galloway, W.E., Whiteaker, T.L., Curry, P.G., 2011, History of Cenozoic North American drainage basin evolution, sediment yield, and accumulation in the Gulf of Mexico basin. Geosphere, v. 7 no. 4 p. 938-973.

Holland, D. S., J. B. Leedy, and D. R. Lammlein, 1990, Eugene Island Block 330 field—U.S.A., offshore Louisiana, *in* E. A. Beaumont and N. H. Foster, eds., Structural traps III, tectonic fold and fault traps: AAPG Treatise of Petroleum Geology, Atlas of Oil and Gas Fields, p. 103–143.

Jackson, M. P. A., and C. Cramez, 1989, Seismic recognition of salt welds in salt tectonics regimes (abs.): SEPM Gulf Coast Section, 10th Annual Research Conference, Program and Extended Abstracts, Houston, Texas, p. 66–71.

Marton, G., and R. T. Buffler, 1994, Jurassic reconstruction of the Gulf of Mexico Basin: International Geology Review, v. 36, p. 545– 586.

Morley, C.K., and Wonganan, N., 2000. Normal fault displacement characteristics, with particular reference to synthetic transfer zones, Mae Moh mine, northern Thailand. Basin Research v. 12, 307-327.

Morley, C.K., S. Gabdi, and Seusutthiya, K., 2007. Fault superimposition and linkage resulting from stress changes during rifting: Example of 3D seismic data, Phitsanulok Basin, Thailand. Journal of Structural Geology v. 29, p. 646-663.

Peacock, D.C.P., 2002. Propagation, interaction and linkage in normal fault systems: Earth-Science Reviews v. 58, 121-142.

Rowan, M. G., B. D. Trudgill, B. S. Hart, S. Nelson, and P. B. Flemings, 1998, Three-dimensional geometry and evolution of a salt-related growth-fault array: Eugene Island 330 field, offshore Louisiana, Gulf of Mexico: Marine and Petroleum Geology, v. 15, p. 309–328.

Rowan, M. G., B. D. Trudgill, and M. P. A. Jackson, 1999, Salt-related fault families and fault welds in the northern Gulf of Mexico: American Association of Petroleum Geologists Bulletin, v. 83, No.9, p.1454-1484.

Salvador, A., 1987, Late Triassic-Jurassic paleogeography and origin of Gulf of Mexico basin: AAPG Bulletin, v. 71, no. 4, p. 419-451.

Salvador, A., 1991, Origin and development of the Gulf of Mexico Basin, in A. Salvador, ed., The Gulf of Mexico Basin: Geological Society of America, The geology of North America, v.J, p. 389-444.

Sumner, H. S., B. A. Robison, W. K. Dirks, and J. C. Holliday, 1990, Morphology and evolution of salt/minibasin systems: lower shelf and upper slope, central offshore Louisiana (abs.): GSA Annual Meeting, Programs with Abstracts, Dallas, Texas, p. 48.

Vail, P. R., R. M. Mitchum, Jr., R. G. Todd, J. M. Widmier, S. I. Thompson, J. B. Sangree, J. N. Bubb, and W. G. Hatlelid, 1977, Seismic stratigraphy and global changes of sea level, *in* C. E. Payton, ed., Seismic stratigraphy: applications to hydrocarbon exploration: AAPG Memoir v. 26, p. 49–212.